

Modulation and Coding for NOMA and RSMA

Hamid Jafarkhani, *Fellow, IEEE*, Hossein Maleki, *Student Member, IEEE*, and
Mojtaba Vaezi, *Senior Member, IEEE*

(Invited Paper)

Abstract—Next generation multiple access (NGMA) serves as an umbrella term encompassing transmission schemes distinct from conventional orthogonal methods. As a prominent candidate of NGMA, non-orthogonal multiple access (NOMA) emerges as a promising solution, enhancing connectivity by allowing multiple users to concurrently share time, frequency, and space. However, NOMA faces challenges in practical implementation, particularly in canceling inter-user interference. In this paper, first, we discuss the principles behind NOMA and review the conventional NOMA methods and results. Then, to address the above challenges, we present asynchronous transmission and interference-aware modulation techniques, leading to decoding free from successive interference cancellation. The goal is to design constellations that dynamically adapt to interference, minimizing bit error rates (BERs) and enhancing user throughput in the presence of inter-user, inter-carrier, and inter-cell interference. The traditional linkage between minimizing BER and increasing spectral efficiency is addressed, with the exploration of deep autoencoders for end-to-end communication as a new concept with significant potential for improving BERs. Interference-aware modulation techniques can revolutionize constellation design and communication over non-orthogonal channels. Rate-splitting multiple access (RSMA) is another promising interference management technique in multi-user systems. Beyond addressing existing challenges and misconceptions in finite-alphabet NOMA, this paper offers fresh insights to the field and provides an overview of code-domain NOMA schemes, trellis-coded NOMA, and RSMA as other potential candidates for NGMA. Additionally, we discuss the evolution of channel coding towards low-latency communication and examine the modulation and coding schemes in fifth-generation cellular networks. Finally, we examine future research avenues and challenges, highlighting the importance of addressing them for the practical realization of NOMA from a theoretical concept to a functional technology.

Index Terms—NGMA, NOMA, RSMA, asynchronous NOMA, code-domain NOMA, sparse code multiple access, trellis-coded NOMA, quadrature amplitude modulation, uniform and non-uniform modulation, channel coding, interference-aware constellation, deep learning, autoencoder, 5G, 6G.

I. INTRODUCTION AND HISTORICAL NOTES

The next generation of communication systems is expected to deliver improved end-user experience by offering new applications and services such as industry automation, smart cities, virtual and augmented reality, remote medical surgery, self-driving cars, and uncrewed aerial vehicles (UAVs). These

envisioned services pose many challenging requirements, such as low latency, high data rates, massive connectivity, high reliability, and support of diverse quality of service. The need for massive connectivity in fifth-generation (5G) wireless networks and beyond is mainly pushed by the explosion of the Internet of things (IoT) devices, as projected by leading industry including Cisco and Ericsson [1]. Particularly, 6G wireless networks require a connection density of 10^7 devices/km², which is 1000 times higher than that of 4G and 10 times higher than that of 5G networks [1]–[3]. The requirements in terms of improving reliability, spectral efficiency, and energy efficiency are also stringent. In this context, the roles of multiple access in general and modulation and coding in particular are crucial toward achieving these goals.

Non-orthogonal multiple access (NOMA) [4] is perhaps the most prominent candidate for next generation multiple access (NGMA). NOMA increases the number of connected devices and enhances the spectral efficiency of communication by enabling multiple users to share time, frequency, and space, thus accommodating a larger number of users compared to conventional orthogonal multiple access (OMA) schemes. NOMA facilitates massive connectivity by allowing the concurrent service of multiple users within the same resource block, such as a time slot, sub-carrier, or spreading code. It has actively been considered by academia [4]–[9], standardization bodies, and industry [10]–[13]. An intriguing aspect of NOMA is its flexibility in integration with various technologies, including orthogonal frequency division multiplexing (OFDM) which is the multiple access method in 4G and 5G. That means a NOMA user has the capability to share a single *resource block* of OFDM with one or more additional users.

Despite its significant promise and immense academic work in this field, NOMA has not been incorporated into any standards yet. Several factors contribute to this. A primary reason is that the theoretical gains of NOMA were not achieved in practical implementations [14]. There are primary challenges that make it difficult to achieve NOMA's theoretical gains in practice. They include the difficulty of canceling inter-user interference introduced by NOMA (such as the complexity of successive interference cancellation), sensitivity of NOMA to channel state information (CSI), and non-synchronous nature of multi-user communication. Another reason for this shortfall is the absence of novel modulation schemes addressing inter-user interference introduced by NOMA. Overall, there has been limited research and innovation on finite-alphabet NOMA. A third contributing factor is the rise of competitive solutions, such as massive multiple-input multiple-output (MIMO), millimeter-wave (mmWave), and narrow-band IoT, which have effectively tackled some of the requirements for

Hamid Jafarkhani and Hossein Maleki are with Center for Pervasive Communications and Computing, University of California at Irvine, Irvine, CA 92697 USA (e-mails: hamidj and malekih@uci.edu). Their work was supported in part by the NSF Awards CNS-2229467 and CCF-2328075. Mojtaba Vaezi is with the Department of Electrical and Computer Engineering, Villanova University, Villanova, PA 19085, USA (e-mail: mvaezi@villanova.edu). His work was supported by the U.S. National Science Foundation under Grant ECCS-2301778. Corresponding authors: Hamid Jafarkhani and Mojtaba Vaezi.

massive connectivity and spectrum efficiency through innovative solutions and the fact that many theoretical NOMA results are limited to single antenna cases.

Nonetheless, inheriting the rich theoretical background of the broadcast channel (BC) [15], NOMA still holds great promise as a future multi-user transmission technique, referred to as NGMA. Besides, emerging methods like rate-splitting multiple access (RSMA) have presented themselves as new potential candidates for NGMA. RSMA utilizes successive interference cancellation (SIC) to decode a portion of the interference and treats the remaining interference as noise. Thus, RSMA is in between space division multiple access (SDMA), which treats interference as noise, and NOMA, which decodes the interference of the users with weaker channels and removes it from the received signal.

With a specific focus on NOMA and RSMA, this article delves into current and future modulation and coding schemes for NGMA. Modulation and coding techniques play a critical role in achieving the ultimate goal of digital communication, which is transmitting a maximum number of bits reliably, i.e., with a small bit error rate (BER). Moreover, the emphasis here is on finite-alphabet and asynchronous NOMA, representing a crucial step in evaluating NOMA's gains in more practical settings and advancing research toward the integration of NOMA into wireless standards.

A. Motivation and Objectives

Modulation techniques, like quadrature amplitude modulation (QAM), are employed to increase the bit rate (spectral efficiency) while resulting in an acceptable BER. Current modulation techniques are, however, designed several decades ago with point-to-point communication in mind [16]–[19]. They have predefined, inflexible symbols and their constellation shaping is oblivious to interference, whereas modern communication systems are limited by interference more than by any other single effect [20]. Interference appears in these networks in different forms such as inter-user interference (IUI), inter-cell interference (ICI), and inter-symbol interference (ISI). These all distort the received constellations in one way or another and thus reduce the reliability of communications by increasing the BER. The typical practical solution is then to sacrifice the spectral efficiency and limit the number of users by allocating orthogonalized resources to each user or by using low-rate and high-energy constellations.

The described interference scenarios share a common issue: they can displace a constellation symbol from its predefined decoding region (boundary), leading to decoding errors and, consequently, symbol and bit errors. This challenge arises because current modulation techniques, such as QAM, were originally designed for point-to-point systems without interference. These modulation techniques feature predefined constellation symbols and their shape is insensitive to interference. The rigidity of these constellations poses a significant hurdle to improving the BER and spectral efficiency in today's interference-limited communication systems. Therefore, there is a need for innovative interference-aware modulation techniques to meet key performance indicators in future wireless

communication networks, including spectral efficiency, the number of supported devices, and high reliability.

A key goal of this paper is to present NGMA modulation and coding methods that reduce decoding BERs and increase the number of users and their throughput for a given number of resource blocks in the presence of inter-user and inter-cell interference. Minimizing BER and increasing spectral efficiency are linked together [21, Fig. 1] and are traditionally optimized by designing modulation and coding schemes. We present a comprehensive survey of modulation schemes, both with and without coding, for both OMA and NOMA scenarios. In the context of NOMA, the survey critically evaluates the implications of superimposed signals on symbol overlapping and BER. Then, we propose using deep autoencoders for end-to-end (E2E) NOMA. Deep learning-based E2E communication is a novel concept with significant potential. As a concrete example, this approach outperforms the MIMO precoder in terms of BER with/without the channel's knowledge [22]–[25].

In line with the fundamental objective of digital communication, which revolves around the reliable transmission of a maximal number of bits, our focus in this work is on exploring various avenues that pave the way for reliable and feasible non-orthogonal transmission. Instead of integrating NOMA with emerging and existing communication technologies, our work centers around understanding the essential steps required to transform non-orthogonal transmission, specifically NOMA, from a theoretical research topic into a practical and feasible technology. Toward this goal, our discussion encompasses practical considerations, including asynchronous transmission, SIC-free decoding, trellis-coded NOMA, interference-aware constellation design, end-to-end communications, and numerous other aspects detailed in the following section.

B. Contributions and Insights

This paper comprehensively explores existing and emerging solutions related to synchronous and asynchronous NOMA, code-domain NOMA, trellis-coded NOMA, uniform, non-uniform, and interference-aware constellation design, bit-interleaved coded modulation, SIC-free decoding, and end-to-end deep learning-based NOMA. Additionally, the paper provides a state-of-the-art overview of RSMA and discusses open problems and future directions in NGMA. Particularly, we contribute to

- Exploring the utilization of asynchronous transmission to tackle synchronization challenges inherent in multi-user and distributed systems, such as those found in uplink and downlink NOMA.
- Reviewing the structure of transmitters and receivers in code-domain NOMA and categorizing various code-domain NOMA schemes accordingly.
- Investigating the effectiveness of non-uniform modulation, trellis-coded NOMA, and bit-interleaved coded modulation with iterative decoding to approach the capacity region of downlink NOMA.¹

¹Unless otherwise stated, downlink NOMA refers to the Gaussian broadcast channel.

- Debunking misconceptions surrounding power allocation in NOMA, which may have arisen from assumptions tied to a specific type of modulation and decoding.
- Reviewing modulation and coding schemes utilized in 5G and discussing the road to reduce latency in 6G.
- Introducing the innovative concept of interference-aware constellation design and end-to-end NOMA and demonstrating its merit.
- Conducting a review of uplink and downlink RSMA and exploring its interconnections with NOMA.
- Highlighting research directions and open problems related to the above topics, with a specific emphasis on advancing NOMA as a feasible and practical technique.

In light of the above contributions, we gain diverse insights that propel NOMA from a theoretical concept towards a practical technology. We hope that these insights, as listed below, may trigger advancements to pave the way for NOMA's inclusion in wireless standards in the near future.

- 1) Contrary to conventional wisdom, which states that asynchronous transmission results in increased overall interference and performance degradation due to extra ISI, we show that asynchronous transmission decreases the overall interference. This unexpected outcome occurs because the reduction in IUI outweighs the impact of the added ISI.
- 2) We demonstrate that drawing general conclusions about NOMA power allocation solely based on a specific type of modulation and decoding may lead to misconceptions.
- 3) Interference-aware constellation design is a practical approach to realize non-overlapping super-constellations in NOMA. Attaining this objective becomes challenging, if not impossible, when utilizing established constellations like QAM for NOMA users.
- 4) For MIMO-NOMA systems, the joint design of constellations and precoding for all MIMO sub-channels holds great potential.

C. Structure

Figure 1 illustrates the organization of the paper, providing an overview of the topics covered in each section.

In Section II, we discuss different techniques under the umbrella of NOMA. These could be primarily categorized into power-domain NOMA (P-NOMA) and code-domain NOMA (C-NOMA) [5]. C-NOMA includes schemes like sparse code multiple access (SCMA) [26], pattern division multiple access (PDMA) [27], low-density signature/spreading (LDS) [28], and others. P-NOMA is explored in both uplink and downlink, along with asynchronous NOMA. The integration of both P-NOMA and C-NOMA into OFDM systems is also discussed.

In Section III, we explore the evolution of modulation techniques for both OMA and NOMA scenarios, to achieve a desirable BER versus signal-to-noise ratio (SNR) independent of channel coding or in conjunction with it. This section emphasizes that simply employing existing modulation schemes for NOMA users without modification can cause symbol overlapping and BER issues. We then discuss non-

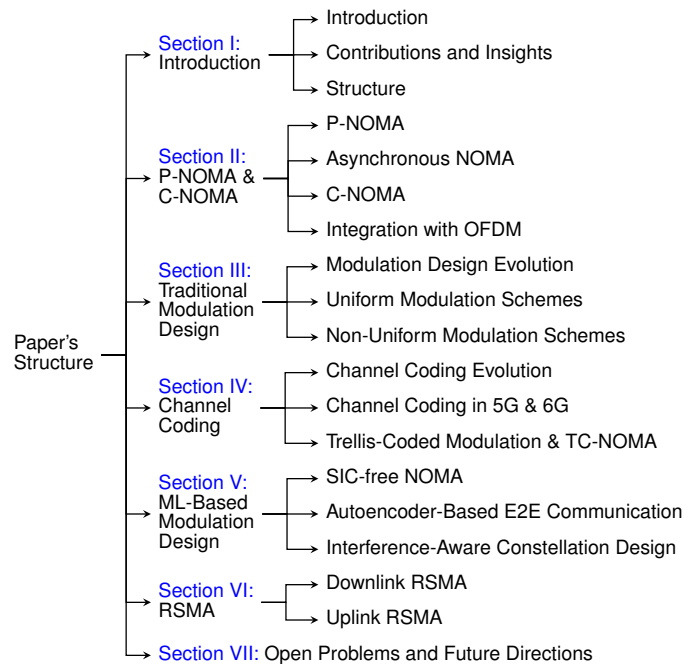


Fig. 1: Structure of the paper.

uniform constellations and their advantages, particularly with bit-interleaved coded modulation.

Section IV discusses the channel codes utilized in different generations of cellular networks, with a particular emphasis on modulation and coding schemes in 5G networks. We explore the evolution of channel coding techniques to meet the growing demands of ultra-reliable low-latency communications (URLLC). Additionally, we cover trellis-coded modulation for both OMA and NOMA scenarios, emphasizing the role of joint detection methods in enhancing performance.

Section V introduces interference-aware constellation design, incorporating SIC-free NOMA and autoencoder-based E2E communication. Autoencoders are utilized to create super-constellations with distinguishable symbols, transitioning from block-by-block to E2E communication. The section includes IUI-aware NOMA, ICI-resilient NOMA, and modulation strategies for MIMO-NOMA.

In Section VI, we review RSMA, discussing its origin and advantages in both downlink and uplink scenarios. Uplink RSMA achieves the capacity region of the Gaussian multiple access channel (MAC) without time sharing, while downlink RSMA is advantageous with imperfect CSI at the transmitter. We briefly explore the use of RSMA in connection with different technologies, including integrated communication and sensing, reconfigurable intelligent surfaces, and UAVs.

Section VII highlights research areas for NGMA, addressing non-uniform modulation in NOMA with bit-interleaved coded modulation. Challenges in E2E NOMA and MIMO-NOMA modulation are discussed. Limited feedback and CSI present open problems, including robust MIMO-NOMA system design with estimated and quantized CSI.

D. Related Works

Numerous survey papers have appeared on NOMA and

TABLE I: List of Key Abbreviations.

Acronym	Description
3GPP	3rd Generation Partnership Project
AE	Autoencoder
AI	Artificial intelligence
A-NOMA	Asynchronous NOMA
AWGN	Additive white Gaussian noise
BC	Broadcast channel
BER	Bit error rate
BICM	Bit-interleaved coded modulation
CDMA	Code division multiple access
C-NOMA	Code-domain NOMA
CSI	Channel state information
CSIT	Channel state information at the transmitter
E2E	End-to-end
ICI	Inter-cell interference
IDMA	Interleave division multiple access
IGMA	Interleave-grid multiple access
IoT	Internet of things
ISAC	Integrated sensing and communications
ISI	Inter-symbol interference
IUI	Inter-user interference
LDS	Low-density signature/spreading
LPMA	Lattice partition multiple access
LTE	Long Term Evolution
MAC	Multiple access channel
MCS	Modulation and coding scheme
MIMO	Multiple-input multiple-output
ML	Machine learning
NGMA	Next generation multiple access
NOMA	Non-orthogonal multiple access
NR	New Radio
OFDM	Orthogonal frequency division multiplexing
OMA	Orthogonal multiple access
PDMA	Pattern division multiple access
P-NOMA	Power-domain NOMA
PSK	Phase-shift keying
QAM	Quadrature amplitude modulation
QPSK	Quadrature phase-shift keying
RB	Resource block
RIS	Reconfigurable intelligent surface
RSMA	Rate-splitting multiple access
SCMA	Sparse code multiple access
SDMA	Space division multiple access
SER	Symbol error rate
SIC	Successive interference cancellation
SISO	Single-input single-output
SNR	Signal-to-noise ratio
SVD	Singular value decomposition
TCM	Trellis-coded modulation
TC-NOMA	Trellis-coded NOMA
UAV	Uncrewed aerial vehicle
URLLC	Ultra-reliable low-latency communications

RSMA in recent years. For example, see [7]–[9] for NOMA and [29] for RSMA. However, many of these survey papers are not directly related to this paper as their focus is not on modulation, finite-alphabet NOMA, or RSMA. The most related works are [30]–[32].

II. P-NOMA & C-NOMA

4G cellular networks have been architected around orthogonal radio resource allocation techniques not allowing for overlapping resource allocation. For instance, a *resource block (RB)* in Long Term Evolution (LTE), which spans 180kHz, cannot be shared among multiple users; it must be exclusively assigned to one user. This resource allocation approach has two limitations in the context of massive IoT:

- With the rapid growth of massive IoT devices, there would not be enough spectrum to allocate a dedicated RB to each device.²
- Massive IoT users typically do not exhaust an entire RB, rendering such resource allocation inefficient.

Due to the above challenges, the communication system design has recently undergone a transformation, shifting from an orthogonal resource allocation to a non-orthogonal one [5]. This paradigm shift encompasses various aspects including waveform design, multiple access, and random access [5]. Particularly, NOMA has attracted significant attention as a promising multiple access technique.

It should be highlighted that the proposed NOMA techniques for the uplink and downlink are distinct, rooted in the inherent differences between communication requirements for each direction. The downlink predominantly serves human-centric communications, characterized by larger packets and higher data rates. Conversely, the uplink involves an extensive array of uncoordinated devices transmitting small packets at low data rates. Consequently, addressing the demands of massive, low-rate IoT devices in the uplink mandates a unique set of techniques compared to P-NOMA which is good for the downlink channels.

It is worth noting that, P-NOMA has been studied by the 3rd Generation Partnership Project (3GPP) for LTE in TR 36.859, Release 13 [35]. It has also been studied for New Radio (NR) in TR 38.812, Release 16 [36]. Also, there are several P-NOMA-related survey papers worth mentioning, including [32], [37]–[39]. These works cover various topics including

²Interestingly, the concept of allocating more than one user to one RB has already been successfully implemented in 2G under the name of voice services over adaptive multi-user channels on one slot (VAMOS) which is used to increase the capacity of voice services by allowing multiple users to share the same time slot. In the simplest case, it is known as the adaptive QPSK (AQPSK) modulation scheme. It enables scheduling two users on in-phase (I) and quadrature-phase (Q) channels, thus doubling the number of users served by a single radio resource [33], [34]. Additionally, allocation of different power levels for each user is possible [33], [34].

With the above definition of NOMA, which involves using one RB for multiple users' signals, VAMOS is a NOMA scheme. There is, however, a subtle difference. The constellation symbols of users try to be orthogonal (one is mapped to the I channel and the other to the Q channel). In other words, half of the constellation points are for the first user and the other half are for the second user. However, in the NOMA modulation schemes considered in [35] and this paper, by receiving every symbol, we can reconstruct information for both users. Therefore, the two schemes are different in terms of transmission rates.

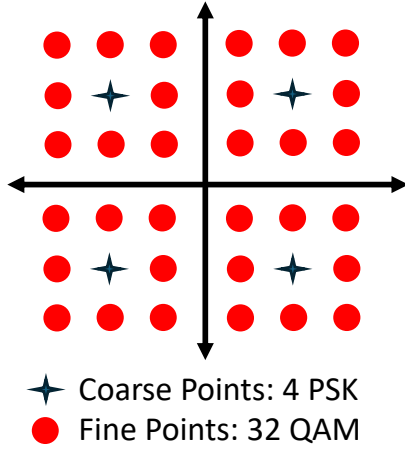


Fig. 2: An example of superposition coding. The constellation for the user with weaker channel is 4-PSK while the constellation for the user with stronger channel is 8-QAM. The overall superposed constellation is called 32-QAM.

grant-free NOMA, resource management mechanisms, and others.

A. P-NOMA

To increase the efficiency of wireless networks, the concurrent transmission of different users is unavoidable. Such a concurrent transmission in a wireless multi-user network results in interference among different signals. Therefore, one of the most distinctive features of multi-user wireless networks is the interference phenomenon. As a result, dealing with interference is very important when shifting from the single-user paradigm to a multi-user paradigm. To deal with interference, currently, communication standards rely on assigning separate time, frequency, and code resources to different users such that each user utilizes only one such a given resource in an orthogonal multiple access framework. This is a huge waste of resources and to curtail it cellular networks utilize frequency reuse in cells that are far from each other. Nevertheless, in each cell, and at each time, frequency, and code, only one user is served using a resource that is orthogonal to other resources. Therefore, the main source of interference will be the leak from users of adjacent resources due to the imperfection of the filters or the inter-cell interference due to the frequency reuse. However, NOMA relies on assigning more than one user to each resource, for example by employing superposition coding at the transmitter and SIC at the receiver. In fact, superposition coding is not new and has been used in achieving the capacity of the degraded BC [15] as well as the single-antenna Gaussian BC which is always degraded. In addition, combined with an appropriate transmitter, SIC at the receiver is capable of approaching the boundaries of the capacity region of both the degraded BC and MAC [40].

To study the main principles behind P-NOMA, let us take a downlink P-NOMA system as an example. It consists of one base station (BS) and K users. Let us assume the transmit power of User k 's signal is P_k and $\sum_{k=1}^K P_k = P$, where P

is the total transmit power of the BS. The transmitted signal s is defined as

$$s = \sum_{k=1}^K \sqrt{P_k} s_k, \quad (1)$$

where s_k is the transmitted symbol for User k . Let us denote the channel coefficient between the BS and User k by h_k . Then, the received signal at User k is given by

$$y_k = h_k \sum_{l=1}^K \sqrt{P_l} s_l + \eta_k, \quad (2)$$

where η_k is the additive Gaussian noise, $\eta_k \sim \mathcal{CN}(0, \sigma_k^2)$. For simplicity of the notation, we assume the same noise power for all users, i.e., $\sigma_k^2 = \sigma^2$. Obviously, different users generate interference for each other and their decoders should manage the interference. P-NOMA manages the interference by decoding the signal of users with weaker channels and canceling it from the received signal. As such, in P-NOMA, it is important to know the relative strength of the users' channels to understand which signals can be decoded for interference cancellation. The main principle behind P-NOMA decoding is that stronger channels, i.e., channels with larger channel magnitudes $|h_k|$, will have larger capacities. Therefore, they can support higher rates. As a result, they can successfully decode the symbols of the weaker users with lower rates.

Without loss of generality, let us assume that $|h_1|^2 \geq |h_2|^2 \geq \dots \geq |h_K|^2$, i.e., a lower index represents a stronger user. For any $k < K$, the capacity of User k is higher than that of User l , for $l = k+1, \dots, K$. Therefore, using SIC, User k can decode the signal for Users $k+1, \dots, K$ and remove their interference before decoding its own signal. Under the assumption of perfect SIC, the throughput of User k for a case with K users can be calculated by

$$R_k = \log \left(1 + \frac{P_k |h_k|^2}{|h_k|^2 \sum_{l=1}^{k-1} P_l + \sigma^2} \right), \quad k = 1, \dots, K. \quad (3)$$

It is clear from (2) and (3) that the throughput values depend heavily on the power allocation and the channels. The co-channel interference makes the resource allocation problem in P-NOMA a non-convex optimization problem. The power allocation for a two-user P-NOMA system is studied in [41]. Power allocation for multiple users sharing one channel, i.e., multi-user NOMA, is investigated in [42]–[44]. The solution to the power minimization problem can be obtained using the uplink-downlink duality. In general, *resource management* is an important aspect of the transmitter design in different NOMA scenarios. In addition, user grouping is essential for balancing spectral efficiency, fairness, and system throughput. While having a single group is ideal in theory [5], practical limitations like the complexity of SIC necessitate multiple groups [45]. As group size increases, the SIC complexity rises. Typically, users are grouped by channel quality, pairing those with strong conditions with those having weaker conditions to enhance performance.

While the above analysis is based on capacity formulas, i.e., error-free decoding, similar principles can be applied to a practical modulation scheme that can cause errors. In what

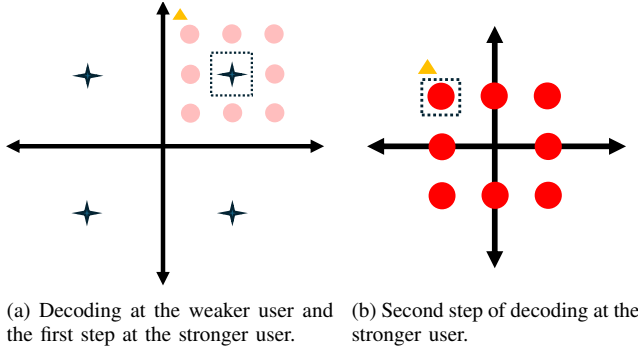


Fig. 3: An example of SIC decoding.

follows, we present an example of superposition coding and SIC decoding for traditional modulation schemes.

Example: An example of superposition coding using 4-phase-shift keying (PSK) and 8-QAM constellations for two users is shown in Fig. 2. In this example, the input bits of the user with weaker channel, i.e., smaller $|h_k|$, are modulated with a 4-PSK modulation as shown by the coarse points in Fig. 2. The input bits for the user with stronger channel are modulated with an 8-QAM modulation. As described in (1), the transmitted symbol is the weighted sum of the two modulated symbols. In this example, we consider equal power allocation that results in a 32-QAM constellation shown by the fine points in Fig. 2.

Figure 3 shows the SIC technique for decoding the superposed signal of the two users in Fig. 2 at the receiver. As shown in Fig. 3a, the receiver of the weaker user only decodes the coarse points by mapping the received signal to the nearest point in the corresponding PSK constellation. Practically, this means that the weaker user is considering the symbol of the stronger user as noise. The stronger user is also able to decode the coarse points since its channel is stronger than that of the weak user. Therefore, the stronger user decodes the symbol of the weaker user, using the same approach, and subtracts the effects of the decoded coarse symbol from the received signal. This will cancel the weaker user's interference from the stronger user's received signal. The remaining signal is decoded using the corresponding constellation (8-QAM) as shown in Fig. 3b. The modulation constellations in this example are chosen to make the example visually more appealing. However, the example works for any choice of constellations. A more practical example may choose a 4-QAM constellation for the stronger user, instead of 8-QAM, that results in an overall 16-QAM modulation.

B. Asynchronous NOMA

Traditional modulation and coding schemes assume perfect symbol synchronization. The performance of many existing modulation and coding schemes will severely degrade without symbol-level synchronization. Because of the distributed nature of multi-user networks and the effects of multipath and propagation delays, signals from different users experience different time delays to the receiver [46]. Perfect synchronization requires feedback and coordination, which complicates the system greatly. Having multiple antennas at

the receiver makes the matter more complicated. For example, assuming a multiple antenna receiver in uplink NOMA, one can synchronize the received signal perfectly at one of the receive antennas but other antennas may experience imperfect timing synchronization among received signals. Even if such a complete synchronization is possible, it is not clear if it is desirable. The possible advantages along with the difficulties in achieving perfect synchronization motivate a thorough analysis and design of NOMA systems under imperfect timing synchronization. In fact, symbol-level asynchrony has been advantageous in managing interference in some communication systems as discussed in [46]–[48]. Similar principles can be applied to NOMA to design asynchronous NOMA (A-NOMA) [49]–[52]. In this section, we discuss the principles behind asynchronous NOMA for both uplink and downlink.

Uplink A-NOMA: Let us assume User k transmits $\sqrt{P_k}\mathbf{s}_k[n]$, where $\mathbf{s}_k[n]$ is the n th element of vector \mathbf{s}_k denoting the n th normalized transmitted symbol and P_k denotes the transmit power. Assuming the pulse-shaping filter $p(\cdot)$ and a frame length of N , the transmitted signal from User k will be $\sum_{n=1}^N \sqrt{P_k}\mathbf{s}_k[n]p(t - nT)$. Considering the relative time delay of τ_k for User k , i.e., a time delay of $\tau_k T$, and the corresponding channel h_k , the signal from User k arrives at the receiver as $\sum_{n=1}^N h_k \sqrt{P_k}\mathbf{s}_k[n]p(t - nT - \tau_k T)$. Then, the received signal at the BS is given by

$$y(t) = \sum_{n=1}^N \sum_{k=1}^K h_k \sqrt{P_k}\mathbf{s}_k[n]p(t - nT - \tau_k T) + \eta(t), \quad (4)$$

where $\eta(t)$ denotes the additive white Gaussian noise (AWGN) with a power spectral density of σ^2 . Unlike the case with perfect synchronization, in addition to IUI, the received signal includes ISI as well. The set of sufficient statistics is found by proper filtering at the receiver, i.e., a matched filter with the impulse response $p(t)$, and over-sampling K times, each time synched with one of the users [46]. In other words, the receiver samples at $t_n = nT + \tau_k T$ to generate K sets of samples, $k = 1, \dots, K$, at each discrete-time $n = 1, \dots, N$. Figure 5 illustrates one possible structure of the decoder including oversampling. As shown in the figure, the sampling rate is still $f_s = 1/T$, i.e., the same as that of the synchronous case, but there are K parallel branches of sampling.

When sampled synched with User k 's signal, the relative delay of User l 's signal is $\tau_{kl} = \tau_l - \tau_k$. The resulting samples can be collected in an $N \times 1$ vector \mathbf{y}_k as

$$\mathbf{y}_k = \sum_{l=1}^K h_l \sqrt{P_l} \mathbf{R}_{kl} \mathbf{s}_l + \boldsymbol{\eta}_k, \quad (5)$$

where the (n, m) th element of the $N \times N$ Toeplitz matrix \mathbf{R}_{kl} is

$$[\mathbf{R}_{kl}]_{n,m} = g(\tau_{kl}T + (m - n)T), \quad m, n = 1, \dots, N, \quad (6)$$

in which $g(t) = p(t) * p(t)$, where $*$ denotes the convolution, and the noise vector $\boldsymbol{\eta}_k$ has the co-variance matrix $\mathbb{E}[\boldsymbol{\eta}_k \boldsymbol{\eta}_k^H] = \sigma^2 \mathbf{R}_{kl}$. Using a square-root Nyquist pulse, $p(t)$, like the practically common root raised cosine (RRC) pulse shape, $\mathbf{R}_{kk} = \mathbf{I}_N$ and $\mathbf{R}_{kl}^T = \mathbf{R}_{lk}$. An example of the received

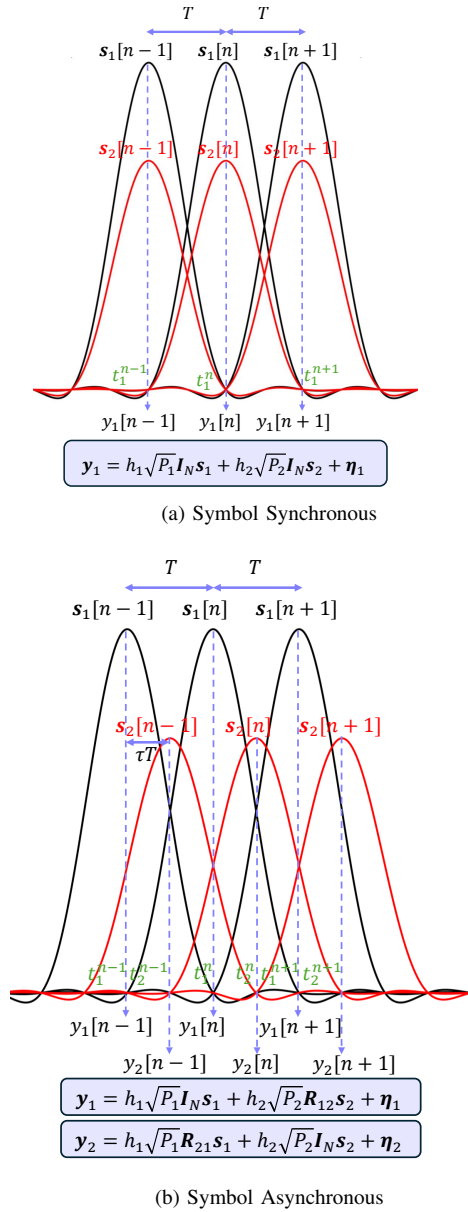


Fig. 4: Sufficient statistics for synchronous and asynchronous NOMA. In asynchronous NOMA, the output of the matched filter is sampled twice, each time synched with one of the users.

signals and the corresponding sufficient statistics for two users is shown in Fig. 4. To collect sufficient statistics in A-NOMA, the receiver should perform oversampling, compared with synchronous NOMA. For the example of two users in Fig. 4, the number of samples in A-NOMA is twice that of the synchronous NOMA. Note that for the case with perfect synchronization, when all delays τ_k are the same, we have $\mathbf{R}_{kl} = \mathbf{I}_N$, i.e., there is no ISI. Therefore, the perfect synchronization results in the conventional uplink P-NOMA system model of

$$\mathbf{y} = \sum_{l=1}^K h_l \sqrt{P_l} \mathbf{s}_l + \boldsymbol{\eta}, \quad (7)$$

where compared to (5), the index k is dropped as all resulting

K equations are identical.

As shown in (7), in a perfectly synchronized NOMA system, at each time instant, only the IUI, from the same time-instant, degrades the performance. Therefore, SIC can provide the optimal performance. However, in A-NOMA, not only IUI but also ISI degrades the performance. Therefore, new challenges arise with asynchronous transmission.

The conventional wisdom suggests that because of the additional ISI, asynchronous transmission increases the overall interference and the overall performance is degraded. However, surprisingly, asynchronous transmission in fact decreases the overall interference, as the reduction in IUI outweighs the addition of ISI [51]. On the other hand, because of the ISI, the conventional SIC is not optimal anymore and the design of efficient sequence detection methods is required [52]. More specifically, to remove the stronger users' signals, all the symbols in a frame need to be decoded which adds delay and complexity to the system. In addition, because of the timing asynchrony, sufficient statistics results in over-sampling and the corresponding sampling diversity [46] that improves the overall performance.

To manage the above issues, one can collect the K vector equations (5) in a matrix format. The resulting input-output matrix equation can be represented as a virtual MIMO system

$$\mathbf{y} = \mathbf{R}\mathbf{H}\mathbf{s} + \boldsymbol{\eta}, \quad (8)$$

where \mathbf{y} , \mathbf{R} , \mathbf{H} , \mathbf{s} and $\boldsymbol{\eta}$ represent the set of samples, the timing offsets matrix, the effective channel matrix, the transmitted symbols (including the assigned power), and the noise vector, respectively. The formulation of the problem with a virtual MIMO system enables the use of various interference mitigation methods and decoder designs developed in the literature for MIMO systems [53].

To quantify the effects of asynchronous transmission, let us focus on a two-user uplink P-NOMA system. Figure 4 shows the received signals of such a system. It can be modeled as an asynchronous MAC with a typical rate-region shown in Fig. 6. As proved in [52] and depicted in Fig. 6, not only does A-NOMA outperform synchronous NOMA, but also SIC is not optimal for A-NOMA. There are several conclusions proved in [52] and shown in Fig. 6:

- Intentionally creating a $\tau = 0.5$ symbol timing mismatch between the two signals with double time oversampling can enlarge the rate-region.
- While the maximum sum-rate using SIC for uplink NOMA is independent of the decoding order, the maximum sum-rate of A-NOMA depends on the decoding order. For example, in Fig. 6, the SIC pentagon rate-region vertices corresponding to the decoding orders $\{1, 2\}$ and $\{2, 1\}$ for A-NOMA provide sum-rates of 1.302 and 1.254, respectively. On the other hand, the corresponding vertices for NOMA provide the same sum-rate of 1.233.
- When perfect synchronization is lacking, SIC is not optimal anymore.

The above observations can guide the principles behind designing practical transceivers for asynchronous multiple access

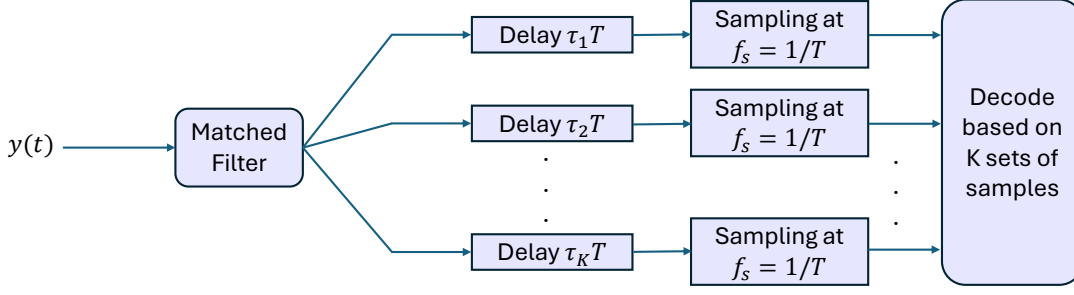


Fig. 5: Decoder structure for uplink A-NOMA. After matched filtering, the signal is sampled K times, each time synchronized with one of the K users, to generate sufficient statistics. Then, the resulting samples are used for decoding.

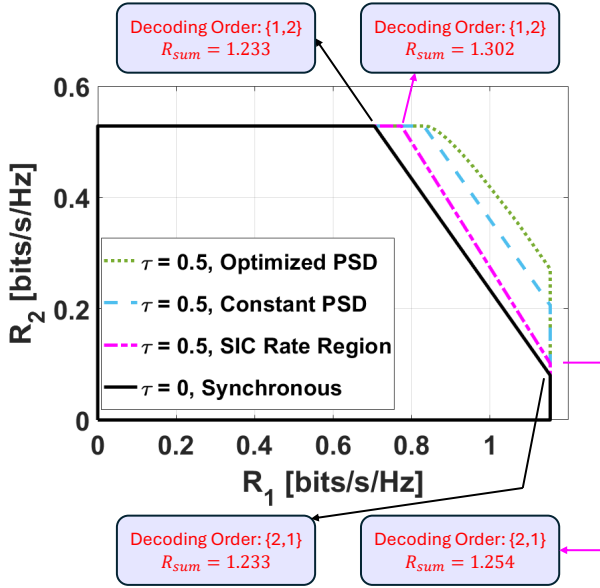


Fig. 6: Different rate-regions for $P_1 = P_2 = 10$ dBm, $|h_1|^2 = \sigma^2$, and $|h_2|^2 = 0.2\sigma^2$, using root raised cosine pulse shaping with $\beta = 0.5$. Different decoding orders in SIC result in different sum rates in asynchronous NOMA.

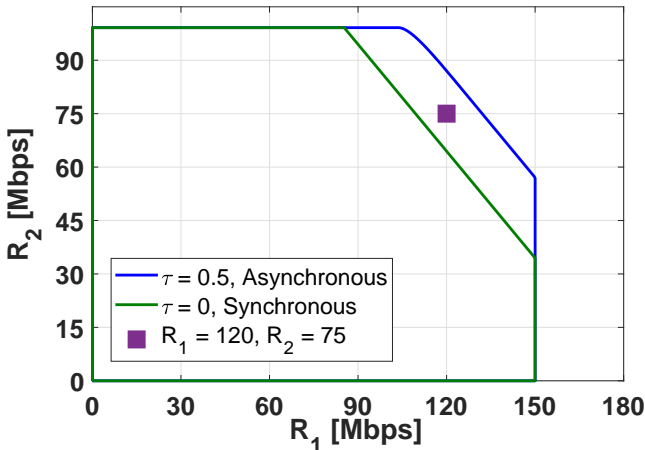


Fig. 7: An example of asynchronous NOMA operational point that is not achievable by synchronous NOMA.

systems. For example, a practical A-NOMA transceiver that creates an intentional $\tau = 0.5$ symbol asynchrony between the two users' signals has been designed in [52]. The operational point achieved by such an A-NOMA transceiver, shown in Fig. 7, is outside of the synchronous NOMA's capacity region and therefore is not achievable by any synchronous NOMA transceiver.

Downlink A-NOMA: In a downlink NOMA system, the superposition is performed at the transmitter and the transmitted signal is received by the intended users. Therefore, unlike uplink NOMA, the transmitter has full control of the time asynchrony and can intentionally add any desired set of time delays. In fact, adding intentional time delays at the transmitter is beneficial and can improve the performance [51]. Using the same notation developed for the uplink A-NOMA, the transmitted signal, including the added intentional time delays, can be written as

$$s(t) = \sum_{n=1}^N \sum_{k=1}^K \sqrt{P_k} s_k[n] p(t - nT - \tau_k T), \quad (9)$$

and the received signal by User k is

$$y_k(t) = h_k s(t) + \eta_k(t). \quad (10)$$

Similar to the case of uplink A-NOMA, the set of sufficient statistics includes over-sampling K times, each time synched with the signal of one of the users. After proper match filtering and over-sampling, the set of samples at the k th receiver can be represented in the following vector [54]

$$\mathbf{y}_k = h_k \sum_{l=1}^K \sqrt{P_l} \mathbf{R}_{kl} \mathbf{s}_l + \boldsymbol{\eta}_k. \quad (11)$$

Note that the perfect synchronization results in the conventional system model of $y_k[n] = h_k \sum_{l=1}^K \sqrt{P_l} s_l[n] + \eta_k[n]$. Using SIC, each user decodes all the signals from weaker users and removes them from the received signal. Then, it considers the remaining interference from the stronger users as noise and decodes its own symbols. This system is called asynchronous P-NOMA (AP-NOMA) in Fig. 8 and Fig. 9.

In downlink NOMA, the virtual MIMO system in (11) resembles a multiuser system. As such, apart from SIC, other techniques for multiuser communications can be applied as well. For example, since the transmitter has access to all signals, after superposition coding, it can perform precoding

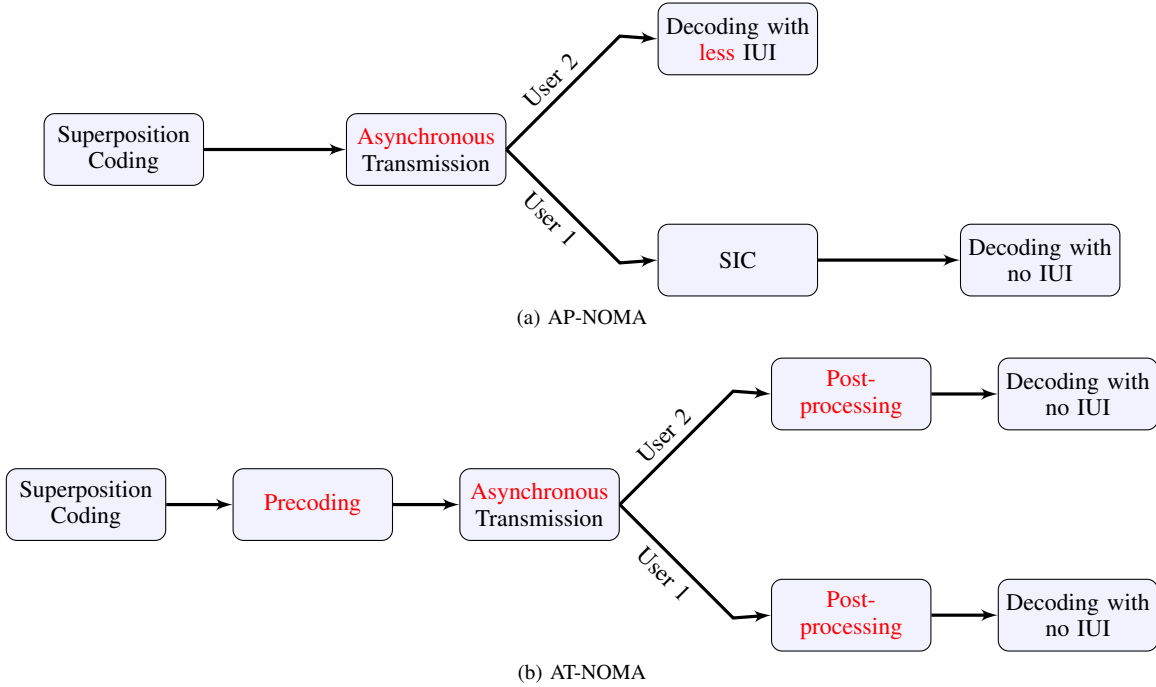


Fig. 8: Downlink asynchronous NOMA schemes. (a) AP-NOMA: The user with stronger channel decodes the signal of the other user and removes its interference. (b) AT-NOMA: The transmitter sends the signal toward the eigenvectors of the effective virtual MIMO system. The receiver uses post-processing, in the direction of the corresponding eigenvector, to recover its signal.

in the direction of matrix \mathbf{R} 's eigenvectors to further improve the performance. The decoder of such a system is named asynchronous time-domain NOMA (AT-NOMA). At User k , AT-NOMA uses post-processing, in the direction of the corresponding eigenvector, to recover its signal. Figure 8 shows the block diagram of such a system that does not include a SIC block for decoding [51]. The corresponding rate regions are shown for two users in Fig. 9. As shown in Fig. 9, AT-NOMA's rate-region is larger than that of AP-NOMA and both of them enlarge the achievable rate-region of P-NOMA.

In addition, for systems with M transmit antennas, transmit beamforming can be implemented as well. Considering an $M \times 1$ beamforming vector \mathbf{W}_k for User k , the asynchronous transmitted signal, including intentional time delays, is [54]

$$s(t) = \sum_{k=1}^K \mathbf{W}_k \sum_{n=1}^N s_k[n]p(t - nT - \tau_k T). \quad (12)$$

Then, the received signal at User k is

$$y_k(t) = \mathbf{h}_k^H \sum_{l=1}^K \mathbf{W}_l \sum_{n=1}^N s_l[n]p(t - nT - \tau_l T) + \eta_k(t), \quad (13)$$

where \mathbf{h}_k is User k 's channel. As before, the set of sufficient statistics after match filtering and over-sampling can be collected in the following vector [54]

$$\mathbf{y}_k = \sum_{l=1}^K \mathbf{R}_{kl} \mathbf{h}_k^H \mathbf{W}_l \mathbf{s}_l + \boldsymbol{\eta}_k. \quad (14)$$

The above input-output relationship is very similar to that of a MIMO system and the corresponding receiver designs from the MIMO literature can be used for decoding [53], [54].

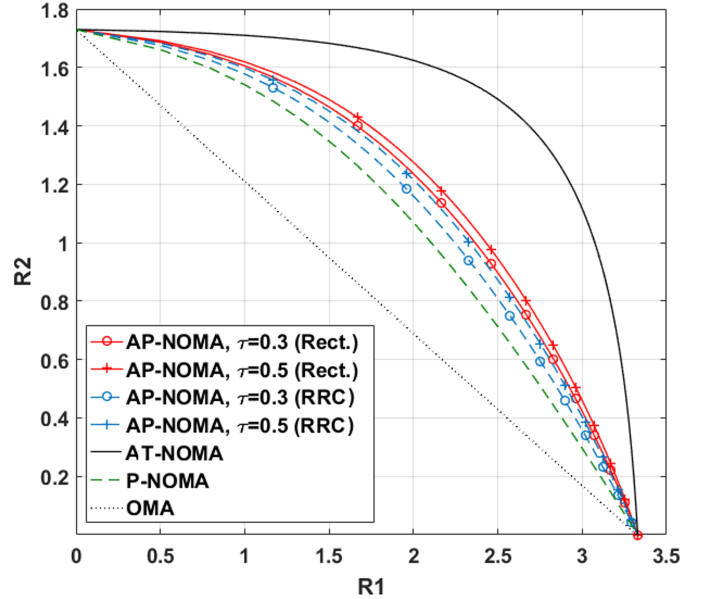


Fig. 9: Rate regions of different NOMA systems for $|h_1|^2 = 10\sigma^2$ and $|h_2|^2 = \sigma^2$.

C. C-NOMA

In the uplink, C-NOMA refers to a diverse range of non-orthogonal transmission techniques [5], [55], [56]. C-NOMA techniques revolve around the concept of allowing more than one user to share the same resource block, marking a distinct departure from OMA techniques. On the other hand, C-NOMA distinguishes itself from P-NOMA by requiring a signature, such as a spreading code, for the differentiation of users

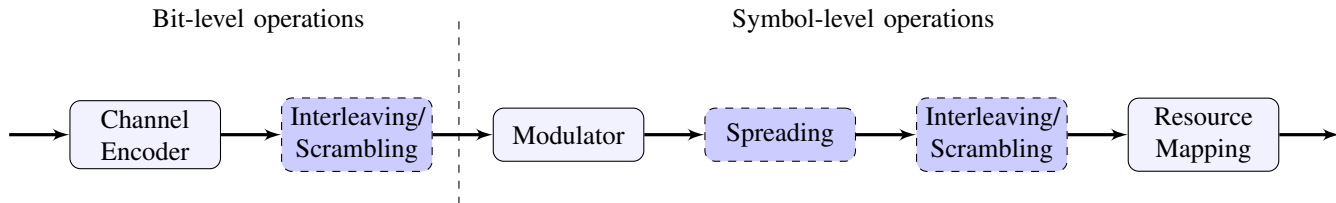


Fig. 10: The general structure of a C-NOMA transmitter. It includes essential components represented by solid blocks, which are necessary for any C-NOMA scheme. In addition, individual C-NOMA schemes may include one or more of the dashed blocks, depending on the specific requirements and characteristics of the scheme. Therefore, the presence of the dashed boxes depends on the type of C-NOMA scheme being implemented.

and the cancellation of inter-user interference. In contrast, P-NOMA achieves this through the variation in power allocation to each user. Given the predominant emphasis on uplink communication in IoT, C-NOMA emerges as a promising way to accommodate IoT users, especially those with limited resources such as simple sensors.

The range of C-NOMA techniques is extensive. A major category within C-NOMA schemes is notably influenced by code division multiple access (CDMA). CDMA is a multiple access technique where data symbols are spread over a set of user-specific, mutually-orthogonal codes. An adaptation of CDMA is LDS-CDMA, where spreading codes exhibit low density, meaning only a small fraction of code elements are non-zero [57]. Resource *overloading* is the common theme of many non-orthogonal access methods which allows the number of supportable users to be more than the number of available resources, i.e., K users share N resources in a non-orthogonal fashion ($K > N$). With this, each scheme needs a multiple access *signature* to differentiate users and cancel inter-user interference.

We next explore the transmitter and receiver structures and classification of C-NOMA techniques.

1) *Transmitter Structure*: A simplified, generic structure of a C-NOMA transmitter is depicted in Fig. 10 [55], [56], [58]. Different NOMA schemes apply their signatures in one or more of the dashed blocks in Fig. 10. For example, the LDS-CDMA signature is a short spreading sequence applied in the ‘spreading’ block followed by a unique interleaver for each user, resulting in a sparse signature matrix. Thus, LDS-CDMA is a symbol-based C-NOMA applying both spreading and interleaving after modulation. Sparse resource element (RE) mapping has emerged as a category of multiple access signatures within several C-NOMA schemes, such as SCMA, PDMA, and interleave-grid multiple access (IGMA). In these schemes, the intentional transmission of zeros occurs in specific REs to make resource mapping sparse. An illustration of such a sparse resource mapping is provided in the matrix below:

	UE1	UE2	UE3	UE4	UE5	UE6	UE7	UE8	UE9
RE1	0	1	0	0	1	0	1	0	0
RE2	1	0	0	0	0	1	0	1	0
RE3	0	1	0	1	0	0	0	0	1
RE4	0	0	1	0	1	0	1	0	0
RE5	1	0	0	1	0	0	0	0	1
RE6	0	0	1	0	0	1	0	1	0

According to the above resource allocation matrix, a total of

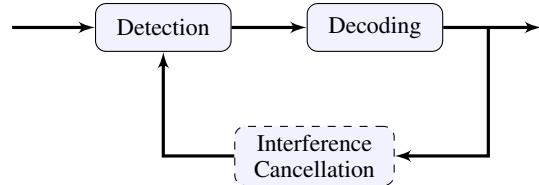


Fig. 11: A high-level structure of a C-NOMA receiver.

9 user equipments (UEs) are mapped to 6 resource elements. Each UE is assigned access to two REs, and each IGMA is accessed by three different UEs. For instance, RE1 accommodates UE2, UE5, and UE7 while UE4 utilizes RE3 and RE5. Further, it is noteworthy that UE-specific signatures exhibit, at most, a one-position overlap, because a pair of columns do not overlap in more than one position.

2) *Receiver Structure*: The fundamental components of a high-level C-NOMA receiver consist of three key building blocks: a detector, a channel decoder, and interference cancellation [55], as depicted in Fig. 11. In the following, we briefly elaborate on the functionality of each block.

The detection block, more precisely, the multi-user detection block, addresses challenges arising from multiple users sharing the same channel. It could employ various techniques [55], including adaptive filtering and optimization algorithms like minimum mean squared error (MMSE) [59], matched filter, maximum a posteriori [60], and message passing algorithm [61], to separate signals from different users.

While the detection block handles scenarios where multiple users transmit simultaneously, and is commonly used in multiple access systems, the *decoding block* serves as a fundamental process in communication systems. Its applicability extends to both single-user and multi-user environments, encompassing error correction and the reconstruction of the original message or data. The decoding block ensures the accurate recovery of information from received signals.

Interference cancellation block may or may not exist. As an example, to decode a UE’s data packet, only MMSE detection and channel decoding could be executed. Nonetheless, interference cancellation is commonly used. This cancellation process can occur successively, in parallel, or through a hybrid approach. MMSE-SIC is a well-known scheme in this context where interference cancellation is performed successively. This technique is commonly utilized in symbol-level spreading schemes, where interference cancellation can take either a ‘hard’ or ‘soft’ form. In the hard interference cancellation

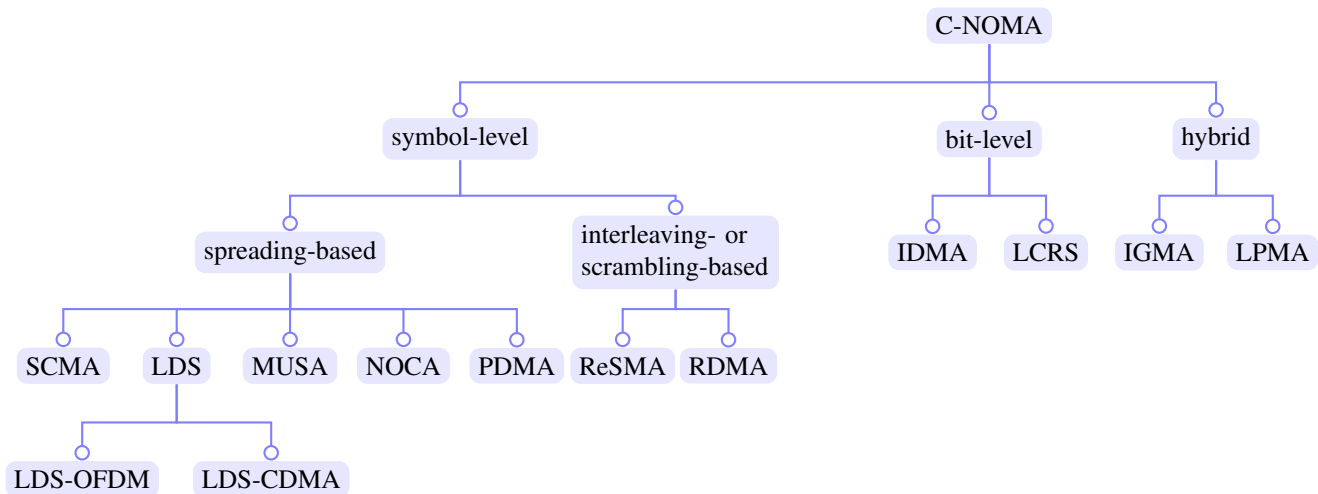


Fig. 12: Various C-NOMA schemes proposed in 3GPP 5G radio access network meetings. C-NOMA techniques encompass operations such as interleaving, scrambling, and spreading, which can be executed at the symbol-level, bit-level, or a combination of both.

approach, interference is subtracted once a user's signal is successfully decoded. On the other hand, in the soft interference cancellation method, the output of the decoder includes soft information. This soft information is then used to reconstruct symbols, involving the consideration and processing of probabilistic or continuous-valued information, rather than relying on discrete, hard decisions.

3) *Categories*: C-NOMA schemes can be classified in different ways. As can be seen in Fig. 12, C-NOMA related operations can be done in the *bit-level* (before modulator), *symbol-level* (after modulator), and *hybrid*. For this reason, as also shown in Fig. 10, C-NOMA schemes may be categorized as follows:

- *Symbol-level spreading-based*: Most NOMA schemes fall into this category where a spreading sequence serves as a signature to distinguish users. Earlier, we discussed examples of such signatures in the context of a resource allocation matrix. Notable instances of this category include SCMA [62] proposed by Huawei, non-orthogonal coded access (NOCA) [63] proposed by Nokia, multi-user shared access (MUSA) [64] proposed by ZTE, PDMA [65] suggested by CATT, and LDS-CDMA, as well as LDS-OFDM [57], [66].
- *Symbol-level interleaving/scrambling-based*: In this category, a symbol-level interleaver/scrambler is used to distinguish the users. Resource spread multiple access (ReSMA) [67] and repetition division multiple access (RDMA) [68] are examples of this category.
- *Bit-level interleaving/scrambling-based*: This category involves bit-level operations, specifically utilizing an interleaver or a scrambler at the bit-level to distinguish users [69]. A bit-level scrambler is advantageous in terms of lower processing delay and memory requirements compared to a bit-level interleaver [36]. Examples of this category include interleave division multiple access (IDMA) [69] suggested by InterDigital and low-code-rate spreading (LCRS) [70] proposed by Intel. Release 15 NR

already supports a bit-level scrambler for randomization, which can be leveraged for C-NOMA as well.

- *Hybrid*: Certain NOMA schemes may combine multiple methods. For instance, IGMA [60], proposed by Samsung, incorporates both bit-level interleaving and sparse mapping in its design. Lattice partition multiple access (LPMA) is another example in this category [71].

C-NOMA schemes can be categorized differently, as illustrated in Fig. 13. In this representation, the classification is based on the utilization of scrambling/interleaving and spreading operations. Thus, methods that use spreading are in one group, while methods that use interleaving—whether at the bit or symbol level—are in another group.

4) *Prominent Schemes*: Here, we explore several prominent C-NOMA schemes in more details.

- *LDS-CDMA*: This C-NOMA scheme represents a non-orthogonal variant of CDMA. While in CDMA, data symbols are spread over user-specific, mutually-orthogonal codes, LDS-CDMA deviates from this norm by utilizing non-orthogonal codes. LDS underscores that spreading codes exhibit low density, i.e., only a small fraction of code elements are non-zero [57]. This low-density feature allows for the utilization of near-optimal message passing algorithms with practical complexity. However, despite its moderate detection complexity, LDS-CDMA may encounter performance degradation for constellation sizes larger than quadrature phase-shift keying (QPSK).
- *SCMA*: As one of the most renowned C-NOMA schemes, SCMA uses a multi-dimensional codebook where incoming data bits are directly mapped to codewords selected from a layer-specific codebook [72]. Each codeword represents a spread transmission layer. In contrast to LDS-CDMA (and CDMA), where spreading and bit-to-symbol mapping are conducted separately, SCMA integrates these two steps by directly mapping incoming bits to a spread codeword within the SCMA codebook sets. Similar to LDS, the sparsity of codewords in SCMA

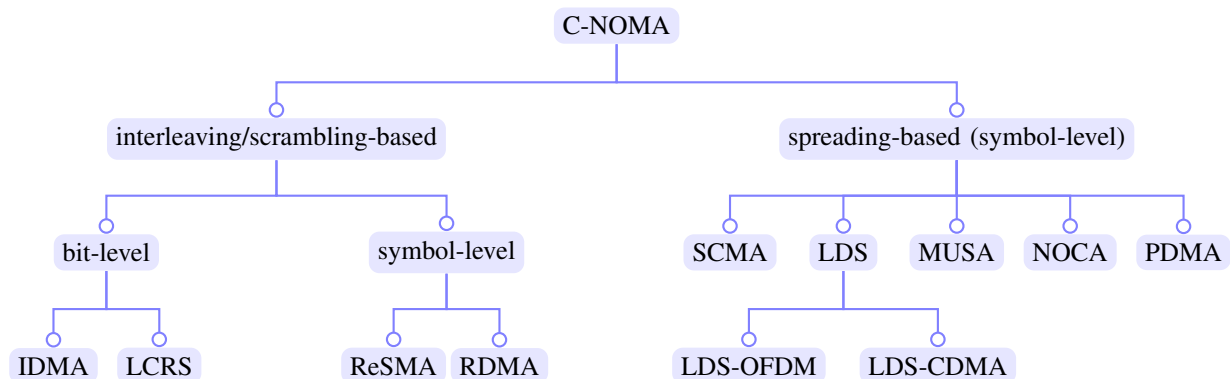


Fig. 13: C-NOMA schemes classified based on scrambling/interleaving and spreading operations.

allows for the implementation of low-complexity reception techniques [73]. SCMA also leverages additional degrees of freedom in the design of multi-dimensional constellations, outperforming LDS [72]. Importantly, the sparser SCMA codewords can tolerate more overloading, facilitating massive IoT connectivity in the uplink. However, it is worth noting that a sparser code results in lower coding gain.

While SCMA can be used for the downlink as well [62], [74], [75], the decoding complexity remains high for low-cost devices, limiting SCMA's ability to efficiently support massive IoT connectivity in the downlink [75].

5) *SDMA*: SDMA is a technique used to exploit the spatial dimension for improving system capacity and performance. Multi-user transmit beamforming or SDMA allows simultaneous communication with different users by directing radio frequency signals towards specific users. In SDMA, multiple users are served simultaneously on the same frequency channel but are separated spatially using MIMO techniques. A careful design of beamforming vectors, utilizing antenna arrays, results in minimizing the average transmit power while maintaining a desired quality of service for each user [76]. Each user has a distinct spatial signature, which is leveraged to create separate beams or spatial channels. By employing beamforming techniques, the base station can direct the signal energy to specific users, thereby reducing inter-user interference and enhancing signal quality. SDMA systems are usually designed to beam directly towards a user while reducing the interference experienced by other users. For example, SDMA uses linear precoding to separate users in the spatial domain and any interference from the other users will be treated as noise. Suppose \mathbf{H} represents the channel matrix between the base station with M antennas and K users, where $\mathbf{H} \in \mathbb{C}^{K \times M}$. The received signal \mathbf{y} can be expressed as

$$\mathbf{y} = \mathbf{H}\mathbf{W}\mathbf{x} + \boldsymbol{\eta},$$

where \mathbf{W} is the beamforming matrix, \mathbf{x} is the transmitted signal vector, and $\boldsymbol{\eta}$ is the noise vector. The beamforming matrix \mathbf{W} is designed to maximize the SNR for each user while minimizing interference. Typically, the beamforming vector \mathbf{w}_k for User k is chosen to be the dominant eigenvector of the user's channel covariance matrix. This approach ensures

that the signal intended for User k is maximized at the user's location while minimizing the leakage to other users. In a broadcast channel, multi-user linear precoding is often useful when users experience similar channel strengths and the channels are semi-orthogonal or orthogonal. SDMA based on MU-LP is a well-established multiple access technique that builds up the core principle behind many spatial techniques in 4G and 5G such as multi-user MIMO CoMP, coordinated beamforming, network MIMO, millimeter-wave MIMO, and massive MIMO [77]. SDMA's effectiveness heavily depends on accurate CSI at the transmitter. With perfect CSI, the base station can precisely steer beams, achieving significant spatial multiplexing gains. However, in practical scenarios, obtaining perfect CSI is challenging due to factors like channel estimation errors, limited feedback, and feedback delays. To mitigate these issues, robust beamforming techniques and adaptive algorithms are employed, allowing the system to dynamically adjust to varying channel conditions and maintain high performance. Therefore, SDMA, represents a powerful method to enhance the capacity and efficiency of modern wireless communication systems, particularly in high-density user environments.

D. Integration with OFDM

NOMA schemes can be seamlessly integrated into OFDM-based systems to enhance spectral efficiency and support more users [78]–[80]. OFDM's fine-grained frequency division and ability to handle frequency-selective fading and multi-path interference make it a suitable platform for NOMA, as subcarriers can be dynamically allocated based on channel conditions. However, the complexity increases due to the need for SIC at the receiver. In what follows, we briefly explain how different NOMA schemes fit into the OFDM structure:

1) *PD-NOMA in OFDM*: In PD-NOMA, each OFDM subcarrier carries a superimposed signal from multiple users, instead of a symbol from an individual constellation [78]–[80]. This is achieved by using different power levels for each user.

2) *CD-NOMA in OFDM*: Instead of using power levels to differentiate users, CD-NOMA assigns specific code sequences to different users [81]–[83], allowing them to share the same OFDM subcarrier. At the receiver, the design of efficient multi-user detection schemes is crucial to separate and decode each user's signal based on the codes.

III. TRADITIONAL MODULATION DESIGN

This section investigates the design and evolution of modulation techniques for OMA communication and their extension to NOMA communication. Modulation design, or constellation design, deals with the ways symbols can be arranged in constellations, with a particular focus on achieving a desirable BER. This process can be approached independently of channel coding or in conjunction with it. We will discuss both approaches in this section.

A. Modulation Design Evolution

Consider a complex-input, complex-output point-to-point AWGN channel. The channel input s and output y are complex random variables related by

$$y = s + \eta, \quad (15)$$

where η is a complex random variable whose real and imaginary parts are independently and identically distributed (*i.i.d.*) Gaussian random variables. The capacity of this channel is given by the well-known Shannon formula $C = \log(1 + \text{SNR})$ where SNR denotes the signal power over the noise power and C is the capacity measured in nats per channel use.

The proof for achieving the capacity of this channel utilizes a random codeword formed with *i.i.d.* Gaussian components. However, employing a Gaussian codeword in practice is impractical, as the decoding would require an exhaustive search throughout all codewords in the codebook to determine the most probable candidate. This has resulted in the adoption of signaling constellations, or digital modulation techniques, such as PSK and QAM, comprised of a finite number of points in the complex plane. Extensive literature exists on the problem of choosing a set of M symbols with in-phase and quadrature components for transmission. Foschini *et al.* were among the first researchers who studied the signal constellation design that minimizes the probability of error on the AWGN channel under an *average power constraint* [16]. Other notable contributions to constellation design can be found in works such as [17]–[19], [84].

A constellation with M symbols can carry a maximum of $\log_2 M$ information bits per symbol. The average power of a constellation is defined by the mean of the squares of all symbol amplitudes, i.e., $\mathbb{E}\{|s|^2\}$. Consequently, constellations with larger M must position their points in closer proximity to each other [84]. As such, distinct constellations exhibit different BER versus SNR performance for the same channel. The primary objective of constellation design is to identify configurations with the smallest BER. Another highly relevant parameter in this context is the symbol error rate (SER).

Constellation design for modulation schemes has a long, rich history. Initial works primarily concentrated on developing constellations that demonstrated both spectral and power efficiency independent of channel coding [84], [85]. While the pursuit of spectral and power-efficient modulation schemes remains as relevant today as it was then, there has been notable improvement and evolution. The notion of treating coding and modulation as a unified entity [86], called coded modulation, led to the development of *trellis-coded modulation (TCM)*

[87]–[89] and bit-interleaved coded modulation (BICM) [90]–[93] as two prominent examples. Due to its efficiency, BICM is now a standard in various modern communication systems, including WiMax and 4G/5G cellular networks.

B. Uniform Modulation Schemes

1) *OMA*: By adopting OMA as the multiple access scheme, modulation techniques originally designed for point-to-point communication can be used without necessitating major modifications. These modulation methods, such as PSK and QAM, are designed to enhance spectral efficiency (bit per symbol) while maintaining an acceptable BER for a specified power constraint [16]–[19]. Various ways that symbols can be arranged in constellations, with a particular focus on achieving a desirable BER, in the absence of channel coding are discussed in [84]. The paper also studies capacity of those constellations on the AWGN channel assuming optimum coding.

2) *NOMA*: Non-orthogonal transmission is known to be optimal for Gaussian BC [40], [94], [95], which is also referred to as NOMA in this paper. We consider the two-user NOMA for illustration. Assume s_1 and s_2 are the signals for User 1 and User 2 and h_1 and h_2 are their corresponding complex channel gains, respectively. The BS broadcasts superimposed signal $\sqrt{\alpha P}s_1 + \sqrt{\bar{\alpha} P}s_2$, where P is the BS power and α , $0 \leq \alpha \leq 1$, and $\bar{\alpha} \triangleq 1 - \alpha$ are the fractions of total power allocated to the signals of User 1 and User 2, respectively. This is a special case of (1), with $K = 2$ users where $P_1 = \alpha P$ and $P_2 = \bar{\alpha} P$. The received signal at User k , $k \in \{1, 2\}$, is given by

$$y_k = h_k(\sqrt{\alpha P}s_1 + \sqrt{\bar{\alpha} P}s_2) + \eta_k, \quad (16)$$

where η_k is the complex noise at User k . For decoding, assuming $|h_1| \geq |h_2|$, User 1 (the user with a stronger channel gain) first decodes the other user's message and then uses SIC to decode its message free of interference, whereas User 2 (which has a weaker channel gain) treats the signal of the stronger user as noise.

Similar to OMA, achieving the capacity region of NOMA involves the use of random Gaussian codewords, whose decoding is impractical as it requires an exhaustive search over the entire codebook to identify the most probable candidate. In practice, s_1 and s_2 are chosen from a discrete and finite-alphabet set like QPSK modulation. This simplification comes with its costs. For example, for certain values of power allocation coefficient α , the constellations of the two users may overlap. In such cases, the mapping is non-bijective and decoding (SIC or maximum-likelihood decoding) with zero error may not be possible. Figure 14 represents the noiseless superimposed signal when both users use a QPSK constellation. While for $\alpha = 0.2$, we can draw distinctive detection boundaries (bijective mapping), this is not possible for $\alpha = 0.5$. The issue stems from predefined constellations (in this case, QPSK) being individually designed for each user, rather than for the transmitted signal, which is a superposition of the signals from both users. Consequently, the overlap of the superimposed constellation has not been taken into account in the constellation design.

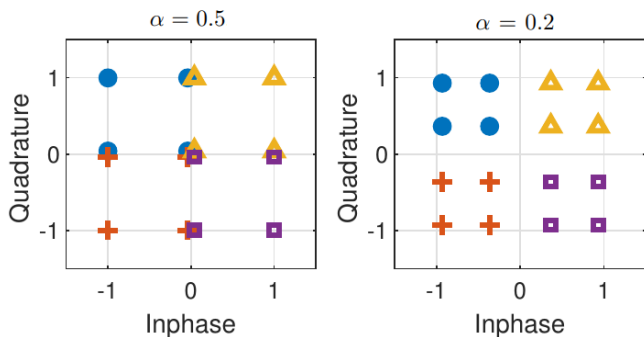


Fig. 14: Superimposed constellations for two different values of α where both NOMA users employ a QPSK constellation. It is observed that $\alpha = 0.5$ leads to a super-constellation with overlapping symbols, i.e., a non-bijective mapping. On the other hand, when $\alpha = 0.2$, a bijective mapping is achieved.

Existing literature extensively relies on the above adoption. Especially, BER and SER analysis for two-user NOMA over AWGN channel with regular constellations is studied by various researchers. To denote some, exact SER expressions for pulse amplitude modulation and QAM are derived in [96]. Analytical bit error probability expressions are derived in [97] when both users employ a QPSK constellation and [98] for QAM. Similarly, BER expressions for binary phase-shift keying (BPSK) modulation are studied in [99]. SER and BER in NOMA with rotated constellations are studied in [100]. BER of NOMA with BPSK and QPSK modulations over fading channels was studied in [101]. A list of papers evaluating NOMA can be found in [31].

Despite their findings, these studies have also contributed to one of the most prevalent misconceptions in NOMA literature. This is the myth that a user with a smaller channel gain should receive higher power. Specifically, many papers have assumed that in a two-user NOMA, α should be smaller than 0.5, where α is the fraction of total power allocated to the user with a stronger channel. While this misconception has been debunked in [102] based on Gaussian inputs, this has also been shown to be incorrect even in the finite-alphabet case by several independent works [103]–[105].

The goal of the above approach is to prevent super-symbol overlapping when utilizing uniform constellations by adjusting the power allocation coefficient and decoding. However, it has long been known that even using uniform constellations that result in overlapping (non-bijective) or partially overlapping super-symbols, it is still possible to decode both NOMA users' information with carefully designed turbo channel coding and iterative decoding [106]. Specifically, when employing BICM with iterative decoding, non-bijective mapping may even outperform bijective ones, as elucidated in Myth 1 in [106] and other works [107]–[109].

Before proceeding to non-uniform constellation design, we would like to emphasize the above discussions in the following remarks.

Remark 1: Drawing general conclusions about NOMA power allocation solely based on a specific type of modulation and decoding is not appropriate and may lead to misconceptions. For instance, as discussed in [105], even within a given

modulation scheme like QAM, successive interference cancellation and maximum likelihood decoding suggest different acceptable values for the power allocation coefficient α .

Remark 2: By leveraging *bit-interleaved coded modulation* with iterative decoding, it is not necessary, or even favorable, to design non-overlapping super-symbols, as detailed in [106, Myth 1] and other references therein. This clarification indicates that there may not be a strict constraint on the power allocation coefficient in NOMA, even within the framework of finite-alphabet inputs. This fact is well-established theoretically and has been noted independently in [102, Myth 1].

So far, we have established that within the framework of finite-alphabet NOMA, it is not mandatory to allocate power in the reverse order of the users' channel gains, contrary to the common belief in many NOMA papers. Specifically, in a two-user NOMA scenario, $\alpha \leq 0.5$ is not a necessity. Such misconceptions arise from limiting assumptions, such as using uniform constellations with SIC decoding, without exploring other established techniques like BICM and maximum likelihood decoding.

With this clarification in mind, in the next subsection, we introduce a less-discussed topic in NOMA literature. Namely, we shift the focus from employing predefined, *uniform* constellation schemes for NOMA users to exploring the possibility of designing/employing *non-uniform* constellations for NOMA users. The goal of designing non-uniform constellations for NOMA users is to ensure that the resulting super-constellation provides a bijective mapping from the beginning.

C. Non-Uniform Modulation

The constellations discussed in the previous subsection exhibit regular shapes. In such a design, the emphasis is almost exclusively on constructing large set of symbols in 2D space with the objective of maximizing the minimum Euclidean distance between them.³ For example, the conventional uniform QAM employs signal points on a regular orthogonal grid. In contrast, *non-uniform constellations*, by relaxing this constraint, provide an added shaping gain that facilitates reception, even under lower SNRs [109], [117], [118]. Non-uniform constellations have found recent applications in digital broadcasting systems.

1) *OMA:* Much of the work in non-uniform constellation is related to point-to-point channels trying to improve the performance at lower SNRs [109], [117], [118]. Non-uniform constellation has been particularly important in the context of video broadcasting and is included in standards like digital video broadcasting terrestrial (DVB-T) and advanced television systems committee (ATSC). The utilization of non-uniform constellations in MIMO channels, along with two signal processing algorithms for MIMO precoding, can be found in [119]. Using a different approach, guessing random additive noise decoding is recently used to design non-uniform

³It is worth noting that the concept of 2D modulation can be extended to multi-dimensional modulation in various ways [110]–[114]. In MIMO systems, spatial modulation utilizes both the antenna index and complex symbols to form a 3D constellation for efficient information transmission [111]. Other forms of multi-dimensional modulation are explored in [112]–[116].

constellations based on channel statistics [120]. This approach is code-agnostic, focusing on identifying the impact of noise on the data.

2) *NOMA*: As highlighted in Remark 2, non-uniform constellations combined with BICM hold potential advantages in NOMA. While it has been noted that superposition of individual uniform constellations generally leads to non-uniform constellations [100], [101], [121]–[123], there has not been an explicit exploration of this opportunity in the existing literature of NOMA. The related topic of *hierarchical modulation*, which involves constellations with non-uniformly spaced signal points, holds a more prominent presence [124]–[126]. Constellation rotation [127]–[129] is another related topic in this area. In fact, the idea of rotating constellations goes back to the design of $\pi/4$ -QPSK for differential coherent detection in [130]. To avoid higher dimensional constellation points collapsing on top of each other and losing diversity, the idea of constellation rotation has been used extensively in the space-time coding literature [131]–[133]. Although the hierarchical modulation and constellation rotation methods may help overcoming rate losses observed in NOMA implementation [14], the design and implementation of non-uniform constellations with BICM could be transformative.

It should be noted that BICM improves error performance of uncoded modulation but presents implementation challenges, especially in low-resource IoT devices. The increased receiver complexity, including de-interleaving and soft-decision decoding, along with higher computational demands and power consumption—particularly when using iterative decoding methods like turbo codes—are significant hurdles. These processes also introduce processing delays and potential latency, crucial considerations in real-time communication systems.

Despite these hurdles, BICM implementation in IoT devices is achievable with a focus on efficient algorithms, hardware support, and complexity-performance trade-off. Optimized algorithms for interleaving and decoding, energy-efficient error-correcting codes tailored for low-power operation, and hardware accelerators for key functions can effectively mitigate these challenges. For example, narrowband IoT demonstrates a practical application of BICM for low-resource devices, employing simplified modulation and coding strategies to enhance reliability while efficiently managing complexity [134], [135]. We will discuss such possible avenues in Section VII-A.

IV. CHANNEL CODING

Channel coding, also referred to as forward error correction, is an indispensable component of today’s wireless communications. These coding techniques introduce redundancy into transmitted data using error correction and error detection codes. The redundancy enables receivers to detect and correct errors that may occur during transmission, thereby enhancing the robustness of communication systems and approaching the capacity limits of wireless channels [89]. It improves cellular network performance metrics such as reliability, throughput, coverage, spectral efficiency, and energy efficiency [136]. In addition, channel coding ensures reliable data transmission by detecting and correcting errors caused by noise and interference, reducing the need for re-transmission and as a

result improving the throughput and latency. It also extends coverage by enhancing data transmission over longer distances and under challenging radio conditions.

A. Channel Coding Evolution from 2G to 5G

Channel coding has evolved significantly since its inception. In early digital communications, simple error detection methods like parity checks were used, while Hamming codes were among the first error-correcting codes applied in computer systems and data protocols. With the advent of more sophisticated coding schemes like Bose-Chaudhuri-Hocquenghem (BCH) and Reed-Solomon codes [137] in the 1960s and convolutional codes [138] in the 1970s, error correction capabilities improved substantially. The development of turbo codes [139] and low-density parity-check (LDPC) codes [140], [141] in the 1990s represented a significant advancement, achieving performance close to the theoretical limits derived by Shannon. Polar codes [142], introduced in 2009, further advanced the field by offering provably capacity-achieving performance with low-complexity encoding and decoding algorithms.

Channel coding has been integral to digital communication in cellular networks since the emergence of 2G technology. With each generation of cellular technology, channel coding has advanced and evolved to meet the increasing demands for reliability and efficiency in data transmission. In addition, different channel coding techniques have been adopted for *control channels* and *data/traffic channels* because of their distinct requirements. Specifically, channel coding for control channels emphasizes robust error detection and correction to ensure reliable transmission of critical signaling information with minimal latency, while coding for data/traffic channels prioritizes maximizing throughput and spectral efficiency.

The tree diagram in Fig. 15 illustrates the channel codes employed in each generation of cellular systems for both control and traffic channels. A more detailed explanations follows.

- **2G**: Convolutional codes were introduced to enhance the reliability of control signaling, improve the quality of digital voice, and support text messaging.
- **3G**: More advanced coding techniques like turbo codes were introduced for data channels, providing better error correction capabilities and supporting higher data rates for mobile internet access. Despite the above change, 3G systems use convolutional codes for control channels.
- **4G**: Turbo codes with enhancements like hybrid automatic repeat request (HARQ) and flexible rate matching were used. By combining error correction coding with re-transmissions, 4G LTE improves data reliability and efficiency. Further, coding schemes in 4G are more adaptable to varying channel conditions and user requirements, allowing for better utilization of available bandwidth and more efficient data transmission.
- **5G**: LDPC codes and polar codes are used for data channels and control channels, respectively, offering enhanced performance for a wide range of applications, including IoT, autonomous driving, and URLLC communications. LDPC codes were adopted for data channels due to

their superior performance in error correction and lower decoding complexity at high data rates.

B. Channel Coding and Modulation in 5G & 6G

Here, we first present some details of the channel coding and modulation techniques used in 5G systems. We then discuss possible road maps for the channel coding in 6G.

1) *Channel Coding and Modulation in 5G*: In wireless systems, a *physical channel* refers to the actual medium via which data is transmitted between the network and the UE. In total, there are six physical channels in 5G NR, as described below:

- Physical downlink control channel (PDCCH): Transmits downlink control information.
- Physical uplink control channel (PUCCH): Carries uplink control information.
- Physical broadcast channel (PBCH): Handles UE synchronization and broadcasts essential system information.
- Physical random access channel (PRACH): Ensures initial network access and resource allocation.
- Physical downlink shared channel (PDSCH): Transports downlink data payloads.
- Physical uplink shared channel (PUSCH): Transmits uplink data payloads.

Two of these channels, PDCCH and PUCCH, carry most of the control information in the downlink and uplink, respectively. PBCH and PRACH are responsible for tasks such as UE synchronization initial access to the network. As their names suggest, PBCH and PRACH are downlink and uplink channels, respectively. Actual information payloads, including text messages, audio/video call data, and web streams, are transmitted over shared channels PDSCH and PUSCH, for downlink and uplink, respectively.

TABLE II: Channel Coding and Modulation in 5G Physical Channels

	Channel	Coding	Modulation	Adaptive
Downlink	PBCH	Polar	QPSK	✗
	PDCCH	Polar	QPSK	✗
	PDSCH	LDPC	M -QAM*	✓
Uplink	PRACH	—	—	✗
	PUCCH	Polar	BPSK, QPSK	✗
	PUSCH	LDPC	M -QAM*	✓

* $M \in \{4, 16, 64, 256, 1024\}$

Table II summarizes the channel coding and modulation used in each channel. PRACH does not employ channel coding or modulation; instead, it utilizes Zadoff-Chu sequences for tasks such as initial access synchronization, random access, uplink control information, and channel sounding [143]. The table also indicates whether adaptive coding and modulation is used in each channel. An index, called modulation and coding scheme (MCS) index, determines how data is encoded

and modulated before transmission and thus decides on the number of useful bits per symbol based on radio signal quality. A higher signal quality allows sending more data per symbol. MCS index selection depends on radio conditions and block error rate (BLER). This is determined by a quantity called *channel quality indicator* and is adjusted dynamically by the BS. 5G NR supports M -QAM modulation with $M \in \{4, 16, 64, 256, 1024\}$ for the PDSCH [144]. There are 32 MCS indices (0-31), with indices 29-31 reserved for re-transmissions. 3GPP Specification 38.214 [144] has provided four tables for PDSCH MCS indices. With M -QAM modulation and target coding rate R , the spectral efficiency of transmission is given by $r \log_2 M$. The highest spectral efficiency is achieved with 1024-QAM and a coding rate $r = \frac{948}{1024}$, resulting in 9.2578 bits per symbol. The lowest spectral efficiency is achieved with 4-QAM (QPSK) and a coding rate $r = \frac{30}{1024}$, resulting in 0.0586 bits per symbol.

It also worth noting that the NR LDPC coding process encompasses several stages [143] such as code block segmentation, cyclic redundancy check attachment, LDPC encoding, rate matching, and bit interleaving. These steps collectively ensure robust and efficient data transmission in 5G networks.

2) *Channel Coding Road to 6G*: As wireless systems evolve toward 6G, latency requirements become increasingly stringent. Particularly, URLLC is one of the main use cases of 5G and beyond, envisioned to bridge the digital and physical realms. This ensures that a given data packet will be delivered within a very short time frame, such as in the order of 1 ms, and with a very high reliability, e.g., 99.999% [1]. End-to-end delay consists of three components: 1) the access delay, 2) the computation delay, and 3) the transmission delay [145], [146]. These tasks involve transmitting essential data and performing computations on both ends, such as compressing data at one end and decompressing it at the other end as well as channel encoding and decoding. These elements form a latency budget that must meet strict real-time requirements.

This has led to the exploration of channel coding techniques with shorter block lengths and reduced complexity. Arkan [147] made significant progress in this direction by introducing polarization-adjusted convolutional codes and demonstrating that a convolutional pre-transformation can effectively enhance BLER for short codes with sequential decoding [148]. There has been several recent improvements including deep learning-based polar codes [149]. Polar codes are not the only family of codes being studied for low-delay communication. Various other channel codes, including LDPC, turbo, and convolutional codes, have been considered [150]. Other channel codes, such as analog fountain codes, analog BCH codes, and Raptor codes could also be considered toward this goal.

Finally, we should emphasize that channel codes are developed independently of whether multiple access techniques are orthogonal or non-orthogonal. Current research in the intersection of NOMA and channel coding predominantly focuses on evaluating NOMA performance using specific channel codes tailored for this purpose. Additionally, joint source-channel coding represents another approach for achieving low-latency communication, as explored in studies such as [151]–[153].

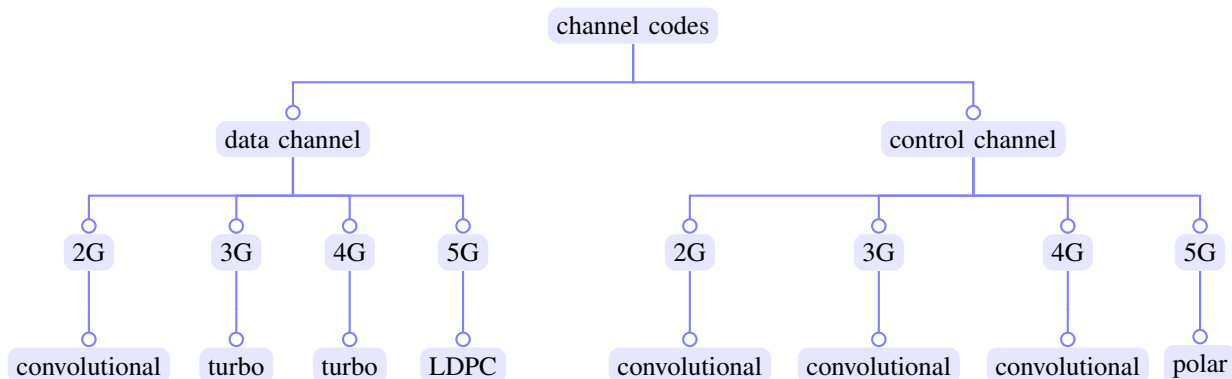


Fig. 15: Evolution of channel codes from 2G to 5G. Data and control channels typically apply different types of channel codes.

C. Trellis-Coded Modulations

1) *OMA*: The main idea behind TCM is to combine coding and modulation to increase the coding gain [154]. To achieve this, a given constellation is expanded and then partitioned into a hierarchy of subsets with increasing minimum Euclidean distances. For encoding, a trellis, representing a finite-state machine, decides which subset should be used to maximize the coding gain at each time slot. TCM's finite-state machine and underlying modulation can be represented using convolutional codes as well. The main design challenge is how to assign subsets to trellis paths to maximize the coding gain. A TCM codeword includes a sequence of transmitted symbols chosen through the finite-state machine and the corresponding set partitioning. The free distance between two possible codewords is defined as the squared Euclidean distance between the two coded sequences. Analogous to how the minimum Euclidean distance determines the performance of a modulation scheme, the minimum free distance specifies the performance of a TCM [154].

Figures 16 and 17 show an example of a 4-state TCM using the 8-PSK constellation. For maximum-likelihood decoding, the Viterbi algorithm is utilized to find the most likely valid path, a path starting at State 0 and merging to State 0, and the corresponding transmitted bits [154].

2) *NOMA*: In this section, we discuss trellis-coded multiple access (TCMA) [155] and trellis-coded NOMA (TC-NOMA) [156]. While the main principles work for any number of users, for the sake of brevity, we focus on a downlink system with two users. Also, while the choice of TCM for each user can be different, we utilize the TCM encoder in Fig. 17 for both users. The BS modulates the input bits using TCM to generate two sets of symbols, $a_1(n)$ and $a_2(n)$ for Users 1 and 2, respectively. To improve the performance, $a_2(n)$'s constellation can be rotated, for example by the optimal rotation $\frac{\pi}{8}$ [156]. In TCMA, the encoder superimposes the two outputs $a_1(n)$ and $a_2(n)$ by transmitting $a_1(n) + a_2(n)$. On the other hand, similar to P-NOMA, TC-NOMA superimposes the symbols of different users on different power levels and transmits $\sqrt{P_1}a_1(n) + \sqrt{P_2}a_2(n)$. Optimal power allocation can be done to maximize the resulting minimum free distance [87] and maintain a constraint on the total power, i.e., $P_1 + P_2 \leq P$

To recover the transmitted bits, the receiver can employ

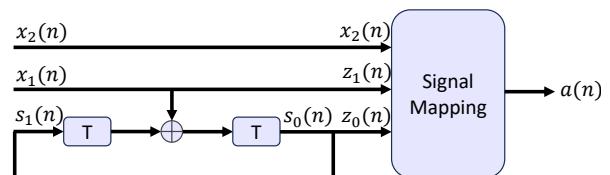


Fig. 16: Illustration of an 8-PSK 4-state TCM encoder. The coded bits go through a rate-1/2 convolutional code.

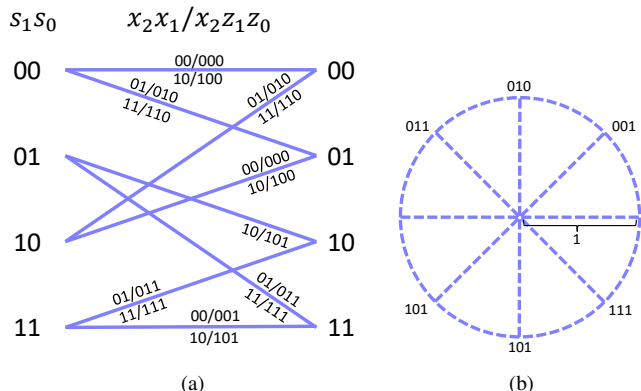


Fig. 17: Encoder and bit-mapping for an 8-PSK 4-state TCM. (a) Trellis representation of 8-PSK 4-state TCM, (b) The mapping of 8-PSK constellation.

SIC to separately decode the two bit streams, as discussed for P-NOMA before. In other words, the stronger user, User 1, decodes the symbols of the weaker user, User 2, and cancels the corresponding interference before decoding its own bits. The weaker user decodes its signal by assuming the symbols of the other user as noise.

In addition, joint detection using tensor product of trellises is also possible and greatly improves the performance [156]. First, we describe the underlying tensor product of trellises [157], [158] which is essential for the joint detection. Let us assume User 1 in TC-NOMA utilizes trellis T_1 with r_1 states $S_i^{(1)}$, $i = 1, \dots, r_1$. Similarly, T_2 , the trellis of User 2, contains r_2 states $S_j^{(2)}$, $j = 1, \dots, r_2$. Then, the tensor product $T_1 \otimes T_2$ is defined as a $(r_1 \times r_2)$ -state trellis with states $S_i^{(1)} S_j^{(2)}$, $i = 1, \dots, r_1, j = 1, \dots, r_2$. A state transition from $S_i^{(1)} S_j^{(2)}$ to $S_k^{(1)} S_l^{(2)}$ in $T_1 \otimes T_2$ exists if and only if transitions

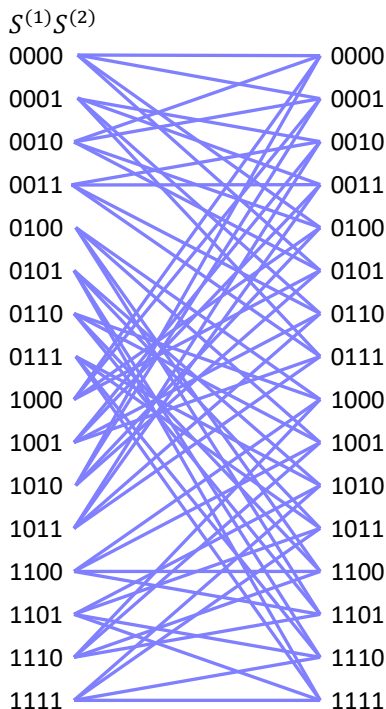


Fig. 18: The underlying 16-state trellis generated by the tensor product of two 4-state trellises.

from $S_i^{(1)}$ to $S_k^{(1)}$ and from $S_j^{(2)}$ to $S_l^{(2)}$ exist in T_1 and T_2 , respectively. A similar definition for the tensor product of more than two trellises works as well. Figure 18 shows the tensor product of the trellis in Fig. 17 by itself.

TC-NOMA is equivalent to a TCM using the trellis in Fig. 18 including transitions from $S_i^{(1)}S_j^{(2)}$ to $S_k^{(1)}S_l^{(2)}$ with the superimposed symbol $\sqrt{P_1}a_1 + \sqrt{P_2}a_2$. Therefore, the Viterbi algorithm can be applied to the equivalent TCM for joint detection. Overall performance of the TC-NOMA can be optimized by appropriate power allocation. Additional fairness criteria can be included as well [156]. Figure 19 depicts BER vs SNR of different NOMA systems using 8-PSK and the 4-state TCM encoder in Figs. 16 and 17 for $P_1 = 0.3$, $P_2 = 1$, $|h_1|^2 = 2$, and $|h_2|^2 = 1$. Joint detection of TC-NOMA symbols outperforms the uncoded NOMA and TCMA schemes.

V. MACHINE LEARNING-BASED MODULATION DESIGN

A common characteristic of modulation techniques, as discussed in Section III, is their initial design with point-to-point communication in mind. These techniques are characterized by predefined, inflexible symbols, and their constellation shaping is oblivious to interference. In contrast, one notable shift in today's communication systems, especially in cellular networks, is the move from point-to-point to multi-user communication with multiple transmitters. With this paradigm shift, additional challenges are presented because inter-user and inter-cell interference are becoming crucial factors in modern communication system design. Despite this evolution, constellations designed decades ago are still employed and interference is often addressed through orthogonal resources or by treating interference as noise.

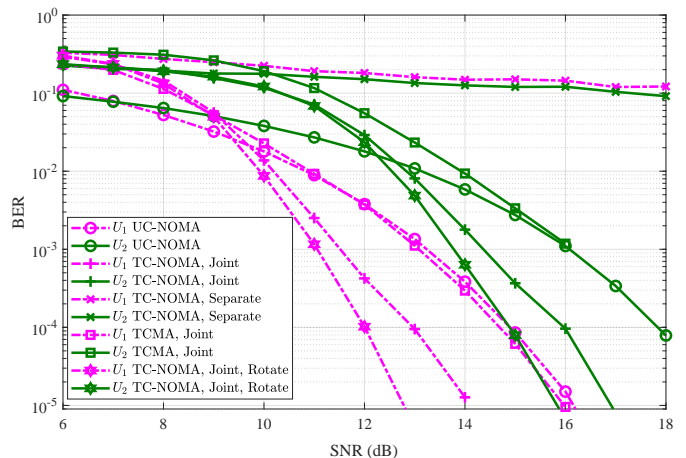


Fig. 19: BER vs SNR of TCMA, uncoded NOMA (UC-NOMA), and TC-NOMA for $P_1 = 0.3$, $P_2 = 1$, $|h_1|^2 = 2$, and $|h_2|^2 = 1$.

Machine learning, particularly its rapidly advancing subset, deep learning [159], is becoming a cornerstone of communication systems [160]. In general, integrating artificial intelligence (AI) into cellular networks has already been initiated with 5G Advanced, and AI is anticipated to play a pivotal role in shaping 6G networks [161]. Machine learning has found different applications across various settings in modulation-related challenges. For instance, machine learning techniques have been effectively applied in automatic modulation classification [162]–[165] and constellation design [166]–[170], among other applications.

In this section, we introduce a novel approach to constellation design for NOMA, termed *interference-aware* constellation design. We aim to design NOMA super-constellations that inherently account for inter-user interference, as opposed to relying on traditional interference-oblivious constellations and attempting to eliminate inter-user interference at the receiver. The objective is to achieve the most distinguishable superimposed symbols for any power allocation such that decoding can be completed without needing SIC. The main performance metric is BER but simplicity of the decoding is as critical.

Designing interference-aware super-constellations using traditional methods is very challenging because the constellation shape at the transmitters needs to be adjusted depending on the interfering signal. Otherwise, symbols of superimposed constellations may overlap, as shown in Fig. 14, which is not desired. AI-based approaches appear as an alternative. Our interference-aware constellation design is essentially an end-to-end autoencoder (AE)-based communication. This is because unlike noise, interference has a structure and autoencoders are useful in exploiting structures in data [171], [172]. In addition AE-based E2E communications simplifies block-by-block communication. Before delving into the details of the design, we will motivate it by explaining the significance of SIC-free decoding in NOMA and provide an introduction to AE-based E2E communication in the following two subsections.

A. SIC-Free NOMA

Superposition coding with successive interference cancellation (SC-SIC) is an optimal approach for achieving the capacity region of the downlink NOMA. In the proof, Gaussian inputs are employed as optimal codewords. Inspired by this theoretical result, SC-SIC is then applied to scenarios where inputs have finite-length and uses finite-alphabet modulations, such as QAM [12], [14], [96], [98]. However, as discussed earlier, it is important to note that such an application may not necessarily uphold the same theoretical assertions [103], [173]. At times, this discrepancy has contributed to misconceptions such as the belief that users with smaller channel gains should receive higher power allocations [96], [98], [174]. Although these misconceptions have been disproved in [102], the subtle distinctions between these theoretical premises and the practical finite-alphabet inputs are of significant importance [105]. We use the distinctions between the two premises—theoretical and finite-alphabet—to motivate SIC-free decoding in the following.

Particularly, while theoretically feasible to achieve successful decoding for both users at any $\alpha \in [0, 1]$ [102], the use of a finite-alphabet input, such as a QAM constellation, requires careful selection of the α value, as noted in Remark 1 in Section III-B. Thus, using SIC decoding with finite-alphabet inputs limits power allocation choices, and thereby the possibility of achieving the entire capacity region.

In scenarios involving finite-alphabet inputs, the research community has explored alternative approaches to bypass the need for SIC. Examples of these approaches are the utilization of lattice-based techniques [175], index modulations [104], and maximum-likelihood decoding [105]. These approaches may collectively be referred to as *SIC-free decoding*. They may offer several advantages such as outperforming SIC with finite-alphabet inputs and succeed in cases where SIC falls short. In our experimental work [14], we conclude that addressing constellation overlapping or finding a better way to implement or bypass SIC is necessary for advancing NOMA as a practical technology. The end-to-end NOMA introduced in this paper is an effective SIC-free NOMA, empowered by autoencoders.

B. Autoencoder-Based E2E Communication

1) *A Primer to Autoencoders*: An *AE* is a learning technique employed to discover a low-dimensional representation of the input data. In words, it creates a layer that has less features than the input layer. It first compresses (encodes) its input data into a lower dimension and then makes use of this lower dimensional representation to recreate (decode) the original data [176]. While autoencoders compress the input via unsupervised learning, autoencoders are used to improve system performance through a training process that tries to minimize the reconstruction error—the difference between the input and reconstructed data.

The loss function quantifies the difference between actual and predicted values. *Binary cross-entropy* is the most common loss function used in classification problems. It treats each element of the AE output as a zero/one classification task. For a training sample \mathbf{y} , the cross-entropy loss is expressed

as $\sum_{i=1}^n (y_i \log p_i + (1 - y_i) \log(1 - p_i))$, where y_i is the i -th element of the training sample \mathbf{y} , n is the length of the vector \mathbf{y} , and p_i is the predicted probability corresponding to y_i . The value of p_i is obtained by passing \hat{y}_i through a sigmoid activation function [159], where \hat{y}_i is the predicted value of y_i . To go from the loss for one training sample to the batch loss \mathcal{L} , the average over a batch of samples is calculated. Alternatively, one may use the *mean squared error* loss function, which calculates the squared differences between the actual and predicted values, i.e., $\sum_{i=1}^n (y_i - \hat{y}_i)^2$, where y_i and \hat{y}_i are respectively the actual and predicted values for the i -th training sample. Again, we average the above value over multiple training samples to get the batch loss \mathcal{L} .

2) *Related Works*: Utilizing autoencoders for end-to-end communication is a novel concept with significant potential for improving BERs. This approach provides a fresh alternative to the prevalent block-by-block design philosophy in contemporary communication systems [22]–[24], [171], [177]–[179]. As illustrated in Fig. 20, the concept is simple, mirroring the fundamental objective of digital communication, i.e., reliably transmitting a maximum number of bits.

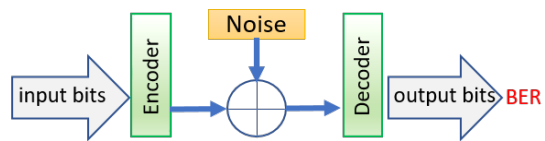


Fig. 20: A simplified diagram of the autoencoder-based point-to-point communication.

Notably, this approach outperforms state-of-the-art MIMO precoders in terms of BER both with and without the channel’s knowledge [22]–[25]. In [25], an end-to-end communication is designed for the point-to-point MIMO channel when the autoencoder learns from the CSI and the transmitted symbols to eliminate the interference at the receiver and estimate the transmitted symbols with small errors. The result is remarkable as the autoencoder system exceeds the performance of the well-known singular value decomposition (SVD)-based MIMO for practical SNRs. The gain is attributed to two factors: 1) AE optimizes the transmission based on finite-alphabet, finite-length inputs whereas SVD is designed for infinite-length Gaussian inputs, and 2) AE enjoys the freedom of non-uniform constellation shapes and is not limited to regular constellations.

C. Interference-Aware Constellation Design

Leveraging autoencoders is a promising approach for crafting a super-constellation with distinguishable symbols, regardless of power allocation coefficients among NOMA users. This contrasts with the traditional methods where each NOMA user is assigned a predefined constellation (e.g., QPSK), and the superposition of these constellations forms the super-constellation. As mentioned earlier, in the conventional approach, the effectiveness of NOMA may be limited due to potential symbol overlap in the super-constellation, depending on power allocation. In contrast, AE-based approach anticipates interference during the design phase, resulting in

constellations with a robust minimum distance, regardless of power allocation. Crucially, this enables SIC-free decoding, particularly vital for resource-limited devices.

1) *IUI-Aware NOMA*: Shifting from the traditional block-by-block approach to end-to-end communication allows for the simultaneous design and optimization of all components, encompassing constellation design. This innovative approach has the potential to substantially reduce BERs. While prior studies [22]–[25] establish a foundation for autoencoder-based end-to-end communication, they primarily concentrate on point-to-point transmissions.

Extending these findings to point-to-*multipoint* scenarios like NOMA poses challenges. The involvement of multiple receivers in NOMA immediately makes the problem more involved as each receiver is only interested in its own message and will have its own loss. Hence, in the training process, each receiver will only feed back the loss of its own message to the transmitter. The first difficulty here is that the transmitter needs to process the losses and adjust its transmission accordingly. The two NOMA users have conflicting interests as they both want to exploit the shared environment for their own benefits. Using autoencoders for communication over NOMA channels in different settings is studied in [177]–[179].

A conceptual architecture of the two-user NOMA network implemented autoencoder is depicted in Fig. 21. The encoder and decoders include batch normalization and fully-connected neural networks (FCNNs). The channel state information (h_1 and h_2) are given to the encoder but they are known only in the corresponding decoders. This end-to-end systems will be trained and tuned to minimize the difference between transmitted (s_k) and received symbols (\hat{s}_k), $k = 1, 2$. As a result, a super-constellation (containing the superposition of the desired and interfering symbols) will be formed. A well-designed and well-trained system will get separable super-constellation symbols.

AE designs typically consist of stacked FCNNs, which may not be suitable for structures resembling SIC. While constructing SIC-like AE structures is feasible, our specific design, as illustrated in Fig. 21, aims to achieve *SIC-free* decoding for NOMA. The key objective is to devise an AE structure capable of creating a super-constellation with distinguishable symbols for any given power allocation coefficient α .

Assume that both users want to transmit 2 bits/symbol, i.e., s_k has two bits each, as illustrated in Fig. 21. Then, unlike Fig. 14, where each user wants to make its own maximum separable 4-symbol constellation and superimpose them, the AE will be trained to build a maximum separable 16-symbol super-constellation. The primary focus is on the shape of the super-constellation rather than that of the individual constellations. An illustrative instance of such AE-generated constellations is presented in Fig. 22. It is noteworthy that these AE-generated constellations vary for each power allocation coefficient α , thereby introducing a dynamic and intelligent aspect to the system. Also, in contrast to traditional constellations such as a fixed 16-QAM constellation, which has inflexible and predefined shapes, the AE has the capability to generate an extensive array of constellations. This brings a new *shaping gain* and lowers BERs at both users, thereby optimizing

performance in diverse scenarios.

The performance of the AE-generated NOMA constellation is evaluated next. The AE-NOMA network is trained with $h_1 = 1$, $h_2 = 2$, $\text{SNR}_1 = 10\text{dB}$, and a loss weight of 10. The noise powers at both receivers are the same. The testing results are shown in Fig. 23. Not surprisingly, the E_b/N_0 requirement for this scenario is much higher than that of QPSK modulation transmitted over a point-to-point AWGN channel where the BER is given by $P_e = \frac{1}{2}\text{erfc}(\sqrt{E_b/N_0})$ [180]. However, comparing the BERs obtained in Fig. 23 with those obtained using QPSK constellations for a two-user NOMA channel, as seen in the literature such as in [181, Fig. 7], reveals that the AE-designed constellations demonstrate much lower BERs at the same E_b/N_0 . This improvement arises because the combination of two QPSK constellations can lead to overlapping symbols, which degrades the BER, as previously discussed. In contrast, our constellations are specifically designed to have distinct symbols, thereby reducing the likelihood of symbol overlap and improving BER performance.

We should also emphasize that, similar to traditional constellations, the learned modulations use a finite set of symbols during each transmission. The key difference is that the symbols may vary from one transmission to another depending on the channel gains. Such a change in constellation symbols poses a significant challenge for traditional decoders, as they need to be informed about the constellation's position each time. However, in the AE-NOMA, this process is handled internally, eliminating the need to inform the decoder about the transmitters' constellation. This is because the transmitter and receivers (Tx , $Rx1$, and $Rx2$ autoencoders in Fig. 21) are trained jointly and can handle those variations.

Numerous research questions revolve around the network's construction and training and the definition of the overall loss function. One possible loss function in Fig. 21 is $\mathcal{L} = w_1\mathcal{L}_1 + w_2\mathcal{L}_2$, where \mathcal{L}_1 and \mathcal{L}_2 are the losses at $Rx1$ and $Rx2$, respectively, and w_1 and w_2 are their weights [177]. In a previous work on a point-to-point channel [25], we trained the network for $\text{SNR}_1 = 10\text{dB}$ and tested it across various SNRs. Given the complexity of the current problem, training multiple AEs, each tailored for distinct SNR or α ranges, may be necessary. Since this problem is more involved, we may need to train multiple AEs each for a certain range of SNR or α . We note that despite the time-consuming nature of training, it is performed offline and the developed model can be used for real-time over-the-fly tests, thereby minimizing computational demands during operational use.

It is worth noting that the goal of the above network is to achieve the most distinguishable super-constellation. This approach may not be the best as emphasized in Remark 2, in Section III-B. Specifically, a potentially improved BER could be achieved by adopting BICM with iterative decoding which allows for overlapping super-symbols. An example of such a design can be found in [182] within the context of point-to-point channels. It is also worth indicating that AE-based NOMA is expected to outperform traditional designs in terms of latency, as E2E communication is generally faster than the block-by-block approach.

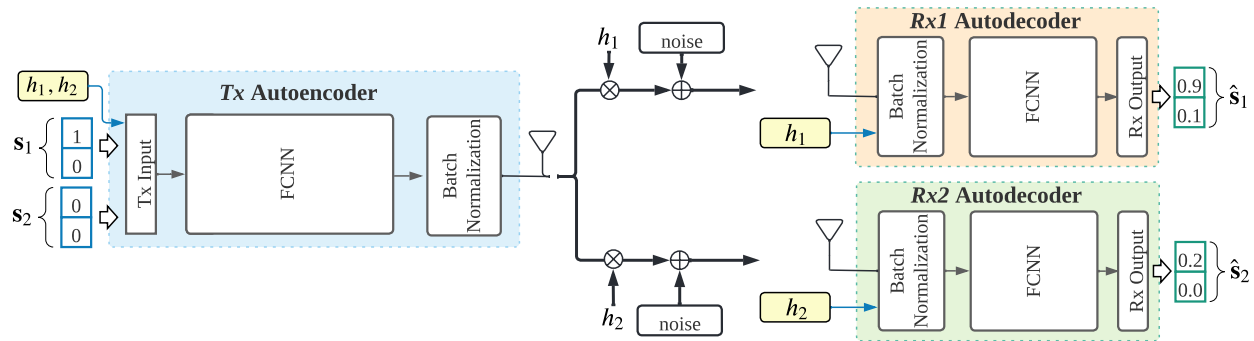


Fig. 21: A conceptual architecture of the two-user NOMA network implemented autoencoder. Both h_1 and h_2 are given to the encoder but they are known only in the corresponding decoders. This end-to-end systems will be trained to form a super-constellation (containing the superposition of the desired and interfering symbols) with separable symbols.

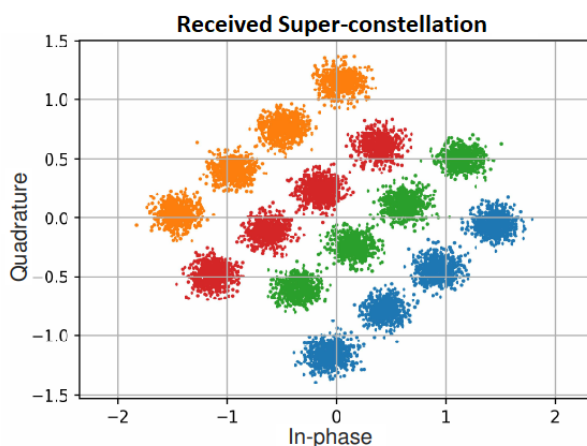
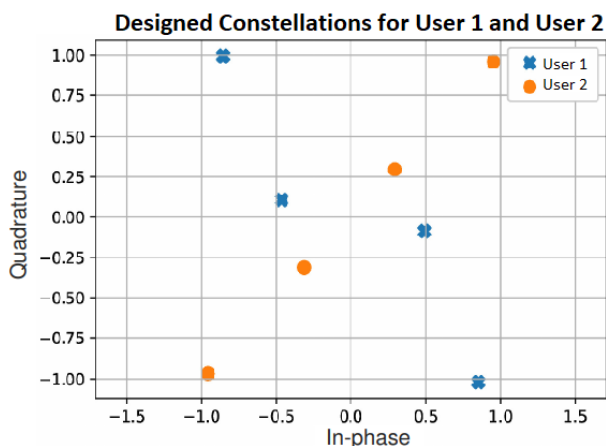


Fig. 22: An example illustrating AE-generated constellations. (top) constellations of the two transmitters. (bottom) super-constellation at the receivers (representing a noisy version of the superimposed constellation at the transmitter). Each color represents a combination of one symbol of user 1 with four distinct symbols from user 2.

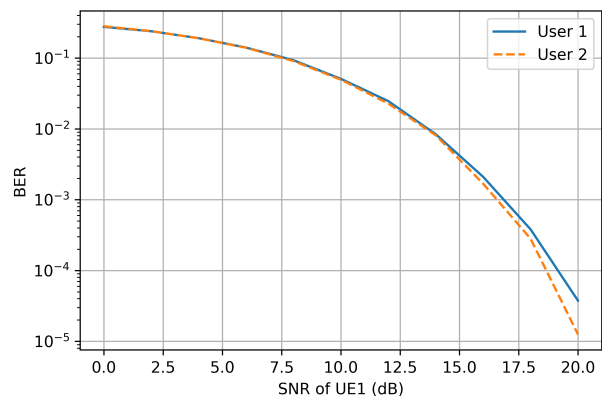


Fig. 23: BER versus SNR of UE1 for a two-user NOMA with $h_1 = 1$ and $h_2 = 2$. The results are for AE-based NOMA.

2) *ICI-Resilient NOMA*: Thus far, our discussion has centered on single-cell NOMA transmission where the spectrum is distributed among multiple users within a single cell. However, contemporary cellular networks operate in a multi-cell environment, aiming to reuse the same frequency band across many or all cells to enhance spectral efficiency. This shared frequency allocation leads to inter-cell interference, causing outages at cell edges and posing a substantial challenge to achieving high throughput [183]–[185]. The issue is worsened by the three-dimensional expansion driven by UAVs [185]. The design of inter-cell interference-aware NOMA becomes notably complex in light of these evolving complexities within contemporary cellular networks.

While multi-cell NOMA has been studied in many papers [186]–[190], these are based on Shannon-theoretic principles and are not directly applicable to finite-alphabet inputs. Recent works on end-to-end communication in interference channels focus on OMA [191]–[193], often comparing their results with basic baselines like QPSK. However, as discussed before, it is known that when both users employ QPSK constellations, BER performance is notably inferior to that where one user employs *rotated* QPSK. Thus, those comparisons are less competitive in terms of BER. In contrast, the approach

in [194], [195] leverages the structure of co-channel interference through interference-resilient constellations adaptable to various interference regimes and topologies, resulting in minimized BER. Indeed, the above works also focus on addressing Z-interference channel [196], also known as one-sided interference channel, in which only one of the users suffers from interference. Therefore, a significant gap exists in the literature regarding constellation design for multi-cell NOMA.

3) *Modulation for MIMO Channels*: MIMO techniques can be broadly divided into open-loop and closed-loop systems [53]. In an open-loop system, there is no feedback from the receiver to the transmitter regarding the channel conditions. Hence, modulation symbols can be directly assigned to different transmit antennas without CSI at the transmitter. We have already covered the modulation techniques used for data channels in 5G NR in Section IV-B and summarized them in Table II. Advanced open-loop MIMO techniques, such as space-time block coding [197]–[199], have been used as modulation schemes for MIMO channels in various scenarios [200, Chapter 4]. These techniques are particularly useful for achieving spatial diversity and improving signal reliability. Space-time block coding is the main block in constructing multiple-antenna differential modulation schemes [201], [202] and trellis codes for MIMO, like super-orthogonal space-time trellis codes [131]. Original goal of space-time block coding was to achieve diversity. However, it is also a building block in closed-loop MIMO systems with limited feedback, like the beamforming/precoding codebooks in WiFi and 5G [203], [204].

Closed-loop MIMO uses feedback from the receiver to inform the transmitter about channel conditions, enabling techniques like beamforming or precoding to adapt. As shown in Fig. 24, modulation symbols are mapped to layers before precoding. Assuming a channel rank of two, the layer mapper takes two symbols (s_1, s_2) and creates two data streams. For a rank of one, it selects one symbol (s_1) and sends it to the precoding block or antenna mapper. With precoding and post-processing, the channel is converted to parallel channels so that two independent data streams, without any coupling between them, are sent. This simplifies the design of the receiver.

As explained above, and shown in Fig. 24, separating precoding and post-processing blocks, modulation schemes used in MIMO channels are the same as those developed for single-input single-output (SISO) channels. The main rationale behind such a separation is the optimality of the precoding and post-processing matrices, obtained from SVD decomposition, to convert the MIMO channel into parallel SISO channels. In such a system, either symbols from a single modulation scheme, such as QPSK, are used across all channels, or symbols from different modulation schemes are assigned based on channel characteristics [205]–[209]. Such techniques separate modulation and precoding schemes, as shown in Fig. 24. These techniques and their representative works can be summarized as, adaptive modulation with SVD precoding, along with optimal bit and power allocation [23], linear precoding for finite-alphabet [205], bit allocation with SVD precoding and water-filling power allocation, bit allocation with SVD precoding

and equal power allocation, and SVD-based deep autoencoder [25]. With a few exceptions, for example [206], the above line of work assumes perfect CSI at the transmitter.

Recent studies have emphasized the advantages of joint modulation and precoding design strategies compared to their separate counterparts. In [112], lattice-based symbol layouts have been proposed to enhance spectral efficiency although they face limitations in fully leveraging MIMO multiplexing gain. The multi-dimensional constellation concept, introduced in [113], is designed to fully leverage MIMO multiplexing gain. This new method designs constellations and precoding by simultaneously optimizing the in-phase and quadrature components for all sub-channels within a MIMO channel. It exhibits superior performance compared to existing finite-alphabet MIMO communication techniques, including current AE-based constellations, as illustrated in [113, Fig. 5]. The BER curves obtained by this method can serve as a lower bound for AE-based constellation design, indicating potential for further enhancement in AE-based end-to-end MIMO systems. This multi-dimensional constellation approach also holds promise for the development of even more sophisticated AE-based end-to-end MIMO-NOMA systems. Several DAE-based finite-alphabet MIMO schemes are introduced in [22], [23], [25].

Lastly, it is crucial to note that a significant portion of downlink MIMO-NOMA literature attempts to adapt SC-SIC decoding of SISO channel to MIMO ones [8], [210], [211]. However, such strategies are strictly sub-optimal for MIMO-NOMA with and without secrecy [95], [212]–[216]. Despite the common extension of SC-SIC (the optimal strategy of SISO-NOMA) to MIMO-NOMA, it is well-established that SC-SIC cannot achieve the capacity region in MIMO-BC (MIMO-NOMA); instead, dirty-paper coding (DPC) is the optimal choice. This point has been highlighted in a few recent MIMO-NOMA works [215]–[217]. In addition, in these works, various linear precoding and power allocation strategies are developed to achieve the DPC-based capacity region of MIMO-NOMA channels. More specifically, Table 1 in [215] lists capacity-achieving signaling design for several related problems. The fact that linear precoding approaches the DPC region is known from various other works [215], [218]–[220]. Further, in [221], the notion of quasi-degraded channels was introduced as a mean to achieve the DPC region using linear precoding. This concept has been applied to other settings, such as network NOMA in [222]. Therefore, when designing modulation and coding for MIMO-NOMA, particularly, when joint design is considered [112], [113], prioritizing the established optimal approach over suboptimal ones is imperative.

The capacity region of uplink MIMO-NOMA, also referred to as MIMO-MAC, is also well-established [223]. This capacity region is the union of pentagons, each corresponding to different transmit covariance matrices, and its boundary is curved, except at the sum-rate point, where it becomes a straight line [223]. Several low-complexity linear methods, such as simultaneous triangularization [224], zero forcing, and linear MMSE with practical codes [225], [226] have been developed to approach the boundary of this region.

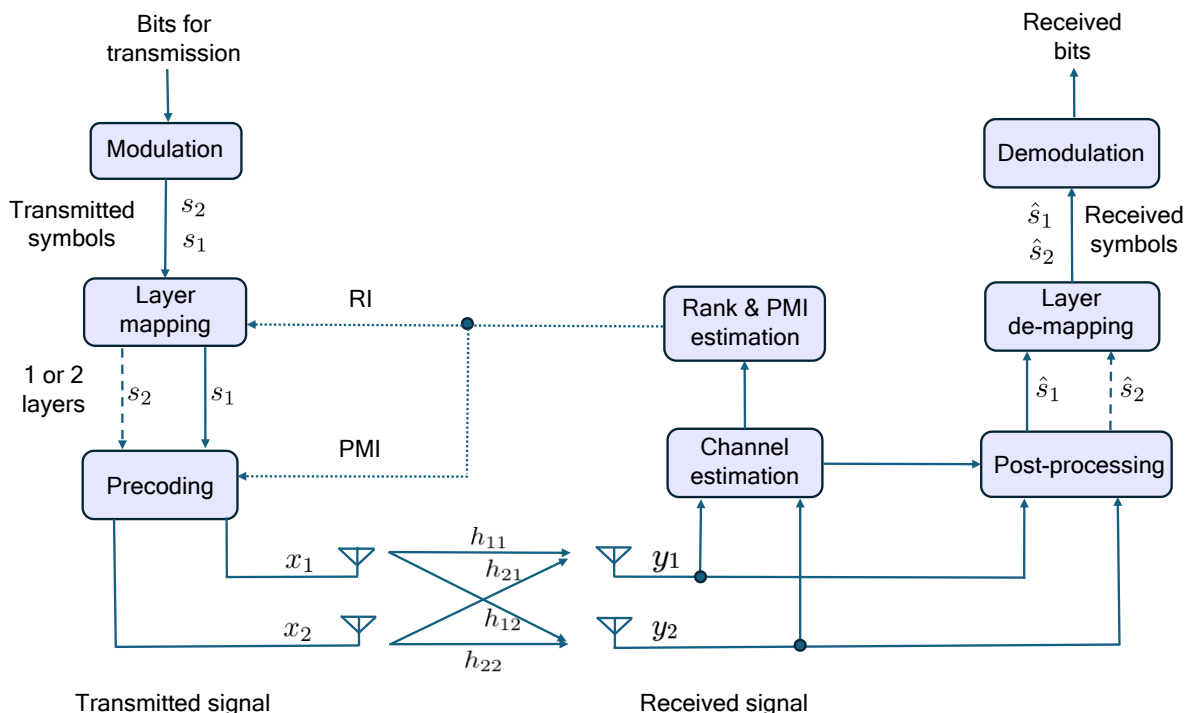


Fig. 24: Block diagram of a 2×2 closed-loop MIMO system. The rank indicator (RI) and precoding matrix indicator (PMI) provide feedback from the receiver to the transmitter. If the channel rank is one, only a single symbol (layer) s_1 is transmitted. If the rank is two, both symbols s_1 and s_2 are transmitted, enhancing data throughput. This scheme can be generalized to an arbitrary number of antennas. Here, modulation and precoding are designed separately.

VI. RSMA

RSMA is a promising interference management technique in multi-user systems. While SDMA treats interference as noise and NOMA decodes interference of the users with weaker channels, RSMA uses SIC to decode a portion of the interference and treats the remaining interference as noise. This unique feature of RSMA allows for a gradual transition between decoding interference in NOMA and treating it as noise in SDMA, enabling a more flexible approach to interference management [227]. The idea of rate splitting was first proposed long ago for a two-user SISO interference channel [228]. The term RSMA was first used around 20 years later in [229] where rate splitting was proposed for a multiple-access channel. Research on downlink RSMA [230]–[232] and its advantages resulted in the revival of the idea.

In what follows, we investigate RSMA under two broad umbrellas of downlink and uplink.

A. Downlink RSMA

To illustrate the framework of downlink RSMA, let us assume a single-layer scheme [233], [234]. Consider a system with K single-antenna users where the BS is equipped with M antennas. Let W_1, \dots, W_K denote the message of Users 1 to K and $\mathbf{h}_1^H, \dots, \mathbf{h}_K^H$ be the channels from the transmitter to Users 1 to K , respectively. In a single-layer scheme, the message of the k th user, W_k , will be split into two parts, namely, common message $W_{c,k}$ and private message $W_{p,k}$. The common parts $\{W_{c,1}, \dots, W_{c,K}\}$ are jointly encoded into the common stream s_c and the private parts

$\{W_{p,1}, \dots, W_{p,K}\}$ are encoded in $\{s_1, \dots, s_K\}$. The data stream vector $\mathbf{s} = [s_c, s_1, \dots, s_K]^T \in \mathbb{C}^{K+1}$ is precoded by $\mathbf{P} = [\mathbf{p}_c, \mathbf{p}_1, \dots, \mathbf{p}_K] \in \mathbb{C}^{M \times (K+1)}$ and the transmitted signal can be written as

$$\mathbf{x} = \mathbf{P}\mathbf{s} = \sum_{k=1}^K s_k \mathbf{p}_k + s_c \mathbf{p}_c. \quad (17)$$

The received signal at User k will be

$$y_k = \mathbf{h}_k^H \mathbf{x} + \eta_k = \sum_{l=1}^K s_l \mathbf{h}_k^H \mathbf{p}_l + s_c \mathbf{h}_k^H \mathbf{p}_c + \eta_k, \quad (18)$$

where η_k is the complex AWGN with variance σ^2 . To recover User k 's intended message, User k should decode the common message and its own private message. The idea behind downlink RSMA is to decode the common message at each user and then subtract it from the received signal, to cancel its interference, and then decode the private message by treating the private messages of all other users as noise. This approach can be considered as partial interference cancellation. For $k = 1, \dots, K$, the rates $R_{k,c}$ and $R_{k,p}$ can be calculated as

$$R_{k,c} = \log \left(1 + \frac{|\mathbf{h}_k^H \mathbf{p}_c|^2}{\sum_{l=1}^K |\mathbf{h}_k^H \mathbf{p}_l|^2 + \sigma^2} \right), \quad (19)$$

$$R_{k,p} = \log \left(1 + \frac{|\mathbf{h}_k^H \mathbf{p}_k|^2}{\sum_{l=1, l \neq k}^K |\mathbf{h}_k^H \mathbf{p}_l|^2 + \sigma^2} \right), \quad (20)$$

where symbols are assumed to be unit-power, i.e., $\mathbb{E}[|s_k|^2] = 1$. To make sure that the common message is decodable by

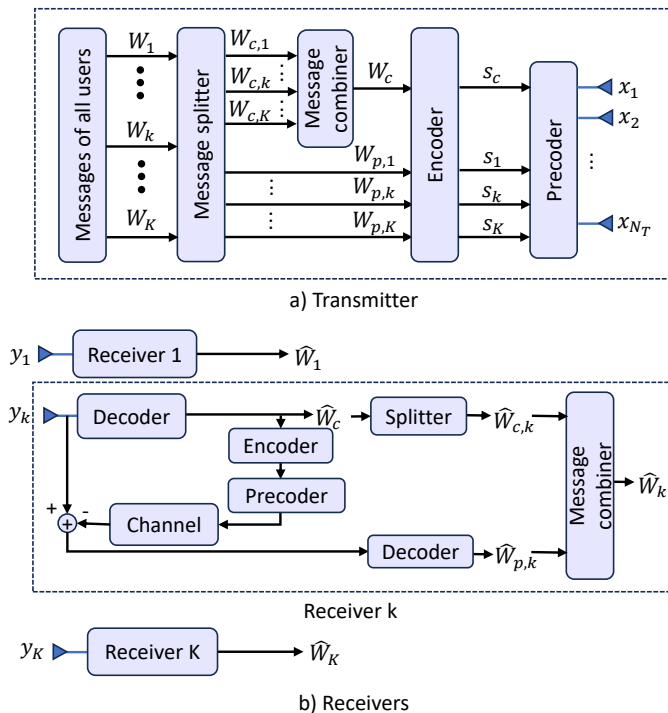


Fig. 25: Transmitter and receiver architecture for a single-layer K -user downlink RSMA system. a) Each user's message is divided into private and common parts. The common parts are combined into a single message. The common message and the private messages are coded and transmitted. b) Each user first decodes the common message and uses SIC to remove interference, treating the messages from other users as noise.

every user, the common rate, R_c , should be at most equal to the minimum of rates given in (19). That is

$$R_c \leq \min\{R_{1,c}, \dots, R_{K,c}\}. \quad (21)$$

The total rate of User k will be the summation of its private message rate and the corresponding portion of the common message rate. The architecture of transmitter and receiver for this system is shown in Fig. 25. More layers can be added to the system by considering common messages that will be decoded by a group of users and treated as noise by the rest [235]. The transmitted signal in (17) is a linear combination of precoded data streams, but nonlinear precoding is also an option [236].

RSMA includes NOMA and SDMA as special cases. When there is no common message, RSMA transforms into SDMA. In a K -user system, where the first user has the strongest channel and the K th user has the weakest channel, designing an RSMA system such that the K th common message is decoded by Users 1 to K , the $(K-1)$ th common message is decoded by Users 1 to $K-1$, \dots , the second common message is decoded by Users 1 and 2, and a private message decoded by User 1 turns RSMA into NOMA. Therefore, performance of RSMA, as a general framework, is never worse than those of SDMA and NOMA.

As a candidate for the NGMA, it is insightful to take a look at the advantages and disadvantages of RSMA. In comparison

to other schemes, RSMA provides robust performance with imperfect channel state information at the transmitter (CSIT) [231], [237]. Having NOMA and SDMA as special cases, RSMA results in better spectral efficiency and energy efficiency [227], [233]. Achieving URLLC stands out as a key feature in the context of NR. A viable solution to enhance latency performance involves the reduction of packet size. Studies in [238], [239] reveal that RSMA can achieve transmission rates similar to those of SDMA and NOMA, yet with shorter block-lengths, resulting in reduced latency. Naturally, these enhancements are accompanied by some associated costs. As one example, the decoding complexity of RSMA is much higher because of SIC and the need to decode common messages. This extra complexity is also present in NOMA; however, SDMA, in contrast, does not require SIC. On the other hand, SDMA lacks control over interference. Dividing the message at the transmitter introduces the challenge of optimizing message splitting, which becomes an additional task at the transmitter. Moreover, every receiver needs to be aware of the splitting/decoding rule to extract its intended message, adding to the complexity of downlink signaling. It is evident that a larger number of streams resulting from message splitting introduces more challenging optimization problems for beamforming and power allocation in RSMA.

To illustrate the concept, so far, we have discussed RSMA for multi-user systems with single-antenna users, i.e., only the transmitter is equipped with multiple antennas. MIMO has become an essential component of communication systems to significantly enhance their performance. Having multiple antennas at the receiver can further improve the performance of RSMA systems. While some works, such as [240], use the term MIMO to refer to systems with multiple single-antenna users and a multiple-antenna transmitter, we apply it specifically to systems where both the transmitter and receivers are equipped with multiple antennas. [241] introduces practical stream combining methods along with regularized block diagonalization precoding for rate-splitting in MIMO broadcast channels, focusing on a single common stream and excluding precoding optimization. In [242], the authors examine a single-layer MIMO-RSMA system. To manage the inter-user interference at the receivers, the system employs linear combinations of the null-space basis vectors from the successively augmented MIMO channel matrices of the users as precoding vectors. [243] studies the precoder optimization problem in MIMO-RSMA with the goal of maximizing the weighted ergodic sum-rate. Precoder design for MIMO-RSMA has been studied in several other papers such as [244], [245]. Uplink MIMO-RSMA has been studied in [246] where the authors focus on increasing energy efficiency by optimizing the transmit covariance matrices and decoding order using statistical CSI. In conclusion, these studies demonstrate that while MIMO systems are highly sensitive to CSI, RSMA proves to be much less affected by channel errors.

The benefits and promising features of RSMA have provoked a surge of research in this area. Therefore, effectiveness of RSMA on many existing problems have been studied. Performance of RSMA with OFDM has been studied in [247] and compared with that of orthogonal frequency division

multiple access and OFDM-NOMA. OFDM is a modulation technique that is widely used in modern wireless communication systems, including 4G (LTE) and 5G networks. It is anticipated that OFDM will continue to be a central component in NGMA. Therefore, ensuring compatibility of new multiple access techniques with OFDM and enhancing overall performance are crucial factors. Application of RSMA to integrated sensing and communications (ISAC) has been studied in several works like [248]–[251]. ISAC is expected to emerge as a pivotal feature in the next generation, seamlessly combining two technologies within a single device. This integration entails the shared utilization of hardware and spectrum for both functionalities. Particularly crucial for smart cities, ISAC enhances continuous environmental monitoring by integrating sensing capabilities into the extensive network of communication base stations. Another rising technology is the reconfigurable intelligent surface (RIS), which enhances communication by establishing new paths between the transmitter and the receiver. Every RIS consists of a large number of elements, often in the thousands, capable of altering the phase of the incident wave. Through careful control and design of these phase changes, an RIS can enhance the received power at the receiver. The large number of elements and passive characteristics of these components pose several challenges that need to be addressed. The integration of RIS in RSMA systems is an intriguing problem that has been explored in various studies, including [252]–[256]. UAV is another enabling technology for the next generation of wireless communications. These aerial platforms, commonly known as drones, offer a versatile and dynamic solution to address various challenges in wireless communications. Equipped with communication systems, UAVs can be deployed to enhance network coverage, particularly in distant or disaster-affected regions where conventional infrastructure may be constrained [257]. Their mobility makes them suitable for duties such as data collection and even acting as relays to extend the network coverage [258]–[260]. As the need for high data rates and low-latency communication increases, incorporating UAVs into communication networks offers a creative and adaptable approach to fulfill these evolving demands [261], [262]. Integration of RSMA into UAV-assisted communication has been studied in several works such as [263]–[267].

B. Uplink RSMA

One of the advantages of uplink RSMA over other multiple access techniques such as NOMA is its ability to achieve the capacity region of the Gaussian MAC without time sharing. Fig. 26 shows the rate region of a two-user Gaussian MAC. Conceptually, this is the same as the black pentagon in Fig. 6. The horizontal and vertical lines up to points A and B are achievable by SIC and changing the order of decoding. As shown in Fig. 26, NOMA can achieve the line AB by time sharing, while RSMA can achieve the line AB without time sharing. If we continue the plot beyond point A without time sharing (i.e., maintaining the decoding order as $\{1,2\}$), we obtain a line extending from point A to intersect the horizontal axis. The same occurs for point B and its extension. The

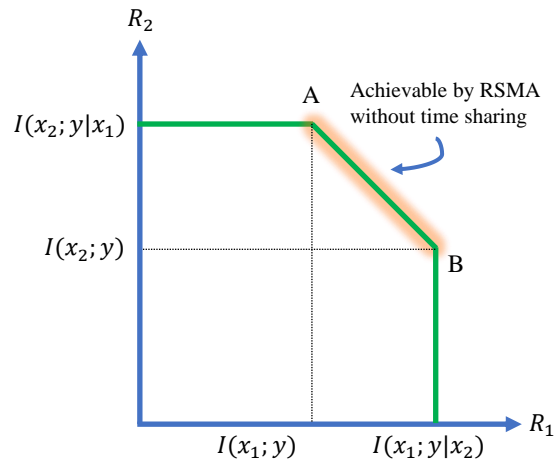


Fig. 26: Capacity region of a two-user Gaussian MAC.

resulting pentagon is the convex hull of these plots, which is achieved through time sharing. This involves decoding in the $\{1,2\}$ order for a portion of the time and switching to the $\{2,1\}$ order for the remaining time. Such a switching may not be desirable.

To illustrate the uplink RSMA's framework, let us consider an uplink system with K single-antenna users and a receiver with N_r antennas. For K users, it is sufficient to split the messages of $K-1$ users to avoid time sharing [29], [229]. Without loss of generality, the message of User k for $k \in \{1, \dots, K-1\}$, denoted by W_k , is split into two parts, $W_{k,1}$ and $W_{k,2}$ and the message of User K remains intact. The messages $W_{k,1}$ and $W_{k,2}$ will be encoded into streams $s_{k,1}$ and $s_{k,2}$ with powers $P_{k,1}$ and $P_{k,2}$, respectively. The message of User K will be encoded to the stream s_K . We assume unit-power constraint on the symbols, i.e., $\mathbb{E}[|s_{k,1}|^2] = \mathbb{E}[|s_{k,2}|^2] = \mathbb{E}[|s_K|^2] = 1$. The transmit signals will be $x_k = \sqrt{P_{k,1}}s_{k,1} + \sqrt{P_{k,2}}s_{k,2}$ for User $k \in \{1, \dots, K-1\}$ and $x_K = \sqrt{P_K}s_K$ for User K . The received signal at the receiver will be

$$\mathbf{y} = \sum_{k=1}^K \mathbf{h}_k x_k + \boldsymbol{\eta}, \quad (22)$$

where \mathbf{h}_k is the channel between User k and the receiver and $\boldsymbol{\eta}$ is the complex additive white Gaussian noise with the covariance matrix $\sigma^2 \mathbf{I}$. The receiver uses filters $\mathbf{w}_{k,1}$ and $\mathbf{w}_{k,2}$ to decode the messages of Users 1 to $K-1$, and uses \mathbf{w}_K to decode the message of User K . Single-layer downlink RSMA, discussed in the previous section, does not require ordering for decoding, because each user simply decodes the common message first and then its own private message. However, ordering is required for downlink RSMA with more than one layer [235]. Similarly, uplink RSMA requires the receiver to decide which message should be decoded first to achieve the optimal performance. This problem has been studied in [268]. Assuming a decoding order π such that $\pi_{k,i} < \pi_{k',i'}$ indicates stream $s_{k,i}$ is decoded before stream $s_{k',i'}$ (for User K we only

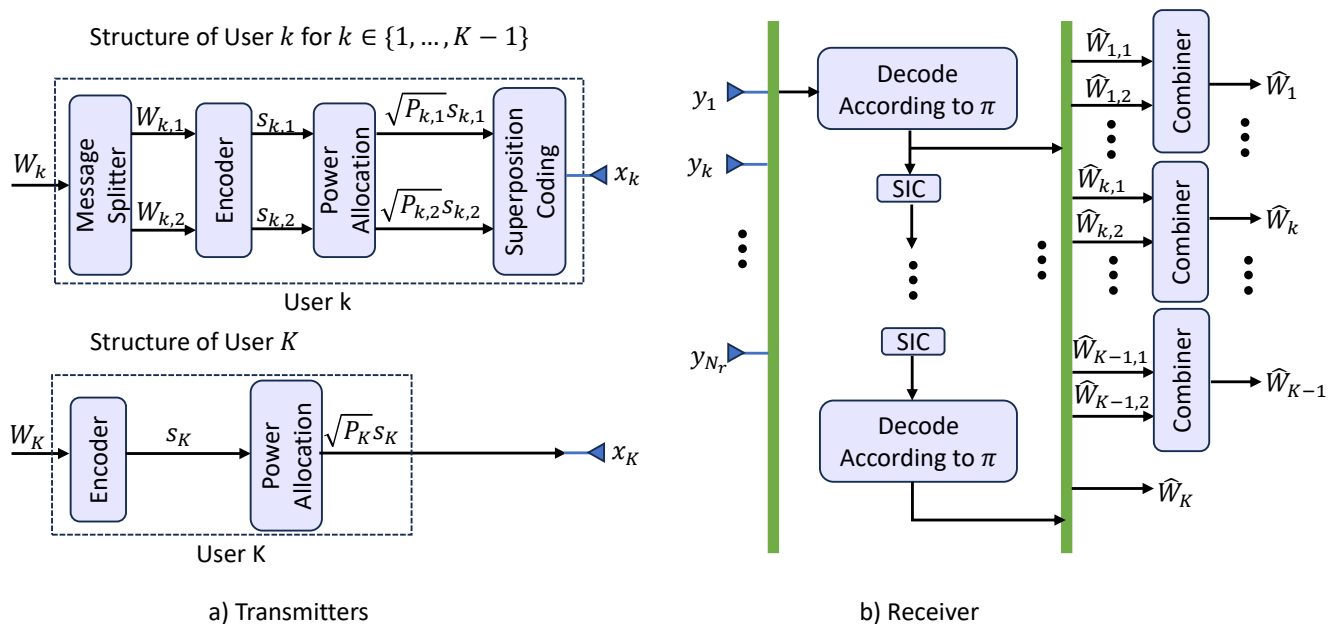


Fig. 27: Uplink RSMA architecture. a) Out of K users, $K - 1$ users split their messages into two parts and use superposition coding to transmit them. b) The receiver determines the optimal decoding order, decodes each user's message, and employs SIC to remove interference.

have π_K), the achievable rates will be

$$R_{k,i} = \log_2 \left(1 + \frac{P_{k,i} |\mathbf{w}_{k,i}^H \mathbf{h}_k|^2}{\sum_{\pi_{k',i'} < \pi_{k',i'}} P_{k',i'} |\mathbf{w}_{k',i'}^H \mathbf{h}_k|^2 + \sigma^2} \right), \quad (23)$$

$$R_K = \log_2 \left(1 + \frac{P_K |\mathbf{w}_K^H \mathbf{h}_k|^2}{\sum_{\pi_K < \pi_{k',i'}} P_{k',i'} |\mathbf{w}_{k',i'}^H \mathbf{h}_k|^2 + \sigma^2} \right) \quad (24)$$

$$i, i' = 1, 2, \quad k, k' = 1, \dots, K - 1.$$

Fig. 27 shows the architecture of the uplink RSMA system. While RSMA for uplink communication was proposed prior to the downlink, the body of literature in this area is very small [269]–[274]. This may be viewed as a drawback of uplink RSMA; however, it also represents a relatively unexplored research area with many open problems. In particular, existing works focus on uplink systems with a single antenna. The next generation is set to deploy multiple antennas for both uplink and downlink. Consequently, tackling multi-antenna uplink RSMA problems can establish a significant and valuable research domain.

VII. OPEN PROBLEMS & FUTURE DIRECTIONS

In this section, we briefly discuss some open problems and future research directions in designing coding and modulation methods for NGMA. While NGMA systems offer numerous advantages, they may introduce new security and privacy challenges, compared to existing communication systems, because of the shared symbols and models.

A. Non-Uniform Modulation for NOMA

It is known that superposition of two uniform constellations generally leads to a non-uniform super-constellations. As this is inherent in NOMA, non-uniform constellations with BICM are transformative shifts for addressing the rate losses observed when implemented with uniform constellations [14], rendering NOMA a practically viable scheme. One possible approach is to have non-uniform constellations for each user and superimpose them to create a non-uniform super-constellation, but this approach may be overly complicated, as the resulting super-constellations would be distinct for each values of the power allocation coefficient α . On the other hand, the direct design of non-uniform constellations for different ranges of α appears to be more promising. In addition, the integration of non-uniform constellations with BICM represents an intriguing and promising avenue for enhancing the practical performance of NOMA. BICM implementation in low-resource IoT devices is challenging due to increased receiver complexity. Therefore, efficient algorithms and hardware are essential to make BICM feasible for IoT. Exploring deep learning-based BICM presents a promising new research avenue [275].

B. Modulation for MIMO-NOMA

As discussed earlier, modulation schemes for MIMO channels often borrow concepts from SISO channels, employing methods like SVD decomposition to treat each channel individually [205], [206]. These techniques treat modulation and precoding separately using various bit allocation strategies. Recent studies advocate for joint modulation and precoding design [112], [113]. The joint multi-dimensional constellation and precoding design proposed in [113] optimizes constellations and precoding simultaneously for all MIMO sub-

channels, demonstrating superior performance compared to existing techniques. This approach is based on two key factors: 1) the collaborative design of modulation and precoding, and 2) leveraging the Mahalanobis distance [276] to effectively utilize sub-channels with varying gains. By treating the MIMO system as a unified multi-dimensional space, rather than separate 2D spaces for in-phase and quadrature-phase, this strategy enhances overall performance. The potential application of these techniques to MIMO-NOMA systems raises intriguing questions with substantial possibilities. Specifically, the design of MIMO-NOMA constellations can draw inspiration in the aforementioned multi-dimensional constellation concept presented in [113].

Additionally, designing modulation schemes based on imperfect or quantized CSI is another promising research direction [206]. Also, like regular MIMO systems, highly correlated channels may result in rank-deficient matrices that require their own studies in MIMO-NOMA systems.

C. AE-Based NOMA

There are several research questions to explore in AE-based constellation design for NOMA. Particularly, future research in this domain should address key challenges, including refining network construction, training, and loss function design. Additionally, a more effective BER may be achieved by exploring bit-interleaved coded modulation with iterative decoding, allowing for overlapping super-symbols. The multi-dimensional constellation design offers a promising avenue for any MIMO problem including MIMO-NOMA. Besides, addressing the complex challenges of inter-cell interference in multi-cell environments is another crucial future research direction for finite-alphabet NOMA. In addition, evaluating the above questions with imperfect CSI and channels with severe multipath and Doppler effects is crucial for understanding the potential improvement in BERs achievable in real-world NOMA transmission. Lastly, non-Gaussian noise channels, such as impulsive noise, can lead to diverse outcomes and offer promising directions for future research. Researchers have investigated NOMA in the presence of impulsive noise [277]. Extending these studies to AE-based NOMA would be useful.

D. Limited Feedback/CSI

Acquiring and distributing CSI to adapt the precoding/beamforming and modulation have been used in different wireless communication systems. For example, 3GPP Release 15 explains the role of CSI in its description of “5G Phase 1 Specifications” in Section 5.2.2 of TS 138.214 [204]. The UE reports CSI parameters to the base station using limited feedback, i.e., a few bits. In most of the discussions so far, it has been assumed that the CSI is known perfectly. Obviously, the number of available feedback bits affects the performance of the NGMA systems, similar to the case of single-user systems [53]. Channel values can be estimated at the receiver by transmitting pilots. The accuracy of the CSI estimation is limited and its error is usually modeled by a Gaussian distribution. In frequency division duplexing

(FDD) scenarios, to use CSI at the transmitter, the receiver should quantize and send back the estimated CSI. Since the channel values are real numbers and only a limited number of feedback bits are available, there will be a quantization error in addition to the estimation error. In NOMA systems that use SIC, the benefits of NOMA heavily depend on the knowledge of channel orders for decoding. As such, it is very important to design the limited/quantized feedback systems to maintain the channel orders. Recently, there have been some studies on the effects of limited/quantized feedback on NOMA systems [211], [278]–[283]. In addition to designing appropriate uniform quantizers to maximize the minimum rate in SISO-NOMA systems, [278] analyzes the performance and demonstrates the catastrophic effects of an incorrect channel order estimation. A more general optimal scalar quantizer that works for both NOMA and A-NOMA is designed in [279]. Designing NOMA systems with very small number of feedback bits that can achieve outage probabilities close to those of full-CSI NOMA systems is possible if the bits are mainly utilized to preserve the user ordering [211], [280]–[282]. An RIS-aided NOMA system with limited feedback is designed in [283] and the rate loss due to quantization is analyzed. Also, there has been some limited research on RSMA systems with limited feedback [230], [284], [285].

Nevertheless, there are still many open problems in this area. For example, the capacity region of NOMA for a given number of feedback bits is not known. Future research directions include the design of the feedback link with optimal quantizers, studying the trade-off between the number of feedback bits and the performance, and analyzing the rate loss due to the limited feedback. One important challenge is to keep the transmitted throughput less than the capacity of the channel. Since the transmitter has only access to a quantized version of the channel gains, its estimate of the possible throughput rates may exceed the real capacity of the channel. This is more severe for downlink NOMA where channels are estimated at different nodes without knowing other channels. If the transmitter of downlink NOMA does not know the correct ordering, because of feedback error or quantization noise, a receiver may try to decode at a rate which is higher than its capacity, resulting in catastrophic outcomes and error propagation. Another challenge is the robust design of MIMO-NGMA systems for estimated and quantized CSI, especially taking into account the impact of precoding/beamforming vectors in designing user grouping methods and decoding order algorithms for each group. When RIS components exist in NOMA systems, estimating the corresponding cascaded channels is a major challenge, especially since RIS elements are usually passive and cannot transmit pilots [286]. Designing appropriate limited feedback mechanisms for such RIS-assisted NOMA systems is another interesting open problem.

E. Effects of mmWave and Terahertz (THz) Channels

By enabling ultra-high data rates up to terabits per second, and massive connectivity, mmWave and THz frequencies are critical for next-generation wireless systems. However, they face challenges like limited coverage, hardware limitations,

and susceptibility to blockages [287]. These channels are sparse, with few significant propagation paths from transmitter to receiver. Their smaller wavelengths allow highly directional antennas and beamforming, focusing energy in specific directions. Thus, communication in these bands is more directional, with signals traveling in defined paths rather than spreading widely.

Both NOMA and RSMA are used with these bands [288]–[292]. The potential for highly directional beamforming in these bands makes NOMA user grouping different from sub-6 GHz channels. Additionally, beamforming will shift from digital to analog or hybrid to reduce power consumption when the number of antennas is high [293]–[295]. Similarly, challenges related to modulation and coding in mmWave and THz bands are mostly hardware-related. High-speed analog-to-digital converters (ADCs) and digital-to-analog converters (DACs) are power-hungry and costly [296], [297]. As an alternative, QAM demodulation in the analog domain has been proposed [296]. Power dissipation of ADCs and DACs reduces by lowering their resolution bits. While low-resolution ADCs and DACs, such as one-bit converters, can simplify hardware design and reduce power consumption, they also increase quantization noise, introducing challenges in signal quality, beamforming precision, and overall performance [298]. NOMA and RSMA are more sensitive to channel imperfections, compared to OMA, since they require CSI for decoding. It is crucial to study the impact of low-resolution converters on both NOMA and RSMA decoders, particularly on SIC. Designing signal processing and machine learning techniques to mitigate these effects is essential for achieving acceptable performance levels.

REFERENCES

- [1] M. Vaezi, A. Azari, S. R. Khosravirad, M. Shirvanimoghaddam, M. M. Azari, D. Chasaki, and P. Popovski, "Cellular, wide-area, and non-terrestrial IoT: A survey on 5G advances and the road toward 6G," *IEEE Commun. Surv. Tut.*, vol. 24, no. 2, pp. 1117–1174, 2022.
- [2] H. Viswanathan and P. E. Mogensen, "Communications in the 6G era," *IEEE Access*, vol. 8, pp. 57063–57074, 2020.
- [3] C.-X. Wang, X. You, X. Gao, X. S. Zhu, Z. Li, C. Zhang, H. Wang, Y. Huang, Y. Chen, H. Haas, J. S. Thompson, E. G. Larsson, M. D. Renzo, W. Tong, P. Zhu, X. Shen, H. V. Poor, and L. Hanzo, "On the road to 6G: Visions, requirements, key technologies, and testbeds," *IEEE Commun. Surv. Tut.*, vol. 25, no. 2, pp. 905–974, 2023.
- [4] Y. Saito, Y. Kishiyama, A. Benjebbour, T. Nakamura, A. Li, and K. Higuchi, "Non-orthogonal multiple access (NOMA) for cellular future radio access," in *Proc. IEEE Veh. Technol. Conf. (VTC Spring)*, pp. 1–5, Jun 2013.
- [5] M. Vaezi, Z. Ding, and H. V. Poor, *Multiple Access Techniques for 5G Wireless Networks and Beyond*. Cham, Switzerland: Springer, 2019.
- [6] L. Dai, B. Wang, Y. Yuan, S. Han, C.-L. I, and Z. Wang, "Non-orthogonal multiple access for 5G: Solutions, challenges, opportunities, and future research trends," *IEEE Commun. Mag.*, vol. 53, no. 9, pp. 74–81, 2015.
- [7] Y. Liu, Z. Qin, M. El-kashlan, Z. Ding, A. Nallanathan, and L. Hanzo, "Non-orthogonal multiple access for 5G and beyond," *Proc. IEEE*, vol. 105, no. 12, pp. 2347–2381, 2017.
- [8] Z. Ding, X. Lei, G. K. Karagiannidis, R. Schober, J. Yuan, and V. K. Bhargava, "A survey on non-orthogonal multiple access for 5G networks: Research challenges and future trends," *IEEE J. Sel. Areas Commun.*, vol. 35, no. 10, pp. 2181–2195, 2017.
- [9] M. Vaezi, G. A. A. Baduge, Y. Liu, A. Arafat, F. Fang, and Z. Ding, "Interplay between NOMA and other emerging technologies: A survey," *IEEE Trans. Cogn. Commun. Netw.*, vol. 5, no. 4, pp. 900–919, 2019.
- [10] 3GPP TD RP-150496, "Study on downlink multiuser superposition transmission," March 2015. [Online]. Available: <https://portal.3gpp.org/desktopmodules/Specifications/SpecificationDetails.aspx?specificationId=2912>.
- [11] Y. Yuan, Z. Yuan, and L. Tian, "5G non-orthogonal multiple access study in 3GPP," *IEEE Commun. Mag.*, vol. 58, no. 7, pp. 90–96, 2020.
- [12] Y. Saito, A. Benjebbour, Y. Kishiyama, and T. Nakamura, "System-level performance evaluation of downlink non-orthogonal multiple access (NOMA)," in *Proc. Int. Symp. Pers. Indoor Mob. Radio Commun. (PIMRC)*, pp. 611–615, Sep 2013.
- [13] A. Benjebbour, A. Li, K. Saito, Y. Saito, Y. Kishiyama, and T. Nakamura, "NOMA: From concept to standardization," in *Proc. IEEE Conf. Stand. Commun. Netw. (CSCN)*, pp. 18–23, 2015.
- [14] Y. Qi, X. Zhang, and M. Vaezi, "Over-the-air implementation of NOMA: new experiments and future directions," *IEEE Access*, vol. 9, pp. 135828–135844, 2021.
- [15] T. Cover, "Broadcast channels," *IEEE Trans. Inf. Theory*, vol. 18, pp. 2–14, Jan 1972.
- [16] G. Foschini, R. Gitlin, and S. Weinstein, "Optimization of two-dimensional signal constellations in the presence of Gaussian noise," *IEEE Trans. Commun.*, vol. 22, no. 1, pp. 28–38, 1974.
- [17] G. Forney, R. Gallager, G. Lang, F. Longstaff, and S. Qureshi, "Efficient modulation for band-limited channels," *IEEE J. Sel. Areas Commun.*, vol. 2, no. 5, pp. 632–647, 1984.
- [18] A. J. Goldsmith and S.-G. Chua, "Variable-rate variable-power MQAM for fading channels," *IEEE Trans. Commun.*, vol. 45, no. 10, pp. 1218–1230, 1997.
- [19] M. F. Barsoum, C. Jones, and M. Fitz, "Constellation design via capacity maximization," in *Proc. IEEE Int. Symp. Inf. Theory (ISIT)*, pp. 1821–1825, 2007.
- [20] J. G. Andrews, "Interference cancellation for cellular systems: A contemporary overview," *IEEE Wireless Commun.*, vol. 12, no. 2, pp. 19–29, 2005.
- [21] G. D. Forney and G. Ungerboeck, "Modulation and coding for linear Gaussian channels," *IEEE Trans. Inf. Theory*, vol. 44, no. 6, pp. 2384–2415, 1998.
- [22] T. J. O'Shea, T. Erpek, and T. C. Clancy, "Deep learning based MIMO communications," *arXiv preprint arXiv:1707.07980*, 2017.
- [23] J. Song, C. Häger, J. Schröder, T. O'Shea, and H. Wymeersch, "Benchmarking end-to-end learning of MIMO physical-layer communication," in *Proc. IEEE Global Commun. Conf. (GLOBECOM)*, pp. 1–6, 2020.
- [24] T. O'Shea and J. Hoydis, "An introduction to deep learning for the physical layer," *IEEE Trans. Cogn. Commun. Netw.*, vol. 3, no. 4, pp. 563–575, 2017.
- [25] X. Zhang, M. Vaezi, and T. J. O'Shea, "SVD-embedded deep autoencoder for MIMO communications," in *Proc. IEEE Int. Commun. Conf. (ICC)*, pp. 1–5, 2021.
- [26] H. Nikopour and H. Baligh, "Sparse code multiple access," in *Proc. Int. Symp. Pers. Indoor Mob. Radio Commun. (PIMRC)*, pp. 332–336, Sep 2013.
- [27] S. Chen, B. Ren, Q. Gao, S. Kang, S. Sun, and K. Niu, "Pattern division multiple access: a novel nonorthogonal multiple access for fifth-generation radio networks," *IEEE Trans. Veh. Technol.*, vol. 66, pp. 3185–3196, Jul 2016.
- [28] A.-I. Mohammed, M. A. Imran, R. Tafazolli, and D. Chen, "Performance evaluation of low density spreading multiple access," in *Proc. IEEE Int. Wireless Commun. Mob. Comput. Conf. (IWCMC)*, pp. 383–388, Aug 2012.
- [29] Y. Mao, O. Dizdar, B. Clerckx, R. Schober, P. Popovski, and H. V. Poor, "Rate-splitting multiple access: Fundamentals, survey, and future research trends," *IEEE Commun. Surv. Tut.*, vol. 24, no. 4, pp. 2073–2126, 2022.
- [30] Y. Cai, Z. Qin, F. Cui, G. Y. Li, and J. A. McCann, "Modulation and multiple access for 5G networks," *IEEE Commun. Surv. Tut.*, vol. 20, no. 1, pp. 629–646, 2017.
- [31] H. Yahya, A. Ahmed, E. Alsusa, A. Al-Dweik, and Z. Ding, "Error rate analysis of NOMA: Principles, survey and future directions," *IEEE Open J. Commun. Soc.*, vol. 4, no. 7, pp. 1682–1727, 2023.
- [32] M. B. Shahab, R. Abbas, M. Shirvanimoghaddam, and S. J. Johnson, "Grant-free non-orthogonal multiple access for IoT: A survey," *IEEE Commun. Surv. Tut.*, vol. 22, no. 3, pp. 1805–1838, 2020.
- [33] 3GPP, "Modulation (Version 9.1.0)," *TS 45.004*, 2010. <https://telecomfiles.com/servidor/views/img/extractos/vamos.pdf>.
- [34] Ericsson, "Evolution of GSM voice," https://www.etsi.org/deliver/etsi_ts/145000_145009/145004/09.01.00_60/ts_145004v090100p.pdf.

- [35] 3rd generation partnership project (3GPP), "Study on downlink multiuser superposition transmission (MUST) for LTE (Release 13)," Technical report 36.859, November 2015.
- [36] 3GPP, "Study on non-orthogonal multiple access (NOMA) for NR (Release 16)," Technical report 38.812, December 2018.
- [37] M. Elbayoumi, M. Kamel, W. Hamouda, and A. Youssef, "NOMA-assisted machine-type communications in UDN: State-of-the-art and challenges," *IEEE Commun. Surv. Tut.*, vol. 22, no. 2, pp. 1276–1304, 2020.
- [38] O. Maraqa, A. S. Rajasekaran, S. Al-Ahmadi, H. Yanikomeroglu, and S. M. Sait, "A survey of rate-optimal power domain NOMA with enabling technologies of future wireless networks," *IEEE Commun. Surv. Tut.*, vol. 22, no. 4, pp. 2192–2235, 2020.
- [39] F. Hussain, R. Hussain, S. A. Hassan, and E. Hossain, "Machine learning in IoT security: Current solutions and future challenges," *IEEE Commun. Surv. Tut.*, vol. 22, no. 3, pp. 1686–1721, 2020.
- [40] T. M. Cover and J. A. Thomas, *Elements of Information Theory*. John Wiley & Sons, 2012.
- [41] Z. Yang, Z. Ding, P. Fan, and N. Al-Dhahir, "A general power allocation scheme to guarantee quality of service in downlink and uplink NOMA systems," *IEEE Trans. Wireless Commun.*, vol. 15, pp. 7244–7257, Aug 2016.
- [42] C.-L. Wang, J.-Y. Chen, and Y.-J. Chen, "Power allocation for a downlink non-orthogonal multiple access system," *IEEE Wireless Commun. Lett.*, vol. 5, pp. 532–535, Aug 2016.
- [43] J. Zhu, J. Wang, Y. Huang, S. He, X. You, and L. Yang, "On optimal power allocation for downlink non-orthogonal multiple access systems," *IEEE J. Sel. Areas Commun.*, vol. 35, pp. 2744–2757, Dec 2017.
- [44] K. N. Doan, M. Vaezi, W. Shin, H. V. Poor, H. Shin, and T. Q. Quek, "Power allocation in cache-aided NOMA systems: Optimization and deep reinforcement learning approaches," *IEEE Trans. Commun.*, vol. 68, no. 1, pp. 630–644, 2020.
- [45] M. S. Ali, H. Tabassum, and E. Hossain, "Dynamic user clustering and power allocation for uplink and downlink non-orthogonal multiple access (NOMA) systems," *IEEE Access*, vol. 4, pp. 6325–6343, 2016.
- [46] M. Ganji and H. Jafarkhani, "Interference mitigation using asynchronous transmission and sampling diversity," in *Proc. IEEE Global Commun. Conf. (GLOBECOM)*, Dec 2016.
- [47] S. Poorkasmaei and H. Jafarkhani, "Asynchronous orthogonal differential decoding for multiple access channels," *IEEE Trans. Wireless Commun.*, vol. 14, pp. 481–493, Jan. 2014.
- [48] M. Avendi and H. Jafarkhani, "Differential distributed space-time coding with imperfect synchronization in frequency-selective channels," *IEEE Trans. Wireless Commun.*, vol. 14, pp. 1811–1822, April 2014.
- [49] J. Cui, G. Dong, S. Zhang, H. Li, and G. Feng, "Asynchronous NOMA for downlink transmissions," *IEEE Commun. Lett.*, vol. 21, no. 2, pp. 402–405, 2017.
- [50] X. Zou, B. He, and H. Jafarkhani, "An analysis of two-user uplink asynchronous non-orthogonal multiple access systems," *IEEE Trans. Wireless Commun.*, vol. 18, pp. 1404–1418, Feb. 2019.
- [51] M. Ganji and H. Jafarkhani, "Time asynchronous NOMA for downlink transmission," in *Proc. IEEE Wireless Commun. Net. Conf. (WCNC)*, Apr. 2019.
- [52] M. Ganji, X. Zou, and H. Jafarkhani, "Asynchronous transmission for multiple access channels: Rate-region analysis and system design for uplink NOMA," *IEEE Trans. Wireless Commun.*, vol. 20, pp. 4364–4378, July 2021.
- [53] H. Jafarkhani, *Space-Time Coding: Theory and Practice*. Cambridge University Press, 2005.
- [54] M. Ganji, X. Zou, and H. Jafarkhani, "Exploiting time asynchrony in multi-user transmit beamforming," *IEEE Trans. Wireless Commun.*, vol. 19, pp. 3156–3169, May 2020.
- [55] 3GPP TR 38.812, "Study on non-orthogonal multiple access (NOMA) for NR," [Online]. Available: <https://portal.3gpp.org/desktopmodules/Specifications/SpecificationDetails.aspx?specificationId=3236>.
- [56] Y. Yuan, "Industry Perspective: 5G non-orthogonal multiple access study," *IEEE Commun. Mag.*, vol. 25, pp. 4–6, October 2018.
- [57] R. Hoshyari, F. P. Wathan, and R. Tafazolli, "Novel low-density signature for synchronous CDMA systems over AWGN channel," *IEEE Trans. Signal Process.*, vol. 56, no. 4, pp. 1616–1626, 2008.
- [58] Y. Chen, A. Bayesteh, Y. Wu, B. Ren, S. Kang, S. Sun, Q. Xiong, C. Qian, B. Yu, Z. Ding, *et al.*, "Toward the standardization of non-orthogonal multiple access for next generation wireless networks," *IEEE Commun. Mag.*, vol. 56, no. 3, pp. 19–27, 2018.
- [59] B. M. Zaidel, O. Shental, and S. S. Shitz, "Sparse NOMA: A closed-form characterization," in *Proc. IEEE Int. Symp. Inf. Theory (ISIT)*, pp. 1106–1110, 2018.
- [60] S. Hu, B. Yu, C. Qian, Y. Xiao, Q. Xiong, C. Sun, and Y. Gao, "Nonorthogonal interleave-grid multiple access scheme for industrial Internet of things in 5G network," *IEEE Trans. Industr. Inform.*, vol. 14, no. 12, pp. 5436–5446, 2018.
- [61] A. Bayesteh, H. Nikopour, M. Taherzadeh, H. Baligh, and J. Ma, "Low complexity techniques for SCMA detection," in *Proc. IEEE Globecom Workshops (GC Wkshps)*, pp. 1–6, 2015.
- [62] H. Nikopour, E. Yi, A. Bayesteh, K. Au, M. Hawryluck, H. Baligh, and J. Ma, "SCMA for downlink multiple access of 5G wireless networks," in *Proc. IEEE Global Commun. Conf. (GLOBECOM)*, pp. 3940–3945, 2014.
- [63] Nokia, Alcatel-Lucent, "Non-orthogonal multiple access for New Radio, 3GPP TSG-RAN WG1 85,R1-165019," May 2016. [Online]. Available: <https://www.3gpp.org/DynaReport/TDocExMtg--R1-85--31662.htm>.
- [64] Z. Yuan, G. Yu, W. Li, Y. Yuan, X. Wang, and J. Xu, "Multi-user shared access for Internet of things," in *Proc. IEEE Veh. Technol. Conf. (VTC Spring)*, pp. 1–5, 2016.
- [65] S. Chen, B. Ren, Q. Gao, S. Kang, S. Sun, and K. Niu, "Pattern division multiple access—a novel nonorthogonal multiple access for fifth-generation radio networks," *IEEE Trans. Veh. Technol.*, vol. 66, no. 4, pp. 3185–3196, 2016.
- [66] R. Hoshyari, R. Razavi, and M. Al-Imari, "LDS-OFDM an efficient multiple access technique," in *Proc. IEEE Vehi Technol. Conf.*, pp. 1–5, 2010.
- [67] Qualcomm, "Resource spread multiple access (RSMA), 3GPP TSG RAN WG1 85,R1-164688," May 2016. [Online]. Available: <https://www.3gpp.org/DynaReport/TDocExMtg--R1-85--31662.htm>.
- [68] <https://www.3gpp.org/DynaReport/TDocExMtg--R1-86--31663.htm>, "New uplink non-orthogonal multiple access schemes for NR, 3GPP TSG RAN WG1 86, 167535," August 2016. [Online]. Available: <https://www.3gpp.org/DynaReport/TDocExMtg--R1-86--31663.htm>.
- [69] L. Ping, L. Liu, K. Wu, and W. K. Leung, "Interleave division multiple-access," *IEEE Trans. Wireless Commun.*, vol. 5, pp. 938–947, Apr 2006.
- [70] Intel, "Multiple access schemes for new radio interface, 3GPP TSG-RAN WG1 84b,R1-162385," April 2016. [Online]. Available: <https://www.3gpp.org/DynaReport/TDocExMtg--R1-84b--31661.htm>.
- [71] D. Fang, Y.-C. Huang, Z. Ding, G. Geraci, S.-L. Shieh, and H. Claussen, "Lattice partition multiple access: A new method of downlink non-orthogonal multiuser transmissions," in *Proc. IEEE Global Commun. Conf. (GLOBECOM)*, pp. 1–6, 2016.
- [72] M. Taherzadeh, H. Nikopour, A. Bayesteh, and H. Baligh, "SCMA codebook design," in *Proc. IEEE Veh. Technol. Conf. (VTC Fall)*, pp. 1–5, 2014.
- [73] W.-C. Sun, Y.-C. Su, Y.-L. Ueng, and C.-H. Yang, "An LDPC-coded SCMA receiver with multi-user iterative detection and decoding," *IEEE Trans. Circuits Syst. I, Reg. Papers.*, vol. 66, no. 9, pp. 3571–3584, 2019.
- [74] S. Tang, L. Hao, and Z. Ma, "Low complexity joint MPA detection for downlink MIMO-SCMA," in *Proc. IEEE Global Commun. Conf. (GLOBECOM)*, pp. 1–4, 2016.
- [75] Z. Ma and J. Bao, *Sparse code multiple access (SCMA)*, pp. 369–416. Cham: Springer International Publishing, 2019.
- [76] R. H. Roy, "Spatial division multiple access technology and its application to wireless communication systems," in *Proc. IEEE Veh. Technol. Conf. (VTC Spring)*, vol. 2, pp. 730–734, 1997.
- [77] Y. Mao, B. Clerckx, and V. O. Li, "Rate-splitting multiple access for downlink communication systems: Bridging, generalizing, and outperforming SDMA and NOMA," *EURASIP J. Wireless Commun. Netw.*, vol. 2018, no. 1, pp. 1–54, 2018.
- [78] A. Tusha, S. Doğan, and H. Arslan, "A hybrid downlink NOMA with OFDM and OFDM-IM for beyond 5G wireless networks," *IEEE Signal Process. Lett.*, vol. 27, pp. 491–495, 2020.
- [79] P. Parida and S. S. Das, "Power allocation in OFDM based NOMA systems: A DC programming approach," in *Proc. IEEE Globecom Workshops (GC Wkshps)*, pp. 1026–1031, 2014.
- [80] Y. Xie, K. C. Teh, and A. C. Kot, "Deep learning-based joint detection for OFDM-NOMA scheme," *IEEE Commun. Lett.*, vol. 25, no. 8, pp. 2609–2613, 2021.
- [81] Z. Liu and L.-L. Yang, "Sparse or dense: A comparative study of code-domain NOMA systems," *IEEE Trans. Wireless Commun.*, vol. 20, no. 8, pp. 4768–4780, 2021.

- [82] A. S. Rajasekaran, M. Vameghestahbanati, M. Farsi, H. Yanikomeroglu, and H. Saeedi, "Resource allocation-based PAPR analysis in uplink SCMA-OFDM systems," *IEEE Access*, vol. 7, pp. 162803–162817, 2019.
- [83] L. Yang, X. Lin, X. Ma, and K. Song, "Clipping noise-aided message passing algorithm for SCMA-OFDM system," *IEEE Commun. Lett.*, vol. 22, no. 10, pp. 2156–2159, 2018.
- [84] R.-J. Essiambre, G. Kramer, P. J. Winzer, G. J. Foschini, and B. Goebel, "Capacity limits of optical fiber networks," *J. Lightwave Technol.*, vol. 28, no. 4, pp. 662–701, 2010.
- [85] F. Davarian and J. T. Sumida, "A multiple digital modulator," *IEEE Commun. Mag.*, vol. 27, no. 2, pp. 36–45, 1989.
- [86] J. L. Massey, "Coding and modulation in digital communication," in *Zurich Sem. Digital Commun.*, 1974, vol. 2, 1974.
- [87] G. Ungerboeck, "Channel coding with multilevel/phase signals," *IEEE Trans. Inf. Theory*, vol. 28, no. 1, pp. 55–67, 1982.
- [88] A. J. Viterbi, J. K. Wolf, E. Zehavi, and R. Padovani, "A pragmatic approach to trellis-coded modulation," *IEEE Commun. Mag.*, vol. 27, no. 7, pp. 11–19, 1989.
- [89] D. J. Costello and G. D. Forney, "Channel coding: The road to channel capacity," *Proc. IEEE*, vol. 95, no. 6, pp. 1150–1177, 2007.
- [90] E. Zehavi, "8-PSK trellis codes for a Rayleigh channel," *IEEE Trans. Commun.*, vol. 40, no. 5, pp. 873–884, 1992.
- [91] G. Caire, G. Taricco, and E. Biglieri, "Bit-interleaved coded modulation," *IEEE Trans. Inf. Theory*, vol. 44, no. 3, pp. 927–946, 1998.
- [92] X. Li and J. A. Ritcey, "Bit-interleaved coded modulation with iterative decoding," in *Proc. IEEE Int. Commun. Conf. (ICC)*, vol. 2, pp. 858–863, 1999.
- [93] A. G. i Fabregas, A. Martinez, G. Caire, et al., "Bit-interleaved coded modulation," *Foundations and Trends® in Communications and Information Theory*, vol. 5, no. 1–2, pp. 1–153, 2008.
- [94] A. El Gamal and Y. H. Kim, *Network Information Theory*. Cambridge University Press, 2011.
- [95] M. Vaezi and H. V. Poor, "NOMA: An information-theoretic perspective," in *Multiple Access Techniques for 5G Wireless Networks and Beyond*, pp. 167–193, Cham, Switzerland: Springer, 2019.
- [96] Q. He, Y. Hu, and A. Schmeink, "Closed-form symbol error rate expressions for non-orthogonal multiple access systems," *IEEE Trans. Veh. Technol.*, vol. 68, no. 7, pp. 6775–6789, 2019.
- [97] E. C. Cejudo, H. Zhu, and O. Alluhaibi, "On the power allocation and constellation selection in downlink NOMA," in *Proc. IEEE Veh. Technol. Conf. (VTC Fall)*, pp. 1–5, 2017.
- [98] T. Assaf, A. J. Al-Dweik, M. S. El Moursi, H. Zeineldin, and M. Al-Jarrah, "Exact bit error-rate analysis of two-user NOMA using QAM with arbitrary modulation orders," *IEEE Commun. Lett.*, vol. 24, no. 12, pp. 2705–2709, 2020.
- [99] M. Aldababsa, C. Göztepe, G. K. Kurt, and O. Kucur, "Bit error rate for NOMA network," *IEEE Commun. Lett.*, vol. 24, no. 6, pp. 1188–1191, 2020.
- [100] W. Han, X. Ma, D. Tang, and N. Zhao, "Study of SER and BER in NOMA systems," *IEEE Trans. Veh. Technol.*, vol. 70, no. 4, pp. 3325–3340, 2021.
- [101] F. Kara and H. Kaya, "BER performances of downlink and uplink NOMA in the presence of SIC errors over fading channels," *IET Commun.*, vol. 12, no. 15, pp. 1834–1844, 2018.
- [102] M. Vaezi, R. Schober, Z. Ding, and H. V. Poor, "Non-orthogonal multiple access: Common myths and critical questions," *IEEE Wireless Commun.*, 2019.
- [103] C. Huppert and M. Bossert, "On achievable rates in the two user AWGN broadcast channel with finite input alphabets," in *Proc. IEEE Int. Symp. Inf. Theory (ISIT)*, pp. 2581–2585, 2007.
- [104] A. Almoahamad, M. O. Hasna, S. Althunibat, and K. Qaraqe, "A novel downlink IM-NOMA scheme," *IEEE Open J. Commun. Soc.*, vol. 2, pp. 235–244, 2021.
- [105] Y. Qi and M. Vaezi, "NOMA decoding: Successive interference cancellation or maximum likelihood detection," in *Proc. Annual Conf. Inf. Sci. Sys. (CISS)*, pp. 1–6, 2024.
- [106] P. A. Hoeher and T. Wo, "Superposition modulation: myths and facts," *IEEE Commun. Mag.*, vol. 49, no. 12, pp. 110–116, 2011.
- [107] T. Wo, *Superposition mapping & related coding techniques*. PhD thesis, 2011. PhD Dissertation.
- [108] X. Ma and L. Ping, "Coded modulation using superimposed binary codes," *IEEE Trans. Inf. Theory*, vol. 50, no. 12, pp. 3331–3343, 2004.
- [109] M. Fuentes, D. Vargas, and D. Gomez-Barquero, "Low-complexity demapping algorithm for two-dimensional non-uniform constellations," *IEEE Trans. Mob. Comput.*, vol. 62, no. 2, pp. 375–383, 2015.
- [110] R. Y. Mesleh, H. Haas, S. Sinanovic, C. W. Ahn, and S. Yun, "Spatial modulation," *IEEE Trans. Veh. Technol.*, vol. 57, no. 4, pp. 2228–2241, 2008.
- [111] S. Guo, H. Zhang, P. Zhang, D. Wu, and D. Yuan, "Generalized 3-D constellation design for spatial modulation," *IEEE Trans. Commun.*, vol. 65, no. 8, pp. 3316–3327, 2017.
- [112] J. Choi, Y. Nam, and N. Lee, "Spatial lattice modulation for MIMO systems," *IEEE Trans. Signal Process.*, vol. 66, no. 12, pp. 3185–3198, 2018.
- [113] X. Zhang and M. Vaezi, "Multi-dimensional joint constellation and precoding design for MIMO systems," *IEEE Wireless Commun. Lett.*, vol. 12, no. 4, pp. 713–717, 2023.
- [114] S. G. Kang, Z. Chen, J. Y. Kim, J. S. Bae, and J.-S. Lim, "Construction of higher-level 3-D signal constellations and their accurate symbol error probabilities in AWGN," *IEEE Trans. Signal Process.*, vol. 59, no. 12, pp. 6267–6272, 2011.
- [115] F. Fazel and H. Jafarkhani, "Quasi-orthogonal space-frequency and space-time-frequency block codes for MIMO OFDM channels," vol. 7, no. 1, pp. 184–192, 2008.
- [116] F. Fazel, A. Grau, H. Jafarkhani, and F. D. Flaviis, "Space-time-state block coded MIMO communication systems using reconfigurable antennas," *IEEE Trans. Wireless Commun.*, vol. 8, no. 12, pp. 6019–6029, 2009.
- [117] N. S. Loghin, J. Zöllner, B. Mouhouche, D. Anzorregui, J. Kim, and S.-I. Park, "Non-uniform constellations for ATSC 3.0," *IEEE Trans. Mob. Comput.*, vol. 62, no. 1, pp. 197–203, 2016.
- [118] C. Fragouli, R. D. Wesel, D. Sommer, and G. P. Fettweis, "Turbo codes with non-uniform constellations," in *Proc. IEEE Int. Commun. Conf. (ICC)*, vol. 1, pp. 70–73, 2001.
- [119] D. Gómez-Barquero, D. Vargas, M. Fuentes, P. Klenner, S. Moon, J.-Y. Choi, D. Schneider, and K. Murayama, "MIMO for ATSC 3.0," *IEEE Trans. Mob. Comput.*, vol. 62, no. 1, pp. 298–305, 2016.
- [120] B. Ozaydin, M. Médard, and K. R. Duffy, "GRAND-assisted optimal modulation," in *Proc. IEEE Global Commun. Conf. (GLOBECOM)*, pp. 813–818, 2022.
- [121] R. Abbas, M. Shirvanimoghaddam, Y. Li, and B. Vucetic, "A multi-layer grant-free NOMA scheme for short packet transmissions," in *Proc. IEEE Global Commun. Conf. (GLOBECOM)*, pp. 1–6, 2018.
- [122] M. Fuentes, L. Christodoulou, and B. Mouhouche, "Non-uniform constellations for broadcast and multicast in 5G new radio," in *Proc. IEEE International Symposium on Broadband Multimedia Systems and Broadcasting (BMSB)*, pp. 1–5, 2018.
- [123] J. Barrucco, J. Montalban, E. Iradier, and P. Angueira, "Constellation design for future communication systems: A comprehensive survey," *IEEE Access*, vol. 9, pp. 89778–89797, 2021.
- [124] M.-S. Alouini, "A recursive algorithm for the exact BER computation of generalized hierarchical QAM constellations," *IEEE Trans. Inf. Theory*, vol. 49, no. 1, pp. 297–307, 2003.
- [125] B. Xiao, K. Xiao, Z. Chen, B. Xia, and H. Liu, "Joint design for modulation and constellation labels in multiuser superposition transmission," *IEEE Trans. Mob. Comput.*, vol. 65, no. 2, pp. 245–259, 2018.
- [126] Z. Yang, Y. Fang, G. Han, and K. M. S. Huq, "Spatially coupled protograph LDPC-coded hierarchical modulated BICM-ID systems: A promising transmission technique for 6G-enabled Internet of Things," *IEEE Internet Things J.*, vol. 8, no. 7, pp. 5149–5163, 2020.
- [127] J. Zhang, X. Wang, T. Hasegawa, and T. Kubo, "Downlink non-orthogonal multiple access (NOMA) constellation rotation," in *Proc. IEEE Veh. Technol. Conf. (VTC Fall)*, pp. 1–5, 2016.
- [128] N. Ye, A. Wang, X. Li, W. Liu, X. Hou, and H. Yu, "On constellation rotation of NOMA with SIC receiver," *IEEE Commun. Lett.*, vol. 22, no. 3, pp. 514–517, 2017.
- [129] E. Khorov, A. Kureev, I. Levitsky, and I. F. Akyildiz, "A phase noise resistant constellation rotation method and its experimental validation for NOMA Wi-Fi," *IEEE J. Sel. Areas Commun.*, vol. 40, no. 4, pp. 1346–1354, 2022.
- [130] P. A. Baker, "Phase-modulation data sets for serial transmission at 2000 and 2400 bits per second," *Trans. Am. Inst. Electr. Eng., Part I: Commun. Electron.*, vol. 81, pp. 166–171, July 1962.
- [131] H. Jafarkhani and N. Seshadri, "Super-orthogonal space-time trellis codes," vol. 49, no. 4, pp. 937–950, 2003.
- [132] H. Jafarkhani and N. Hassanpour, "Super-quasi-orthogonal space-time trellis codes for four transmit antennas," vol. 4, no. 1, pp. 215–227, 2005.
- [133] Y. Zhu and H. Jafarkhani, "Differential modulation based on quasi-orthogonal codes," vol. 4, no. 6, pp. 3005–3017, 2005.

- [134] C. Stierstorfer, R. F. Fischer, and J. B. Huber, "Optimizing BICM with convolutional codes for transmission over the AWGN channel," in *Proc. Int. Zurich Sem. Commun.*, 2010.
- [135] Z. Yang, Y. Fang, Y. Cheng, P. Chen, and D. J. Almkhles, "Protograph LDPC-coded BICM-ID with irregular mapping: An emerging transmission technique for massive Internet of Things," *IEEE Trans. Green Commun. Netw.*, vol. 5, no. 3, pp. 1051–1065, 2021.
- [136] M. Rowshan, M. Qiu, Y. Xie, X. Gu, and J. Yuan, "Channel coding towards 6G: Technical overview and outlook," *IEEE Open J. Commun. Soc.*, vol. 5, no. 4, pp. 2585–2685, 2024.
- [137] R. E. Blahut, *Algebraic Codes for Data Transmission*. New York: Cambridge Univ. Press, 2003.
- [138] A. Viterbi, "Convolutional codes and their performance in communication systems," *IEEE Trans. Commun. Technol.*, vol. 19, no. 5, pp. 751–772, 1971.
- [139] C. Berrou, A. Glavieux, and P. Thitimajshima, "Near Shannon limit error-correcting coding and decoding: Turbo-codes. 1," in *Proc. IEEE Int. Commun. Conf. (ICC)*, vol. 2, pp. 1064–1070, 1993.
- [140] R. Gallager, "Low-density parity-check codes," *IRE Trans. Inf. Theory*, vol. 8, no. 1, pp. 21–28, 1962.
- [141] A. Shokrollahi, "LDPC codes: An introduction," in *Coding, Cryptography and Combinatorics*, pp. 85–110, Springer, 2004.
- [142] E. Arıkan, "Channel polarization: A method for constructing capacity-achieving codes for symmetric binary-input memoryless channels," *IEEE Trans. Inf. Theory*, vol. 55, no. 7, pp. 3051–3073, 2009.
- [143] X. Lin and N. Lee, "5G and Beyond," *Cham, Switzerland: Springer Nature Switzerland AG*, 2021.
- [144] "NR; Physical layer procedures for data (Version 18.2.0)," *3GPP TS 38.214*, 2024. <https://portal.3gpp.org/desktopmodules/Specifications/SpecificationDetails.aspx?specificationId=3216>.
- [145] P. Popovski, F. Chiariotti, K. Huang, A. E. Kalør, M. Kountouris, N. Pappas, and B. Soret, "A perspective on time toward wireless 6G," *Proc. IEEE*, vol. 110, no. 8, pp. 1116–1146, 2022.
- [146] R. Fantacci and B. Picano, "End-to-end delay bound for wireless uVR services over 6G terahertz communications," *IEEE Internet Things J.*, vol. 8, no. 23, pp. 17090–17099, 2021.
- [147] E. Arıkan, "From sequential decoding to channel polarization and back again," *arXiv preprint arXiv:1908.09594*, 2019.
- [148] M. Moradi, A. Mozammel, K. Qin, and E. Arıkan, "Performance and complexity of sequential decoding of PAC codes," *arXiv preprint arXiv:2012.04990*, 2020.
- [149] G. Choi and N. Lee, "Deep polar codes," *IEEE Trans. Commun.*, vol. 72, 2024.
- [150] M. Shirvanimoghaddam, M. S. Mohammadi, R. Abbas, A. Minja, C. Yue, B. Matuz, G. Han, Z. Lin, W. Liu, Y. Li, *et al.*, "Short block-length codes for ultra-reliable low latency communications," *IEEE Commun. Mag.*, vol. 57, no. 2, pp. 130–137, 2018.
- [151] D. Persson, J. Kron, M. Skoglund, and E. G. Larsson, "Joint source-channel coding for the MIMO broadcast channel," *IEEE Trans. Signal Process.*, vol. 60, no. 4, pp. 2085–2090, 2011.
- [152] M. Vaezi and F. Labeau, "Distributed source-channel coding based on real-field BCH codes," *IEEE Trans. Signal Process.*, vol. 62, no. 5, pp. 1171–1184, 2014.
- [153] S. F. Yılmaz, C. Karamanli, and D. Gündüz, "Distributed deep joint source-channel coding over a multiple access channel," in *Proc. IEEE Int. Commun. Conf. (ICC)*, pp. 1400–1405, 2023.
- [154] G. Ungerboeck, "Trellis-coded modulation with redundant signal sets Part I: Introduction," *IEEE Trans. Commun. Technol.*, vol. 25, pp. 5–11, Feb. 1987.
- [155] T. Aulin and R. Espineira, "Trellis coded multiple access (TCMA)," in *Proc. IEEE Int. Commun. Conf. (ICC)*, vol. 2, pp. 1177–1181, 1999.
- [156] X. Zou, M. Ganji, and H. Jafarkhani, "Trellis-coded non-orthogonal multiple access," vol. 9, pp. 538–542, Apr. 2020.
- [157] H. Jafarkhani and V. Tarokh, "Multiple description trellis-coded quantization," *IEEE Trans. Commun.*, vol. 47, pp. 799 – 803, June 1999.
- [158] H. Jafarkhani and V. Tarokh, "Design of successively refinable trellis-coded quantizers," *IEEE Trans. Inf. Theory*, vol. 45, pp. 1490–1497, July 1999.
- [159] I. Goodfellow, Y. Bengio, A. Courville, and Y. Bengio, *Deep learning*, vol. 1. MIT press Cambridge, 2016.
- [160] X. Zhang and M. Vaezi, "Multi-objective DNN-based precoder for MIMO communications," *IEEE Trans. Commun.*, vol. 69, no. 7, pp. 4476–4488, 2021.
- [161] X. Lin, "An overview of 5G advanced evolution in 3GPP release 18," *IEEE Commun. Stand. Mag.*, vol. 6, no. 3, pp. 77–83, 2022.
- [162] T. J. O'Shea, T. Roy, and T. C. Clancy, "Over-the-air deep learning based radio signal classification," *IEEE J. Sel. Topic Signal Process.*, vol. 12, no. 1, pp. 168–179, 2018.
- [163] S. Peng, S. Sun, and Y.-D. Yao, "A survey of modulation classification using deep learning: Signal representation and data preprocessing," *IEEE Trans. Neural Netw. Learn. Syst.*, vol. 33, no. 12, pp. 7020–7038, 2021.
- [164] K. Tekbıyık, A. R. Ekti, A. Görçin, G. K. Kurt, and C. Keçeci, "Robust and fast automatic modulation classification with CNN under multipath fading channels," in *Proc. IEEE Veh. Technol. Conf. (VTC Spring)*, pp. 1–6, 2020.
- [165] R. Wang, Y. Qi, M. Vaezi, X. Jiao, and M. Amin, "Strategies for enhanced signal modulation classifications under unknown symbol rates and noise conditions," in *Proc. IEEE Int. Acoust. Speech Signal Process. (ICASSP)*, pp. 1–5, 2023.
- [166] F. Sohrabi, Y.-F. Liu, and W. Yu, "One-bit precoding and constellation range design for massive MIMO with QAM signaling," *IEEE J. Sel. Topic Signal Process.*, vol. 12, no. 3, pp. 557–570, 2018.
- [167] M. Han, H. Seo, A. T. Abebe, and C. G. Kang, "Deep learning-based codebook design for code-domain non-orthogonal multiple access: Approaching single-user bit-error rate performance," *IEEE Trans. Cogn. Commun. Netw.*, vol. 8, no. 2, pp. 1159–1173, 2021.
- [168] M. J. López-Morales, K. Chen-Hu, and A. G. Armada, "A survey about deep learning for constellation design in communications," in *Proc. IEEE Int. Symp. Communication Syst. Netw. Digital Signal Process. (CSNDSP)*, pp. 1–5, 2020.
- [169] Z. Ma, W. Wu, M. Jian, F. Gao, and X. Shen, "Joint constellation design and multiuser detection for grant-free NOMA," *IEEE Trans. Wireless Commun.*, vol. 21, no. 3, pp. 1973–1988, 2021.
- [170] P. Madadi, J. Cho, C. J. Zhang, and D. Burghal, "AI/ML optimized high-order modulations," in *Proc. IEEE Int. Commun. Conf. (ICC)*, pp. 6373–6378, 2023.
- [171] X. Zhang and M. Vaezi, "Deep autoencoder-based Z-interference channels with perfect and imperfect CSI," *IEEE Trans. Commun.*, vol. 72, no. 2, pp. 861–873, 2024.
- [172] N. Nartasilpa, A. Salim, D. Tuninetti, and N. Devroye, "Communications system performance and design in the presence of radar interference," *IEEE Trans. Commun.*, vol. 66, no. 9, pp. 4170–4185, 2018.
- [173] N. Deshpande and B. S. Rajan, "Constellation constrained capacity of two-user broadcast channels," in *Proc. IEEE Global Commun. Conf. (GLOBECOM)*, pp. 1–6, 2009.
- [174] S. R. Islam, N. Avazov, O. A. Dobre, and K.-S. Kwak, "Power-domain non-orthogonal multiple access (NOMA) in 5G systems: Potentials and challenges," *IEEE Commun. Surv. Tut.*, vol. 19, no. 2, pp. 721–742, 2016.
- [175] M. Qiu, Y.-C. Huang, and J. Yuan, "Downlink non-orthogonal multiple access without SIC for block fading channels: An algebraic rotation approach," *IEEE Trans. on Wireless Commun.*, vol. 18, no. 8, pp. 3903–3918, 2019.
- [176] P. Baldi, "Autoencoders, unsupervised learning, and deep architectures," in *Proc. ICML Workshop on Unsupervised and Transfer Learning*, pp. 37–49, 2012.
- [177] F. Alberge, "Constellation design with deep learning for downlink non-orthogonal multiple access," in *Proc. Int. Symp. Pers. Indoor Mob. Radio Commun. (PIMRC)*, pp. 1–5, 2018.
- [178] V. Ninkovic, D. Vukobratovic, A. Pastore, and C. Anton-Haro, "A weighted autoencoder-based approach to downlink NOMA constellation design," in *Proc. IEEE Int. Works. Signal Process. Adv. Wireless Commun. (SPAWC)*, pp. 1–6, 2023.
- [179] A. Aboutaleb, M. Torabi, B. Belzer, and K. Sivakumar, "Deep learning-based auto-encoder for time-offset sub-faster-than-Nyquist downlink NOMA with timing errors and imperfect CSI," *IEEE J. Sel. Topic Signal Process.*, 2024.
- [180] S. Haykin, *Communication Systems*. John Wiley & Sons, 2008.
- [181] H. Yahya, E. Alsusa, and A. Al-Dweik, "Exact BER analysis of NOMA with arbitrary number of users and modulation orders," *IEEE Trans. Commun.*, vol. 69, no. 9, pp. 6330–6344, 2021.
- [182] S. S. Pradhan and K. Ramchandran, "Distributed source coding using syndromes (DISCUS): Design and construction," *IEEE Trans. Inf. Theory*, vol. 49, no. 3, pp. 626–643, 2003.
- [183] O. El Ayach, S. W. Peters, and R. W. Heath, "The practical challenges of interference alignment," *IEEE Wireless Commun.*, vol. 20, no. 1, pp. 35–42, 2013.
- [184] S. Sun, Q. Gao, Y. Peng, Y. Wang, and L. Song, "Interference management through CoMP in 3GPP LTE-advanced networks," *IEEE Wireless Commun.*, vol. 20, no. 1, pp. 59–66, 2013.

- [185] M. Vaezi, X. Lin, H. Zhang, W. Saad, and H. V. Poor, "Deep reinforcement learning for interference management in UAV-based 3D networks: Potentials and challenges," *IEEE Commun. Mag.*, vol. 62, no. 2, pp. 134–140, 2024.
- [186] W. Shin, M. Vaezi, B. Lee, D. Love, J. Lee, and H. Poor, "Coordinated beamforming for multi-cell MIMO-NOMA," *IEEE Commun. Lett.*, vol. 21, no. 1, pp. 84–87, 2016.
- [187] W. Shin, M. Vaezi, B. Lee, D. Love, J. Lee, and H. Poor, "Non-orthogonal multiple access in multi-cell networks: Theory, performance, and practical challenges," *IEEE Commun. Mag.*, vol. 55, no. 10, pp. 176–183, 2017.
- [188] F. Guo, H. Lu, X. Jiang, M. Zhang, J. Wu, and C. W. Chen, "QoS-aware user grouping strategy for downlink multi-cell NOMA systems," *IEEE Trans. Wireless Commun.*, vol. 20, no. 12, pp. 7871–7887, 2021.
- [189] S. Rezvani, E. A. Jorswieck, N. M. Yamchi, and M. R. Javan, "Optimal SIC ordering and power allocation in downlink multi-cell NOMA systems," *IEEE Trans. Wireless Commun.*, vol. 21, no. 6, pp. 3553–3569, 2021.
- [190] C. W. Sung, Y. Chen, and Y. Gu, "Distributed dual optimization for the uplink of multi-cell NOMA," *IEEE Trans. Commun.*, vol. 69, no. 5, pp. 3135–3146, 2021.
- [191] T. Erpek, T. J. O'Shea, and T. C. Clancy, "Learning a physical layer scheme for the MIMO interference channel," in *Proc. IEEE Int. Commun. Conf. (ICC)*, pp. 1–5, 2018.
- [192] S. Vishwakarma, V. Ummalaneni, M. S. Iqbal, A. Majumdar, and S. S. Ram, "Mitigation of through-wall interference in radar images using denoising autoencoders," in *Proc. IEEE Radar Conf.*, pp. 1543–1548, 2018.
- [193] D. Wu, M. Nekovee, and Y. Wang, "Deep learning-based autoencoder for m-User wireless interference channel physical layer design," *IEEE Access*, vol. 8, pp. 174679–174691, 2020.
- [194] X. Zhang and M. Vaezi, "Deep autoencoder-based Z-interference channels," in *Proc. IEEE Wireless Commun. Net. Conf. (WCNC)*, pp. 1–6, 2023.
- [195] X. Zhang, M. Vaezi, and L. Zheng, "Interference-aware constellation design for Z-interference channels with imperfect CSI," in *Proc. IEEE Int. Commun. Conf. (ICC)*, pp. 1–6, 2023.
- [196] M. Vaezi and H. V. Poor, "Simplified Han-Kobayashi region for one-sided and mixed Gaussian interference channels," in *Proc. IEEE Int. Commun. Conf. (ICC)*, pp. 1–6, 2016.
- [197] S. M. Alamouti, "A simple transmit diversity technique for wireless communications," *IEEE J. Sel. Areas Commun.*, vol. 16, no. 8, pp. 1451–1458, 1998.
- [198] V. Tarokh, H. Jafarkhani, and A. Calderbank, "Space-time block coding for wireless communications: performance results," *IEEE J. Sel. Areas Commun.*, vol. 17, no. 3, pp. 451–460, 1999.
- [199] V. Tarokh, H. Jafarkhani, and A. Calderbank, "Space-time block codes from orthogonal designs," vol. 45, no. 5, pp. 1456–1467, 1999.
- [200] C. Cox, *An Introduction to LTE: LTE, LTE-Advanced, SAE, VoLTE and 4G Mobile Communications*. John Wiley & Sons, 2014.
- [201] V. Tarokh and H. Jafarkhani, "A differential detection scheme for transmit diversity," *IEEE J. Sel. Areas Commun.*, vol. 18, no. 7, pp. 1169–1174, 2000.
- [202] H. Jafarkhani and V. Tarokh, "Multiple transmit antenna differential detection from generalized orthogonal designs," vol. 47, no. 6, pp. 2626–2631, 2001.
- [203] "IEEE standard for information technology–Telecommunications and information exchange between systems - Local and metropolitan area networks–Specific requirements - Part 11: Wireless LAN medium access control (MAC) and physical layer (PHY) specifications," *IEEE Std 802.11-2020 (Revision of IEEE Std 802.11-2016)*, pp. 1–4379, 2021.
- [204] 3GPP, "5G NR Physical layer procedures for data (Version 15.3.0 Release 15)," *TS 138 214*, 2018. https://www.etsi.org/deliver/etsi_ts/138200_138299/138214/15.03.00_60/ts_138214v150300p.pdf.
- [205] C. Xiao, Y. R. Zheng, and Z. Ding, "Globally optimal linear precoders for finite alphabet signals over complex vector Gaussian channels," *IEEE Trans. Signal Process.*, vol. 59, no. 7, pp. 3301–3314, 2011.
- [206] Z. Zhou, B. Vucetic, M. Dohler, and Y. Li, "MIMO systems with adaptive modulation," *IEEE Trans. Veh. Technol.*, vol. 54, no. 5, pp. 1828–1842, 2005.
- [207] Z. Zhou and B. Vucetic, "Adaptive coded MIMO systems with near full multiplexing gain using outdated CSI," *IEEE Trans. Wireless Commun.*, vol. 10, no. 1, pp. 294–302, 2010.
- [208] J. Xia, D. Deng, and D. Fan, "A note on implementation methodologies of deep learning-based signal detection for conventional MIMO transmitters," *IEEE Trans. Mob. Comput.*, vol. 66, no. 3, pp. 744–745, 2020.
- [209] R. S. Prabhu and B. Daneshrad, "Energy-efficient power loading for a MIMO-SVD system and its performance in flat fading," in *Proc. IEEE Global Commun. Conf. (GLOBECOM)*, pp. 1–5, 2010.
- [210] Z. Ding, F. Adachi, and H. V. Poor, "The application of MIMO to non-orthogonal multiple access," *IEEE Trans. Wireless Commun.*, vol. 15, no. 1, pp. 537–552, 2016.
- [211] Z. Ding and H. V. Poor, "Design of massive-MIMO-NOMA With limited feedback," *IEEE Signal Process. Lett.*, vol. 23, no. 5, pp. 629–633, 2016.
- [212] H. Weingarten, Y. Steinberg, and S. S. Shamai, "The capacity region of the Gaussian multiple-input multiple-output broadcast channel," *IEEE Trans. Inf. Theory*, vol. 52, no. 9, pp. 3936–3964, 2006.
- [213] R. Liu, T. Liu, H. V. Poor, and S. Shamai, "Multiple-input multiple-output Gaussian broadcast channels with confidential messages," *IEEE Trans. Inf. Theory*, vol. 56, no. 9, pp. 4215–4227, 2010.
- [214] E. Ekrem and S. Ulukus, "Degraded compound multi-receiver wiretap channels," *IEEE Trans. Inf. Theory*, vol. 58, no. 9, pp. 5681–5698, 2012.
- [215] Y. Qi and M. Vaezi, "Signaling design for MIMO-NOMA with different security requirements," *IEEE Trans. Signal Process.*, vol. 70, no. 3, pp. 1389–1401, 2022.
- [216] Y. Qi, M. Vaezi, and H. V. Poor, "K-receiver wiretap channel: Optimal encoding order and signaling design," *IEEE Trans. Wireless Commun.*, vol. 22, no. 12, pp. 8575–8586, 2023.
- [217] J. Pauls and M. Vaezi, "Secure precoding in MIMO-NOMA: A deep learning approach," *IEEE Wireless Commun. Lett.*, vol. 11, no. 1, pp. 77–80, 2021.
- [218] S. A. A. Fakoorian and A. L. Swindlehurst, "On the optimality of linear precoding for secrecy in the MIMO broadcast channel," *IEEE J. Sel. Areas Commun.*, vol. 31, no. 9, pp. 1701–1713, 2013.
- [219] S. Shi, M. Schubert, and H. Boche, "Rate optimization for multiuser MIMO systems with linear processing," *IEEE Trans. Signal Process.*, vol. 56, no. 8, pp. 4020–4030, 2008.
- [220] D. Park, "Weighted sum rate maximization of MIMO broadcast and interference channels with confidential messages," *IEEE Trans. Wireless Commun.*, vol. 15, no. 3, pp. 1742–1753, 2015.
- [221] Z. Chen, Z. Ding, P. Xu, and X. Dai, "Optimal precoding for a QoS optimization problem in two-user MISO-NOMA downlink," *IEEE Commun. Lett.*, vol. 20, no. 6, pp. 1263–1266, 2016.
- [222] Y. Sun, Z. Ding, X. Dai, M. Zhou, and Z. Ding, "On the application of quasi-degradation to network NOMA in downlink CoMP systems," *IEEE Trans. Wireless Commun.*, vol. 23, no. 2, pp. 978–993, 2024.
- [223] A. Goldsmith, S. A. Jafar, N. Jindal, and S. Vishwanath, "Capacity limits of MIMO channels," *IEEE J. Sel. Areas Commun.*, vol. 21, no. 5, pp. 684–702, 2003.
- [224] A. Krishnamoorthy and R. Schober, "Uplink and downlink MIMO-NOMA with simultaneous triangularization," *IEEE Trans. Wireless Commun.*, vol. 20, no. 6, pp. 3381–3396, 2021.
- [225] Y. Chi, L. Liu, G. Song, C. Yuen, Y. L. Guan, and Y. Li, "Practical MIMO-NOMA: Low complexity and capacity-approaching solution," *IEEE Trans. Wireless Commun.*, vol. 17, no. 9, pp. 6251–6264, 2018.
- [226] L. Liu, Y. Chi, C. Yuen, Y. L. Guan, and Y. Li, "Capacity-achieving MIMO-NOMA: iterative LMMSE detection," *IEEE Trans. Signal Process.*, vol. 67, no. 7, pp. 1758–1773, 2019.
- [227] Y. Mao, B. Clerckx, and V. O. Li in *Proc. IEEE Int. Symp. Wireless Commun. Syst. (ISWCS)*, title=Energy efficiency of rate-splitting multiple access, and performance benefits over SDMA and NOMA, year=2018, pages=1-5.
- [228] A. Carleial, "Interference channels," *IEEE Trans. Inf. Theory*, vol. 24, no. 1, pp. 60–70, 1978.
- [229] B. Rimoldi and R. Urbanke, "A rate-splitting approach to the Gaussian multiple-access channel," *IEEE Trans. Inf. Theory*, vol. 42, no. 2, pp. 364–375, 1996.
- [230] C. Hao, Y. Wu, and B. Clerckx, "Rate analysis of two-receiver MISO broadcast channel with finite rate feedback: A rate-splitting approach," *IEEE Trans. Commun.*, vol. 63, no. 9, pp. 3232–3246, 2015.
- [231] M. Dai, B. Clerckx, D. Gesbert, and G. Caire, "A rate splitting strategy for massive MIMO with imperfect CSIT," *IEEE Trans. Wireless Commun.*, vol. 15, no. 7, pp. 4611–4624, 2016.
- [232] B. Clerckx, H. Joudeh, C. Hao, M. Dai, and B. Rassouli, "Rate splitting for MIMO wireless networks: A promising PHY-layer strategy for LTE evolution," *IEEE Commun. Mag.*, vol. 54, no. 5, pp. 98–105, 2016.
- [233] G. Zhou, Y. Mao, and B. Clerckx, "Rate-splitting multiple access for multi-antenna downlink communication systems: Spectral and energy efficiency tradeoff," vol. 21, no. 7, pp. 4816–4828, 2022.

- [234] B. Matthiesen, Y. Mao, P. Popovski, and B. Clerckx, "Globally optimal beamforming for rate splitting multiple access," in *Proc. IEEE Int. Acoust. Speech Signal Process. (ICASSP)*, pp. 4775–4779, 2021.
- [235] Z. Li, C. Ye, Y. Cui, S. Yang, and S. Shamai, *IEEE J. Sel. Areas Commun.*
- [236] Y. Mao and B. Clerckx, "Beyond dirty paper coding for multi-antenna broadcast channel with partial CSIT: A rate-splitting approach," *IEEE Trans. Commun.*, vol. 68, no. 11, pp. 6775–6791, 2020.
- [237] M. Medra and T. N. Davidson, "Robust downlink transmission: An offset-based single-rate-splitting approach," in *Proc. IEEE Int. Works. Signal Process. Adv. Wireless Commun. (SPAWC)*, pp. 1–5, 2018.
- [238] O. Dizdar, Y. Mao, Y. Xu, P. Zhu, and B. Clerckx, "Rate-splitting multiple access for enhanced URLLC and eMBB in 6G," in *Proc. IEEE Int. Symp. Wireless Commun. Syst. (ISWCS)*, pp. 1–6, 2021.
- [239] Y. Xu, Y. Mao, O. Dizdar, and B. Clerckx, "Rate-splitting multiple access with finite blocklength for short-packet and low-latency downlink communications," *IEEE Trans. Veh. Technol.*, vol. 71, no. 11, pp. 12333–12337, 2022.
- [240] J. Park, J. Choi, N. Lee, W. Shin, and H. V. Poor, "Rate-splitting multiple access for downlink MIMO: A generalized power iteration approach," *IEEE Trans. Wireless Commun.*, vol. 22, no. 3, pp. 1588–1603, 2022.
- [241] A. R. Flores, R. C. de Lamare, and B. Clerckx, "Linear precoding and stream combining for rate splitting in multiuser MIMO systems," *IEEE Commun. Lett.*, vol. 24, no. 4, pp. 890–894, 2020.
- [242] A. Krishnamoorthy and R. Schober, "Downlink MIMO-RSMA with successive null-space precoding," *IEEE Trans. Wireless Commun.*, vol. 21, no. 11, pp. 9170–9185, 2022.
- [243] A. Mishra, Y. Mao, O. Dizdar, and B. Clerckx, "Rate-splitting multiple access for downlink multiuser MIMO: Precoder optimization and PHY-layer design," *IEEE Trans. Commun.*, vol. 70, no. 2, pp. 874–890, 2021.
- [244] R. Diab, A. Krishnamoorthy, and R. Schober, "Precoding and decoding schemes for downlink MIMO-RSMA with simultaneous diagonalization and user exclusion," in *Proc. IEEE Int. Commun. Conf. Workshops (ICC Wkshps)*, pp. 586–591, 2022.
- [245] L. Khamidullina, A. L. de Almeida, and M. Haardt, "Rate splitting and precoding strategies for multi-user MIMO broadcast channels with common and private streams," in *Proc. IEEE Int. Acoust. Speech Signal Process. (ICASSP)*, pp. 1–5, 2023.
- [246] H. Jiang, L. You, A. Elzanaty, J. Wang, W. Wang, X. Gao, and M.-S. Alouini, "Rate-splitting multiple access for uplink massive MIMO with electromagnetic exposure constraints," *IEEE J. Sel. Areas Commun.*
- [247] M. M. Şahin, O. Dizdar, B. Clerckx, and H. Arslan, "Multicarrier rate-splitting multiple access: Superiority of OFDM-RSMA over OFDMA and OFDM-NOMA," *IEEE Commun. Lett.*, vol. 27, no. 11, pp. 3088–3092, 2023.
- [248] Z. Chen, J. Wang, Z. Tian, M. Wang, Y. Jia, and T. Q. S. Quek, "Joint rate splitting and beamforming design for RSMA-RIS-assisted ISAC system," *IEEE Wireless Commun. Lett.*, pp. 1–1, 2023.
- [249] Z. Liu, Y. Jint, B. Cao, and R. Lu, "RISAC: Rate-splitting multiple access enabled integrated sensing and communication systems," in *Proc. IEEE Int. Commun. Conf. (ICC)*, pp. 6449–6454, 2023.
- [250] C. Hu, Y. Fang, and L. Qiu, "Joint transmit and receive beamforming design for uplink RSMA enabled integrated sensing and communication systems," in *Proc. IEEE Wireless Commun. Net. Conf. (WCNC)*, pp. 1–6, 2023.
- [251] C. Xu, B. Clerckx, S. Chen, Y. Mao, and J. Zhang, "Rate-splitting multiple access for multi-antenna joint radar and communications," *IEEE J. Sel. Topic Signal Process.*, vol. 15, no. 6, pp. 1332–1347, 2021.
- [252] Z. Yang, J. Shi, Z. Li, M. Chen, W. Xu, and M. Shikh-Bahaei, "Energy efficient rate splitting multiple access (RSMA) with reconfigurable intelligent surface," in *Proc. IEEE Int. Commun. Conf. (ICC)*, pp. 1–6, 2020.
- [253] R. Zhang, K. Xiong, Y. Lu, P. Fan, D. W. K. Ng, and K. B. Letaief, "Energy efficiency maximization in RIS-assisted SWIPT networks with RSMA: A PPO-based approach," *IEEE J. Sel. Areas Commun.*, vol. 41, no. 5, pp. 1413–1430, 2023.
- [254] S. Pala, M. Katwe, K. Singh, B. Clerckx, and C.-P. Li, "Spectral-efficient RIS-aided RSMA URLLC: Toward mobile broadband reliable low latency communication (mBRLLC) system," *IEEE Trans. Wireless Commun.*, pp. 1–1, 2023.
- [255] H. Niu, Z. Lin, K. An, J. Wang, G. Zheng, N. Al-Dhahir, and K.-K. Wong, *IEEE J. Sel. Areas Commun.*
- [256] S. Dhok and P. K. Sharma, "Rate-splitting multiple access with STAR RIS over spatially-correlated channels," *IEEE Trans. Commun.*, vol. 70, no. 10, pp. 6410–6424, 2022.
- [257] H. Jafarkhani, "Taking to the air to help on the ground: How UAVs can help fight wildfires," in *IEEE ComSoc Technology News*, Oct. 2022.
- [258] C. Diaz-Vilor, A. Lozano, and H. Jafarkhani, "Cell-free UAV networks: Asymptotic analysis and deployment optimization," vol. 22, no. 5, pp. 3055–3070, 2023.
- [259] C. Diaz-Vilor, A. Lozano, and H. Jafarkhani, "Cell-free UAV networks with wireless fronthaul: Analysis and optimization," vol. 23, no. 3, pp. 2054–2069, 2024.
- [260] C. Diaz-Vilor, M. A. Almasi, A. M. Abdelhady, A. Celik, A. M. Eltawil, and H. Jafarkhani, "Sensing and communication in UAV cellular networks: Design and optimization," vol. 23, no. 6, pp. 5456–5472, 2024.
- [261] J. Guo, P. Walk, and H. Jafarkhani, "Optimal deployments of UAVs with directional antennas for a power-efficient coverage," vol. 68, no. 8, pp. 5159–5174, 2020.
- [262] S. Karimi-Bidhendi, G. Geraci, and H. Jafarkhani, "Optimizing cellular networks for UAV corridors via quantization theory," *IEEE Trans. Wireless Commun.*, 2024.
- [263] W. Jaafar, S. Naser, S. Muhaidat, P. C. Sofotasios, and H. Yanikomeroglu, "On the downlink performance of RSMA-based UAV communications," *IEEE Trans. Veh. Technol.*, vol. 69, no. 12, pp. 16258–16263, 2020.
- [264] A. Rahmati, Y. Yapici, N. Rupasinghe, I. Guvenc, H. Dai, and A. Bhuyan, "Energy efficiency of RSMA and NOMA in cellular-connected mmWave UAV networks," in *Proc. IEEE Int. Commun. Conf. Workshops (ICC Wkshps)*, pp. 1–6, 2019.
- [265] S. K. Singh, K. Agrawal, K. Singh, and C.-P. Li, "Outage probability and throughput analysis of UAV-assisted rate-splitting multiple access," *IEEE Wireless Commun. Lett.*, vol. 10, no. 11, pp. 2528–2532, 2021.
- [266] M. Xiao, H. Cui, D. Huang, Z. Zhao, X. Cao, and D. O. Wu, "Traffic-aware energy-efficient resource allocation for RSMA based UAV communications," *IEEE Trans. Netw. Sci. Eng.*, pp. 1–12, 2023.
- [267] X. Liu, J. Feng, F. Li, and V. C. M. Leung, "Downlink energy efficiency maximization for RSMA-UAV assisted communications," *IEEE Wireless Commun. Lett.*, pp. 1–1, 2023.
- [268] Z. Yang, M. Chen, W. Saad, W. Xu, and M. Shikh-Bahaei, "Sum-rate maximization of uplink rate splitting multiple access (RSMA) communication," *IEEE Trans. Mob. Comput.*, vol. 21, no. 7, pp. 2596–2609, 2022.
- [269] O. Abbasi and H. Yanikomeroglu, "Transmission scheme, detection and power allocation for uplink user cooperation with NOMA and RSMA," *IEEE Trans. Wireless Commun.*, vol. 22, no. 1, pp. 471–485, 2022.
- [270] M. Katwe, K. Singh, B. Clerckx, and C.-P. Li, "Rate-splitting multiple access and dynamic user clustering for sum-rate maximization in multiple RISs-aided uplink mmWave system," *IEEE Trans. Commun.*, vol. 70, no. 11, pp. 7365–7383, 2022.
- [271] H. Lu, X. Xie, Z. Shi, H. Lei, N. Zhao, and J. Cai, "Outage performance of uplink rate splitting multiple access with randomly deployed users," *IEEE Trans. Wireless Commun.*, pp. 1–1, 2023.
- [272] M. Katwe, K. Singh, B. Clerckx, and C.-P. Li, "Improved spectral efficiency in STAR-RIS aided uplink communication using rate splitting multiple access," *IEEE Trans. Wireless Commun.*, vol. 22, no. 8, pp. 5365–5382, 2023.
- [273] S. Zhang and W. Chen, "Fairness optimization of RSMA for uplink communication based on intelligent reflecting surface," *arXiv preprint arXiv:2309.02264*, 2023.
- [274] Q. Sun, H. Liu, S. Yan, T. A. Tsiftsis, and J. Yuan, "Joint receive and passive beamforming optimization for RIS-assisted uplink RSMA systems," *IEEE Wireless Commun. Lett.*, vol. 12, no. 7, pp. 1204–1208, 2023.
- [275] G. D. B. Rovella, M. Benammar, T. Benaddi, and H. Meric, "Scalable syndrome-based neural decoders for bit-interleaved coded modulations," *arXiv preprint 2403.02850*, 2024.
- [276] R. De Maesschalck, D. Jouan-Rimbaud, and D. L. Massart, "The Mahalanobis distance," *Chemometrics and intelligent laboratory systems*, vol. 50, no. 1, pp. 1–18, 2000.
- [277] B. Selim, M. S. Alam, J. V. Evangelista, G. Kaddoum, and B. L. Agba, "NOMA-based IoT networks: Impulsive noise effects and mitigation," *IEEE Commun. Mag.*, vol. 58, no. 11, pp. 69–75, 2020.
- [278] X. Liu and H. Jafarkhani, "Downlink non-orthogonal multiple access with limited feedback," *IEEE Trans. Wireless Commun.*, vol. 16, pp. 6151–6164, Sept. 2017.
- [279] X. Zou, M. Ganji, and H. Jafarkhani, "Downlink asynchronous non-orthogonal multiple access with quantizer optimization," vol. 9, pp. 1606–1610, Oct. 2020.

- [280] P. Xu, Y. Yuan, Z. Ding, X. Dai, and R. Schober, "On the outage performance of non-orthogonal multiple access with 1-bit feedback," *IEEE Trans. Wireless Commun.*, vol. 15, no. 10, pp. 6716–6730, 2016.
- [281] Y. Yapıcı, I. Güvenç, and H. Dai, "Low-resolution limited-feedback NOMA for mmWave communications," *IEEE Trans. Wireless Commun.*, vol. 19, no. 8, pp. 5433–5446, 2020.
- [282] P. Swami, M. K. Mishra, V. Bhatia, and T. Ratnarajah, "Performance analysis of NOMA enabled hybrid network with limited feedback," *IEEE Trans. Veh. Technol.*, vol. 69, no. 4, pp. 4516–4521, 2020.
- [283] M. Almasi and H. Jafarkhani, "Reconfigurable intelligent surface-aided NOMA with limited feedback," in *Proc. IEEE Int. Commun. Conf. (ICC)*, 2023.
- [284] M. Wu, Z. Gao, Y. Huang, Z. Xiao, D. W. K. Ng, and Z. Zhang, "Deep learning-based rate-splitting multiple access for reconfigurable intelligent surface-aided tera-hertz massive MIMO," *IEEE J. Sel. Areas Commun.*, vol. 41, no. 5, pp. 1431–1451, 2023.
- [285] G. Lu, L. Li, H. Tian, and F. Qian, "MMSE-based precoding for rate splitting systems with finite feedback," *IEEE Commun. Lett.*, vol. 22, no. 3, pp. 642–645, 2017.
- [286] M. A. Almasi and H. Jafarkhani, "Rate loss analysis of reconfigurable intelligent surface-aided NOMA With limited feedback," *IEEE Open J. Commun. Soc.*, vol. 5, pp. 856–871, 2024.
- [287] I. F. Akyildiz, C. Han, Z. Hu, S. Nie, and J. M. Jornet, "Terahertz band communication: An old problem revisited and research directions for the next decade," *IEEE Trans. Commun.*, vol. 70, no. 6, pp. 4250–4285, 2022.
- [288] L. Zhu, J. Zhang, Z. Xiao, X. Cao, D. O. Wu, and X.-G. Xia, "Millimeter-wave NOMA with user grouping, power allocation and hybrid beamforming," *IEEE Trans. Wireless Commun.*, vol. 18, no. 11, pp. 5065–5079, 2019.
- [289] Z. Wei, L. Zhao, J. Guo, D. W. K. Ng, and J. Yuan, "Multi-beam NOMA for hybrid mmWave systems," *IEEE Trans. Commun.*, vol. 67, no. 2, pp. 1705–1719, 2018.
- [290] M. A. Almasi, L. Jiang, H. Jafarkhani, and H. Mehrpouyan, "Joint beamwidth and power optimization in mmWave hybrid beamforming-NOMA systems," *IEEE Trans. Wireless Commun.*, vol. 20, pp. 1934–1947, April 2021.
- [291] Y. Cai, M. Chen, A. Deng, D. Wang, L. Wang, X. Gao, J. Zhou, Y. Liu, and C. Xiang, "Experimental demonstration of 16QAM/QPSK OFDM-NOMA VLC with LDPC codes and analog pre-equalization," *Applied Optics*, vol. 61, no. 19, pp. 5585–5591, 2022.
- [292] H. Cho, B. Ko, B. Clerckx, and J. Choi, "Coverage increase at THz frequencies: A cooperative rate-splitting approach," *IEEE Trans. Wireless Commun.*, vol. 22, no. 12, pp. 9821–9834, 2023.
- [293] M. A. Almasi, M. Vaezi, and H. Mehrpouyan, "Impact of beam misalignment on hybrid beamforming NOMA for mmWave communications," *IEEE Trans. Commun.*, vol. 67, no. 6, pp. 4505–4518, 2019.
- [294] L. Jiang and H. Jafarkhani, "Multi-user analog beamforming in mmWave MIMO systems based on path angle information," *IEEE Trans. Wireless Commun.*, vol. 18, pp. 608–619, Jan. 2019.
- [295] L. Jiang and H. Jafarkhani, "MmWave amplify-and-forward MIMO relay networks with hybrid precoding/combining design," *IEEE Trans. Wireless Commun.*, vol. 19, pp. 1333–1346, Feb. 2020.
- [296] F. Etemadi, P. Heydari, and H. Jafarkhani, "On analog QAM demodulation for millimeter-wave communications," *IEEE Trans. Circuits Syst. II, Exp. Briefs.*, vol. 66, no. 3, pp. 402–406, 2018.
- [297] H. Wang, H. Mohammadnezhad, and P. Heydari, "Analysis and design of high-order QAM direct-modulation transmitter for high-speed point-to-point mm-wave wireless links," *IEEE J. Solid-State Circuits*, vol. 54, no. 11, pp. 3161–3179, 2019.
- [298] J. Mo and R. W. Heath, "Capacity analysis of one-bit quantized MIMO systems with transmitter channel state information," *IEEE Trans. Signal Process.*, vol. 63, no. 20, pp. 5498–5512, 2015.